First-principles-driven Control-oriented Modeling of the Current Profile Evolution in NSTX-U

Zeki Ilhan, Justin Barton, Mark D. Boyer, Eugenio Schuster

Lehigh University, Bethlehem, PA, USA
Department of Mechanical Engineering and Mechanics
Plasma Control Group

Work Meeting with NSTX-U Team
Princeton Plasma Physics Laboratory

June 25, 2013

Motivation for Current Profile Control in NSTX-U

- Some of the next-step operational goals for NSTX-Upgrade include:
  - Non-inductive sustainment of the high-β spherical torus.
  - High performance equilibrium scenarios with neutral beam heating.
  - Longer pulse durations.

- **Active, model-based, feedback control** of the **current profile** evolution can be useful to achieve those stability and performance criteria.

- **Model-based control** motivated by coupled, nonlinear, multivariable, distributed parameter dynamics of system.

- The $\mathbf{q}$ **profile** is related to the **current profile** in the machine and plays an important role in the stability and performance of a given magnetic configuration.

- The value of the $q_{\min}$ can be controlled by varying the current-drive sources used $\Rightarrow$ ***enables feedback control of the current profile.***

Model-based Control Design Approach

- Our purpose is to convert the accepted and detailed physics based models to a form suitable for control design.
- The actual NSTX-U machine is replaced by the control-oriented model during the iterative control design process:

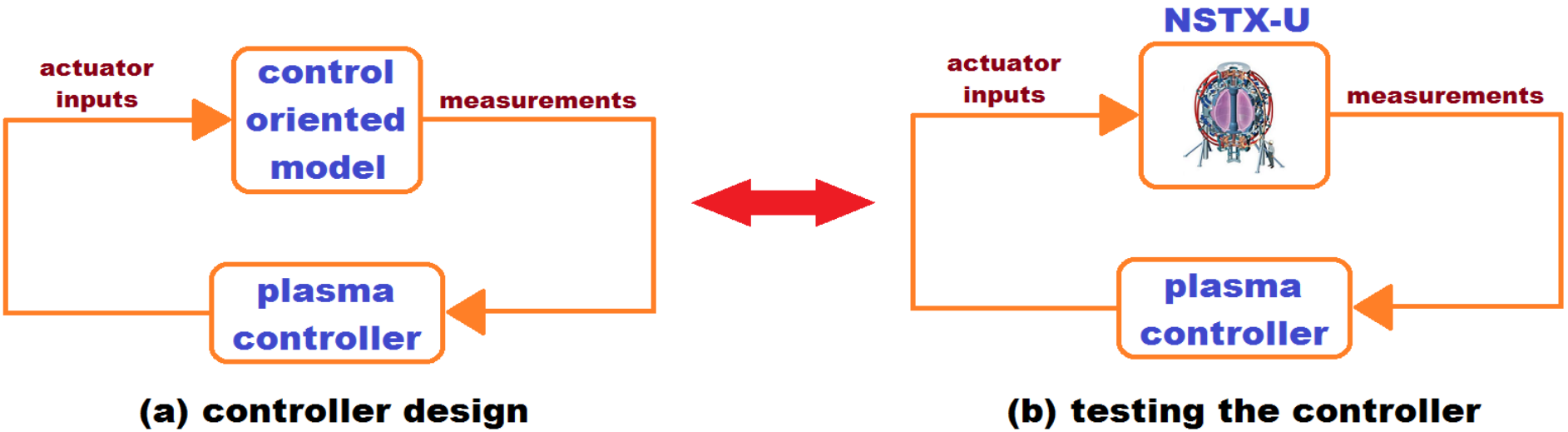

(a) controller design **(b) testing the controller**

- ***We will be modeling for control and not for physical understanding!***
- **The control-oriented model** will need only to **capture the dominant effects** of the current profile evolution.
- **Feedback control** deals with various **model uncertainties**, **adds robustness** in rejecting external disturbances, and **ensures repeatability** of scenarios.

First-Principles-Driven (FPD) Current Profile Modeling

- We develop **control-oriented, physics-based models** for the
  - Electron density profile
  - Electron temperature profile $\rightarrow$ Plasma resistivity profile
  - Non-inductive current deposition
- Modeling of electron temperature admits different levels of approximation. Ad-hoc transport models can be parameterized and tuned to data from experiment or predictive simulations by higher-accuracy transport codes.
- **Empirical models** take a **"separation of variables"** form, i.e., spatial-temporal dependence of plasma parameters is separated.
- These control-oriented models are combined with the magnetic diffusion equation to obtain the desired first-principles-driven (FPD) model.
- Fixed 2D MHD equilibrium $\rightarrow$ Extension to variable equilibrium possible.
- Model includes **nonlinear coupling between different plasma profiles.** FPD modeling allows for **further integration** (e.g., rotation profile).
- FPD models are adaptable to **various tokamaks** and applicable to **various equilibrium configurations** and **operating regimes.**
- FPD modeling approach arbitrarily handles trade-off between simplicity of model and both its physics accuracy and range of validity.

First-principles-driven Current Profile Evolution Model

- In practice, the toroidal current density is usually specified indirectly by the rotational transform $\bar{\iota}$ (or the safety factor $q = \bar{\iota}^{-1}$), which is defined as:

$$q = 1/\bar{\iota} = -d\Phi/d\Psi \tag{1}$$

- Using $\Phi = \pi B_{\phi,0}\rho^2$ and $\hat{\rho} = \rho/\rho_b$, the q profile is expressed as:

$$q(\hat{\rho},t) = -\frac{d\Phi}{d\Psi} = -\frac{d\Phi}{2\pi d\psi} = -\frac{\frac{\partial\Phi}{\partial\rho}\frac{\partial\rho}{\partial\hat{\rho}}}{2\pi\frac{\partial\psi}{\partial\hat{\rho}}} = -\frac{B_{\phi,0}\rho_b^2\hat{\rho}}{\partial\psi/\partial\hat{\rho}} \tag{2}$$

- The evolution of the poloidal magnetic flux is given by

$$\frac{\partial\psi}{\partial t} = \frac{\eta(T_e)}{\mu_0\rho_b^2\hat{F}^2}\frac{1}{\hat{\rho}}\frac{\partial}{\partial\hat{\rho}}\left(\hat{\rho}\hat{F}\hat{G}\hat{H}\frac{\partial\psi}{\partial\hat{\rho}}\right) + R_0\hat{H}\eta(T_e)\frac{<\bar{j}_{NI}\cdot\bar{B}>}{B_{\phi,0}}, \tag{3}$$

  where the parameters $\hat{F}$, $\hat{G}$ and $\hat{H}$ are geometric factors pertaining to the magnetic configuration of a particular plasma equilibrium.

- The geometric factors are defined as

$$\hat{F} = \frac{R_0 B_{\phi,0}}{RB_\phi(R,Z)} \qquad \hat{G} = \left\langle\frac{R_0^2}{R^2}|\nabla\rho|^2\right\rangle \qquad \hat{H} = \frac{\hat{F}}{\left\langle R_0^2/R^2\right\rangle}, \tag{4}$$

First-principles-driven Current Profile Evolution Model

$$\frac{\partial \psi}{\partial t} = \frac{\eta(T_e)}{\mu_0 \rho_b^2 \hat{F}^2} \frac{1}{\hat{\rho}} \frac{\partial}{\partial \hat{\rho}} \left(\hat{\rho} \hat{F} \hat{G} \hat{H} \frac{\partial \psi}{\partial \hat{\rho}} \right) + R_0 \hat{H} \eta(T_e) \frac{< \bar{j}_{NI} \cdot \bar{B} >}{B_{\phi,0}}, \tag{5}$$

- The boundary conditions are given by:

$$\left. \frac{\partial \psi}{\partial \hat{\rho}} \right|_{\hat{\rho}=0} = 0 \qquad \left. \frac{\partial \psi}{\partial \hat{\rho}} \right|_{\hat{\rho}=1} = -\frac{\mu_0}{2\pi} \frac{R_0}{\hat{G}\Big|_{\hat{\rho}=1} \hat{H}\Big|_{\hat{\rho}=1}} I(t), \tag{6}$$

  where $I(t)$ is the total plasma current.

- Magnetic diffusion equation (5) is closed by combining it with **control-oriented models** for electron density and temperature profiles, plasma resistivity and noninductive current drive. In this way, we can obtain the **first-principles-driven** model of $\psi(\hat{\rho}, t)$
  - **Models not designed for physical understanding, i.e., meant to capture dominant physics which affect input-output relationship of system.**
  - **Controller only needs to know about physics relevant to design objective.**

Control Actuators on NSTX-U

- First actuator is **total plasma current,** which is controlled by poloidal field (PF) coil system.
  - By controlling total current inside last closed magnetic flux surface, internal current profile can be modified through resistive diffusion.
- Second actuator is **neutral beam injection (NBI).**
  - NSTX-U is designed to have a second neutral beamline with three new beam sources of more tangential injection.
  - Together with the original beamline, the NSTX-U has a total of 6 NBI beamlet launchers.
  - Beamlet launchers can be configured to inject particles on or off axis.
- Final actuator is **plasma electron density,** which is controlled by gas-feed and pellet launchers.
  - However, tight control of electron density in experiments is challenging due to large recycling at walls.
  - Electron density considered an uncontrolled but measurable input.

Electron Density Model

- Assume tight coupling between electron and ion species in plasma, i.e., $T_e(\hat{\rho},t) \approx T_i(\hat{\rho},t)$ and $n_e(\hat{\rho},t) \approx n_i(\hat{\rho},t)$.
- Assume control action employed to regulate electron density weakly affects radial distribution of the electrons.
- Electron density $n_e(\hat{\rho},t)$ is then modeled as:

$$n_e(\hat{\rho},t) = n_e^{prof}(\hat{\rho})u_n(t) \tag{7}$$

  - $n_e^{prof}(\hat{\rho})$ is a reference electron density profile evaluated at the reference time t_r, i.e.,

$$n_e^{prof}(\hat{\rho}) = n_e(\hat{\rho},t_r) \tag{8}$$

  - $u_n(t)$ regulates time evolution of electron density.

Electron Temperature Model: Heat Transport PDE

- Assuming heat diffusion is dominant transport mechanism, electron heat diffusion equation expressed as:

$$\frac{3}{2}\frac{\partial}{\partial t}\left[n_e T_e\right] = \frac{1}{\rho_b^2 \hat{H}}\frac{1}{\hat{\rho}}\frac{\partial}{\partial \hat{\rho}}\left[\hat{\rho}\frac{\hat{G}\hat{H}^2}{\hat{F}}\left(\chi_e n_e \frac{\partial T_e}{\partial \hat{\rho}}\right)\right] + Q_e, \tag{9}$$

$$\left.\frac{\partial T_e}{\partial \hat{\rho}}\right|_{\hat{\rho}=0} = 0 \qquad T_e(1,t) = T_{e,bdry}(t). \tag{10}$$

- Thermal conductivity χ_e unknown, $\chi_e = f(T_e, n_e, q, s) = k_{\chi_e} T_e^{\gamma} n_e^{\nu} q^{\mu} s^{\pi}$,

$$\theta = \begin{bmatrix}\gamma & \nu & \mu & \pi\end{bmatrix}. \tag{11}$$

  - Nonlinear optimization to determine constants:

$$\min_{\theta} J, \quad J = \int_{t_0}^{t_f}\left\{\sum_{i=1}^{N}\alpha\left[q^{tar}(\hat{\rho}_i,t) - q_(\hat{\rho}_i,t)\right]^2 + \beta\left[T_e^{tar}(\hat{\rho}_i,t) - T_e(\hat{\rho}_i,t)\right]^2\right\}dt$$

Electron Temperature Model: Timescale Separation

- Slowly evolving electron temperature profile evolution modeled as:

$$T_e(\hat{\rho},t) = \begin{cases} k_{T_e}(\hat{\rho},t_r)\left[T_e^{prof}(\hat{\rho},t_r) - T_e^{prof}(\hat{\rho}_{tb},t_r)\right] \\ \times I(t)^{\alpha} P_{tot}(t)^{\gamma} n_e(\hat{\rho},t)^{\lambda} + T_e^{prof}(\hat{\rho}_{tb},t_r), & 0 \le \hat{\rho} \le \hat{\rho}_{tb} \\ T_e^{prof}(\hat{\rho},t_r), & \hat{\rho}_{tb} < \hat{\rho} \le 1 \end{cases} \tag{12}$$

  - k_{T_e} is a constant, $T_e^{prof}(\hat{\rho},t_r)$ is reference electron temperature profile, $\hat{\rho}_{tb}$ is spatial location of transport barrier in plasma and α, γ and λ are constants.

- Constants chosen as $\alpha = 1$, $\gamma = 0.5$ and $\lambda = -1$, i.e.,

$$T_e(\hat{\rho},t) = \begin{cases} k_{T_e}(\hat{\rho},t_r)\left[\dfrac{T_e^{prof}(\hat{\rho},t_r) - T_e^{prof}(\hat{\rho}_{tb},t_r)}{n_e^{prof}(\hat{\rho},t_r)}\right] \\ \times \dfrac{I(t)\sqrt{P_{tot}(t)}}{u_n(t)} + T_e^{prof}(\hat{\rho}_{tb},t_r), & 0 \le \hat{\rho} \le \hat{\rho}_{tb} \\ T_e^{prof}(\hat{\rho},t_r), & \hat{\rho}_{tb} < \hat{\rho} \le 1 \end{cases} \tag{13}$$

Total Injected Power Model

- **Total power** $P_{tot}(t)$ expressed as:

$$P_{tot}(t) = P_{ohm}(t) + P_{aux}(t) - P_{rad}(t) \tag{14}$$

- **Ohmic power** expressed as:

$$P_{ohm}(t) = \int_V j_{tor}^2(\hat{\rho}, t)\eta(\hat{\rho}, t)dV \approx \mathcal{R}(t)I(t)^2, \tag{15}$$

  - $j_{tor}(\hat{\rho}, t)$ is the total toroidal current density,
  - $\mathcal{R}$ is global plasma resistance, which is expressed as:

$$\mathcal{R}(t) \approx 2\pi R_0 \Big/ \int_{\hat{\rho}} \left[\frac{1}{\eta(\hat{\rho}, t)} \frac{dS}{d\hat{\rho}} d\hat{\rho}\right],$$

    where S denotes a magnetic surface within the plasma.

Auxiliary, Radiative Power and Plasma Resistivity

- **Auxiliary power** expressed as:

$$P_{aux}(t) = P_{nbitot}(k) = \sum_{k=1}^{6} P_{nbik}(t) \tag{16}$$

- **Radiative power** modeled as:

$$P_{rad}(t) = \int_{\hat{\rho}} Q_{rad}(\hat{\rho}, t) \frac{dV}{d\hat{\rho}} d\hat{\rho}, \tag{17}$$

where the radiative power density Q_{rad} is modeled as

$$Q_{rad}(\hat{\rho}, t) = k_{brem} Z_{eff} n_e(\hat{\rho}, t)^2 \sqrt{T_e(\hat{\rho}, t)}, \tag{18}$$

with Z_{eff} being the effective average charge of the ions in the plasma.

- **Plasma resistivity** $\eta(T_e)$ scales with electron temperature as:

$$\eta(\hat{\rho}, t) = \frac{k_{sp}(\hat{\rho}, t_r) Z_{eff}}{T_e(\hat{\rho}, t)^{3/2}}, \tag{19}$$

where k_{sp} is a constant.

Auxiliary Noninductive Current Drive Modeling

- **Total noninductive current drive** in NSTX-U is produced by **neutral beam injection** and **bootstrap current:**

$$\frac{\langle \bar{j}_{NI} \cdot \bar{B} \rangle}{B_{\phi,0}} = \frac{\langle \bar{j}_{nbi} \cdot \bar{B} \rangle}{B_{\phi,0}} + \frac{\langle \bar{j}_{bs} \cdot \bar{B} \rangle}{B_{\phi,0}} \tag{20}$$

- Neutral beam current drive modeled as:

$$\frac{\langle \bar{j}_{nbi} \cdot \bar{B} \rangle}{B_{\phi,0}}(\hat{\rho}, t) = k_{nbi}(\hat{\rho}, t_r) j_{nbi}^{dep}(\hat{\rho}, t_r) \frac{T_e(\hat{\rho}, t)}{n_e(\hat{\rho}, t)} P_{nbi}(t) \tag{21}$$

  - k_{nbi} is a constant and $j_{nbi}^{dep}(\hat{\rho}, t_r)$ is reference deposition profile.

- Bootstrap current drive expressed as ($T_e \approx T_i$)) [1], [2]:

$$\frac{\langle \bar{j}_{bs} \cdot \bar{B} \rangle}{B_{\phi,0}}(\hat{\rho}, t) = \frac{k_{JeV} R_0}{\hat{F}(\hat{\rho})} \left(\frac{\partial \psi}{\partial \hat{\rho}} \right)^{-1} \left[2\mathcal{L}_{31} T_e \frac{\partial n_e}{\partial \hat{\rho}} + \{2\mathcal{L}_{31} + \mathcal{L}_{32} + \alpha \mathcal{L}_{34}\} n_e \frac{\partial T_e}{\partial \hat{\rho}} \right] \tag{22}$$

  - $\mathcal{L}_{31}(\hat{\rho})$, $\mathcal{L}_{32}(\hat{\rho})$, $\mathcal{L}_{34}(\hat{\rho})$, $\alpha(\hat{\rho})$ are function of trapped fraction and collisionality.

[1] SAUTER, O. et al., Physics of Plasmas (1999).
[2] SAUTER, O. et al., Physics of Plasmas (2002).

Plasma Stored Energy Modeling

- Under the assumption of the **tight coupling** between the **electron** and **ion** species in the plasma, the stored energy in plasma is expressed as:

$$W = k_{JeV}\left[\int_{\hat{\rho}}\left(\frac{3}{2}n_e(\hat{\rho},t)T_e(\hat{\rho},t)+\frac{3}{2}n_i(\hat{\rho},t)T_i(\hat{\rho},t)\right)\frac{dV}{d\hat{\rho}}d\hat{\rho}\right] \tag{23}$$

  which is a **static mapping** of the plasma stored energy.

- **For control design** purposes, we employ a **dynamic mapping** of the stored energy based on a **zero-dimensional, approximate energy balance** equation:

$$\frac{d\bar{W}}{dt} = -P_{loss} + \underbrace{P_{ohm}+P_{aux}-P_{rad}}_{P_{tot}} = -\frac{\bar{W}}{\tau_{\bar{W}}} + P_{tot}, \tag{24}$$

  where energy confinement scaling $\tau_{\bar{W}}$ is given by IPB98(y,2)

$$\tau_{\bar{W}} = 0.0562 H_H I_p^{0.93} R_0^{1.39} a^{0.58} n_{e19}^{0.41} B_{\phi,0}^{0.15} A_{eff}^{0.19} \kappa^{0.78} P_{tot}^{-0.69} \tag{25}$$

  where a is the plasma minor radius, n_{e19} is the volume average electron density in $10^{19}\mathrm{m}^{-3}$, A_{eff} is the effective ion mass number and κ is the plasma elongation, which is assumed constant.

Magnetic Configuration Parameters and Electron Density and Temperature Reference Profiles

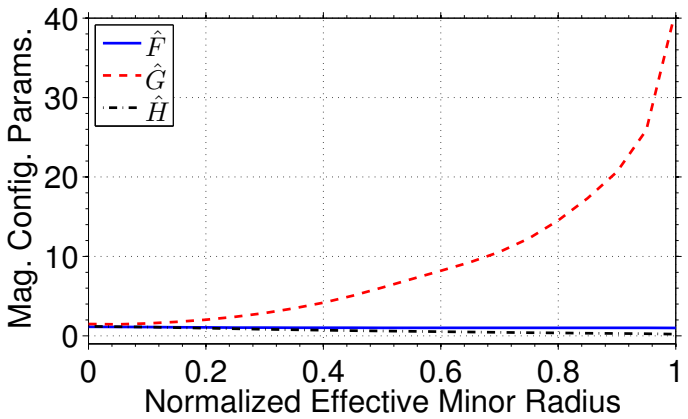

(1) $\hat{F}(\hat{\rho})$, $\hat{G}(\hat{\rho})$, $\hat{H}(\hat{\rho})$

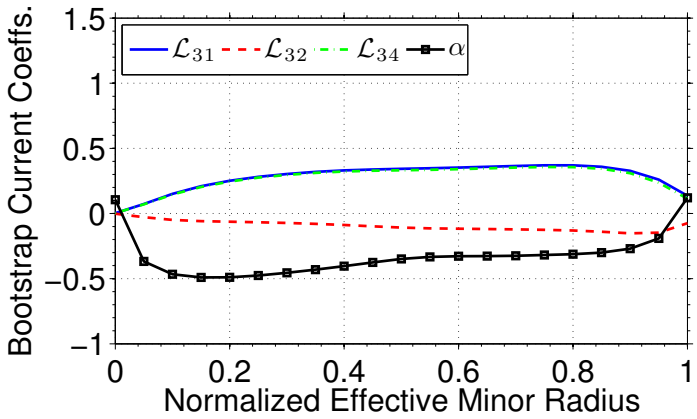

(2) $\mathcal{L}_{31}(\hat{\rho})$, $\mathcal{L}_{32}(\hat{\rho})$, $\mathcal{L}_{34}(\hat{\rho})$, $\alpha(\hat{\rho})$

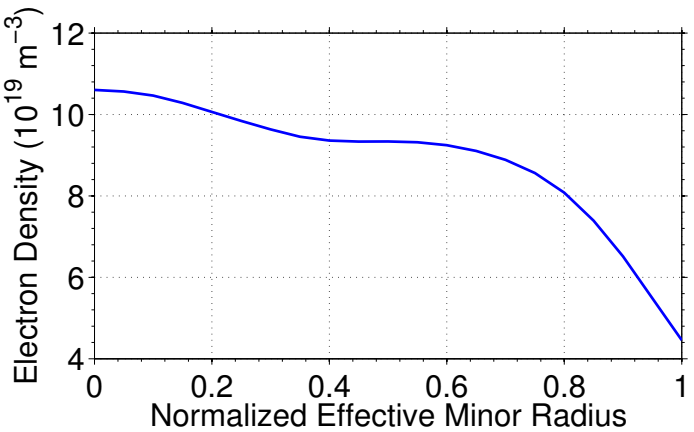

(3) $n_e^{prof}(\hat{\rho})$

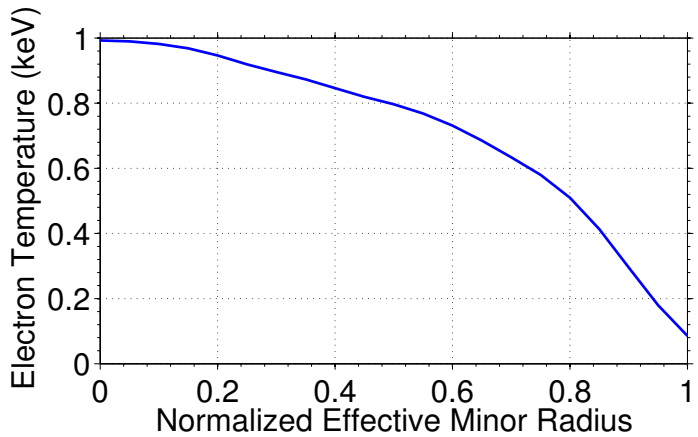

(4) $T_e^{prof}(\hat{\rho})$

Fig. 1: Reference (1) magnetic configuration parameters, (2) bootstrap current coefficients, (3) electron density profile and (4) electron temperature profile.

Model Coefficients and Actuators

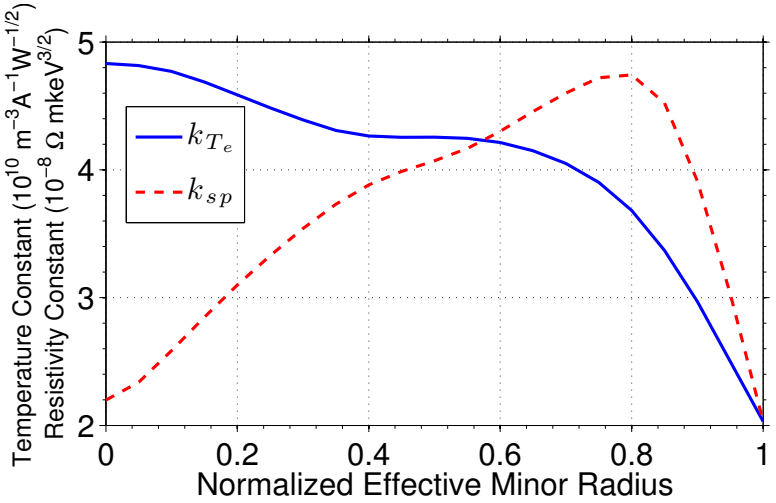

(1) k_{T_e}, k_{sp}

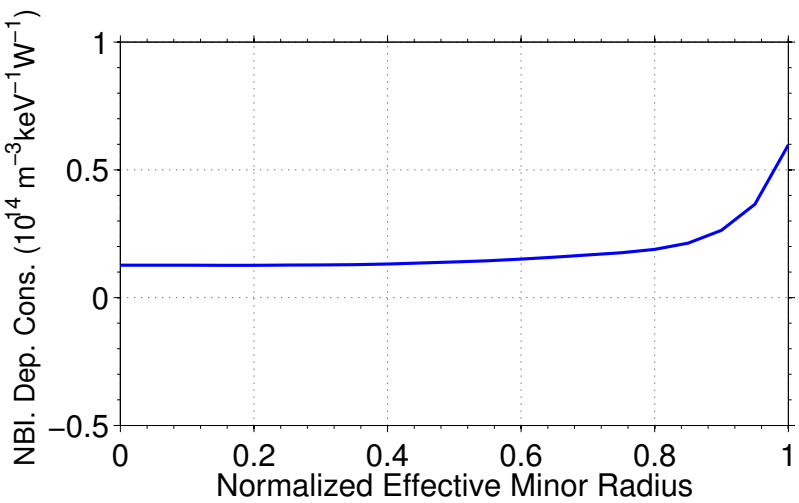

(2) k_{nbi}

Fig. 2: (1) Electron temperature, plasma resistivity, (2) neutral beam model coefficients.

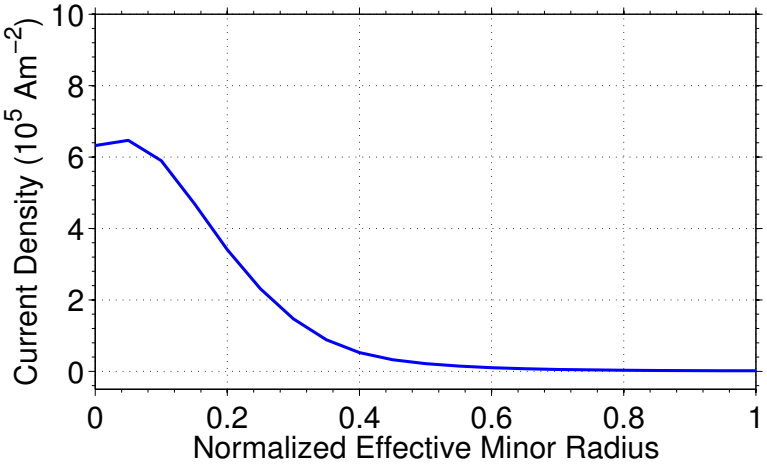

(1) $j_{nbi}^{dep}(\hat{\rho})$

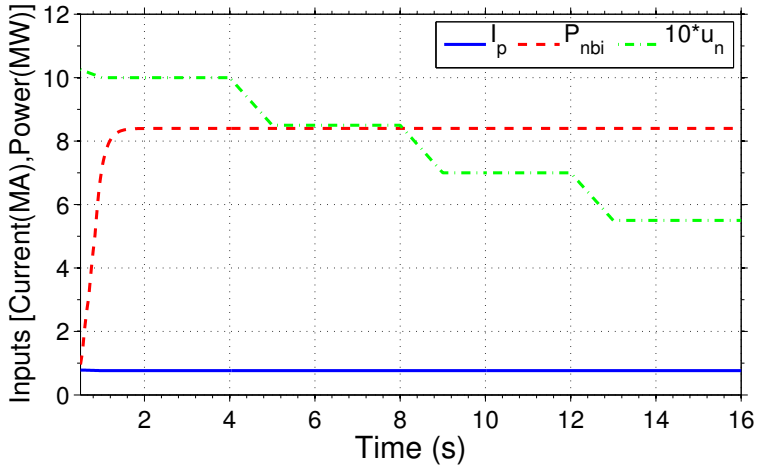

(2) Control Inputs

Fig. 3: (2) Reference NB current deposition profile. (1) Control inputs applied during simulation.

Electron Density and Temperature Profile Comparison

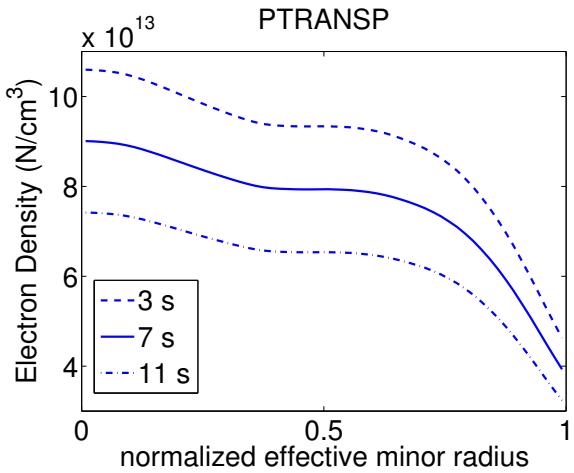

(1) $n_e(\hat{\rho})$

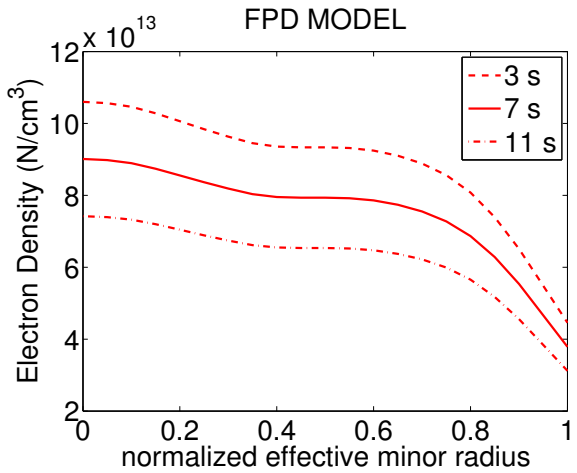

(2) $n_e(\hat{\rho})$

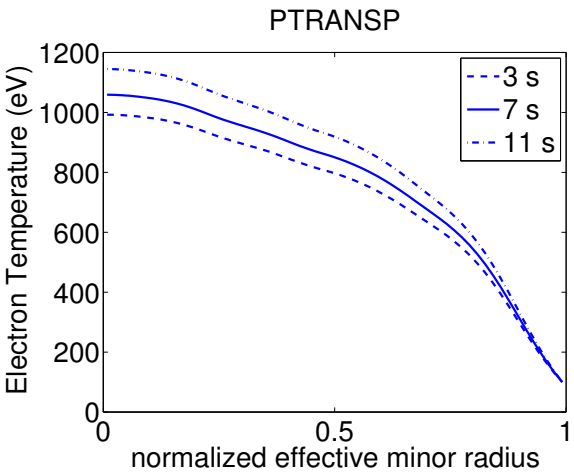

(3) $T_e(\hat{\rho})$

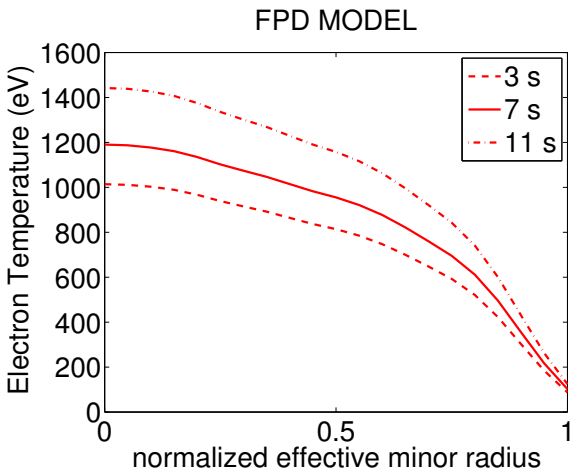

(4) $T_e(\hat{\rho})$

Fig. 4: Plasma profile evolutions comparison: PTRANSP [(1),(3)], control-oriented model [(1),(4)].

Noninductive Current Deposition Profile Comparison

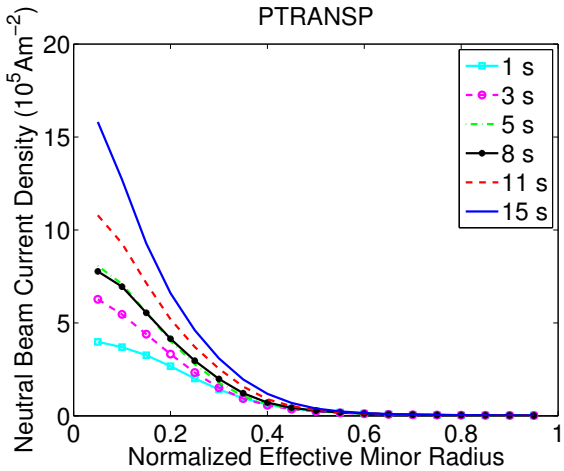

(1) Total Neutral Beam

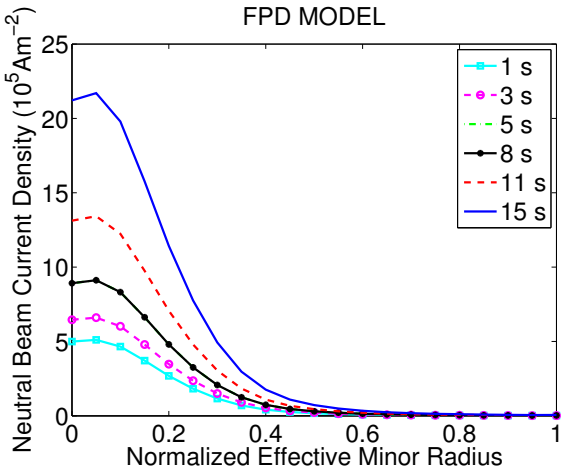

(2) Total Neutral Beam

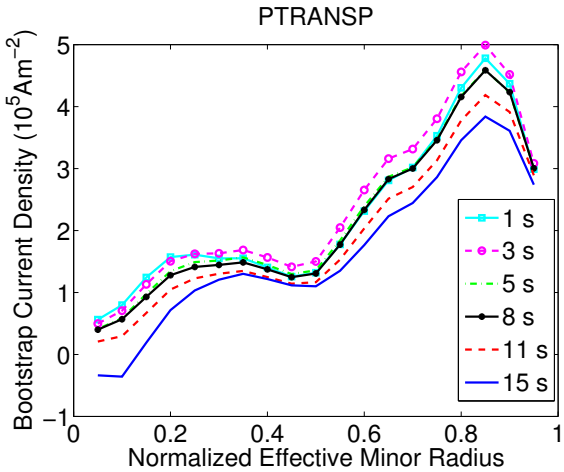

(3) Bootstrap

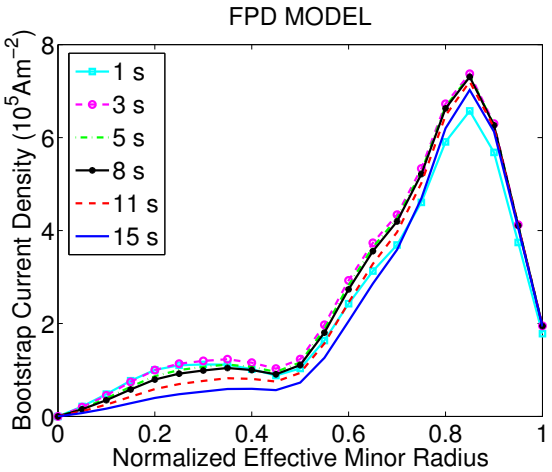

(4) Bootstrap

Fig. 5: Noninductive current deposition profile evolution comparison: PTRANSP [(1),(3)], control-oriented model [(2),(3)].

Net Power and Current Drive Fraction

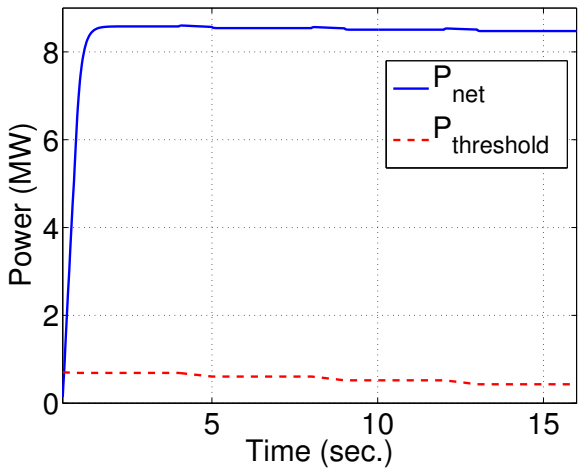

(1) Confinement Regime

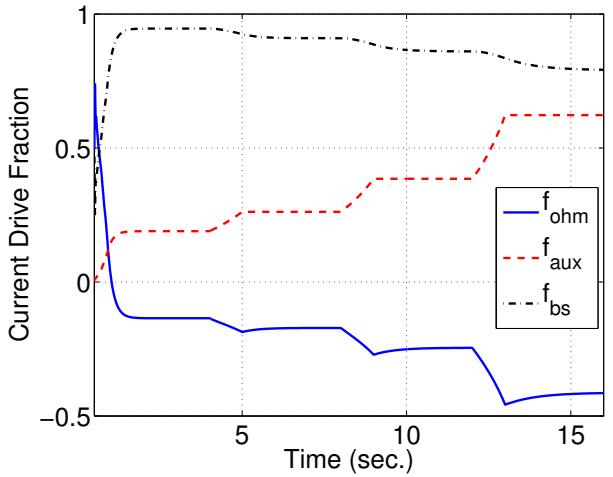

(2) Current Drive Fraction

Fig. 6: (2) Net power across separatrix and L-H threshold power and (3) Current drive fraction.

- Threshold power to enter H-mode is given by [1], [2]:

$$P_{thresh} = \frac{2}{A_{eff}} \left[2.15 e^{\pm 0.107} n_{e20}^{0.782 \pm 0.037} B_{\phi,0}^{0.772 \pm 0.031} a^{0.975 \pm 0.08} R_0^{0.999 \pm 0.101} \right] \quad (26)$$

- If net power through plasma surface $>$ threshold power, plasma will enter H-mode, where

$$P_{net}(t) = P_{tot}(t) - \frac{dW}{dt} \approx \frac{\bar{W}}{\tau_{\bar{W}}} \quad (27)$$

[1] MARTIN, Y. et al., Journal of Physics (2008).
[2] RIGHI, E. et al., Nuclear Fusion (1999).

Poloidal Magnetic Flux Comparison - Time Traces

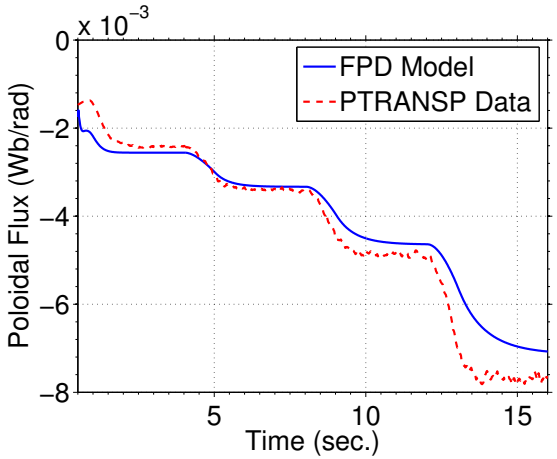

(1) $\hat{\rho} = 0.1$ sec.

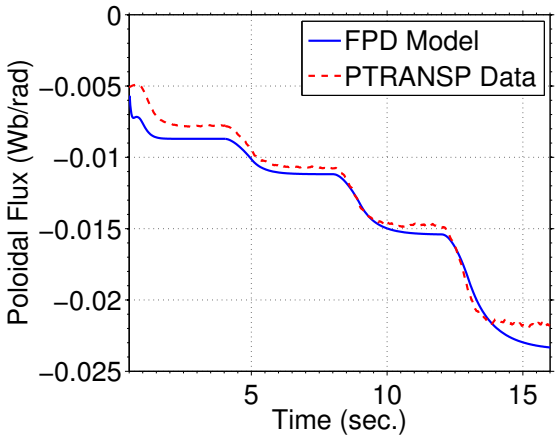

(2) $\hat{\rho} = 0.2$ sec.

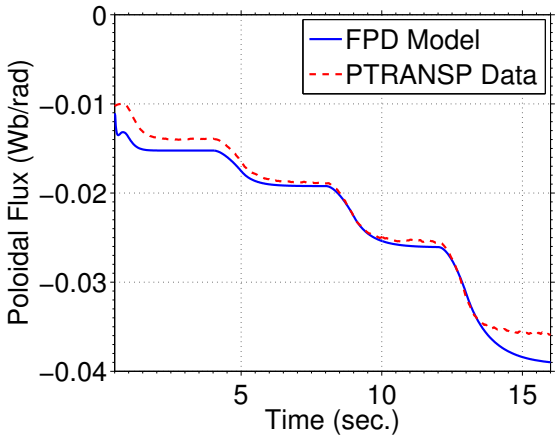

(3) $\hat{\rho} = 0.3$ sec.

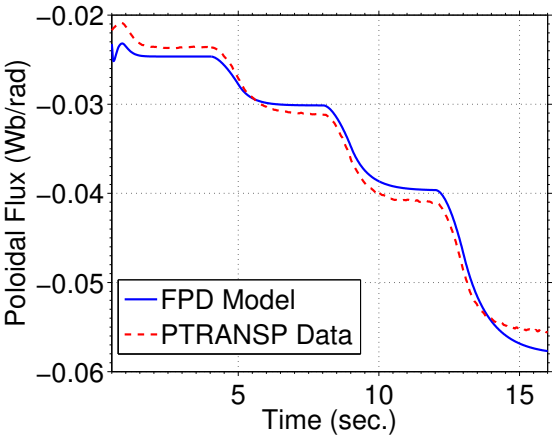

(4) $\hat{\rho} = 0.5$ sec.

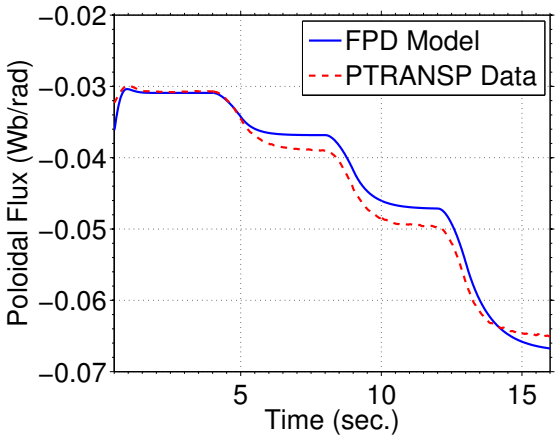

(5) $\hat{\rho} = 0.7$ sec.

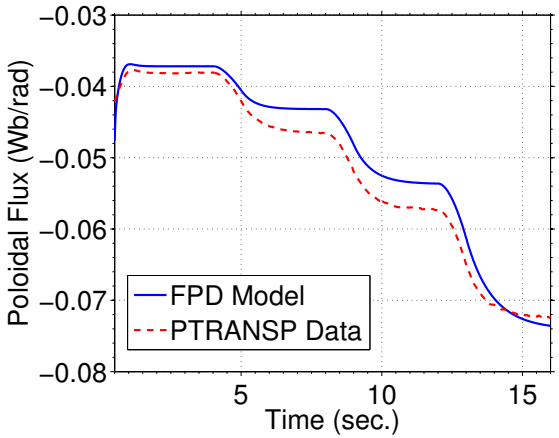

(6) $\hat{\rho} = 0.9$ sec.

Fig. 7: Poloidal magnetic flux evolution comparison.

Poloidal Magnetic Flux Profile Comparison

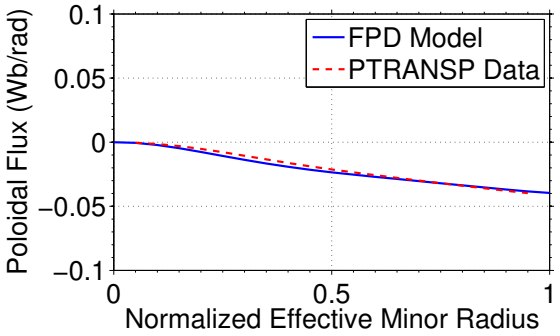

(1) $t = 1$ sec.

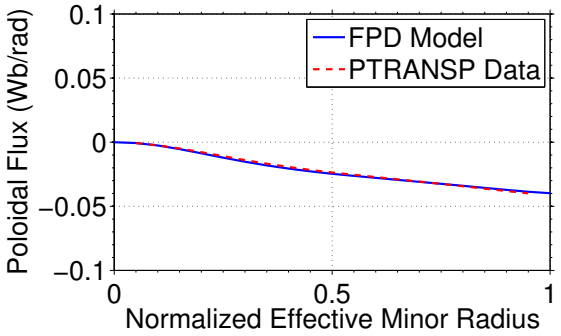

(2) $t = 3$ sec.

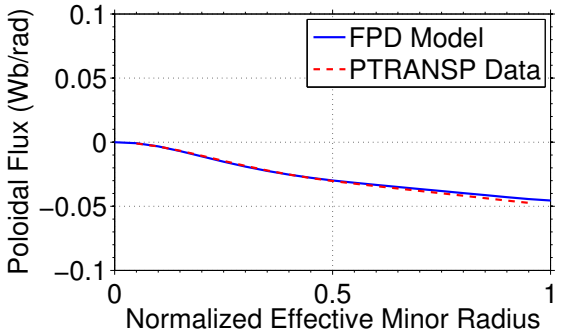

(3) $t = 6$ sec.

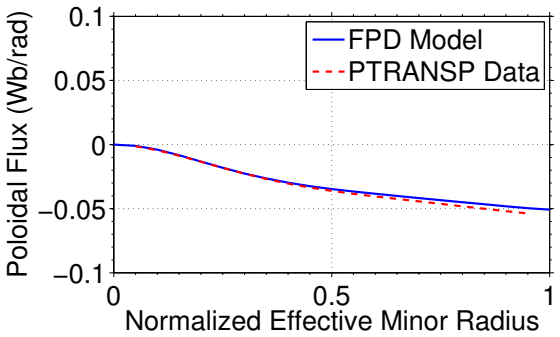

(4) $t = 9$ sec.

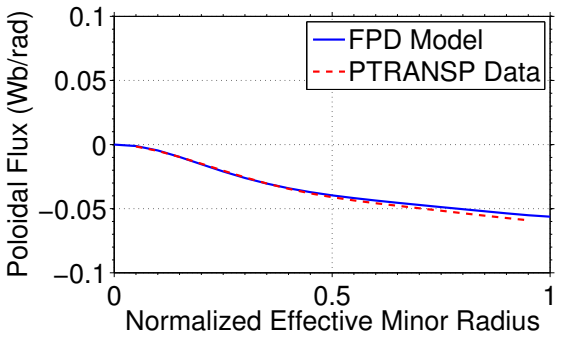

(5) $t = 12$ sec.

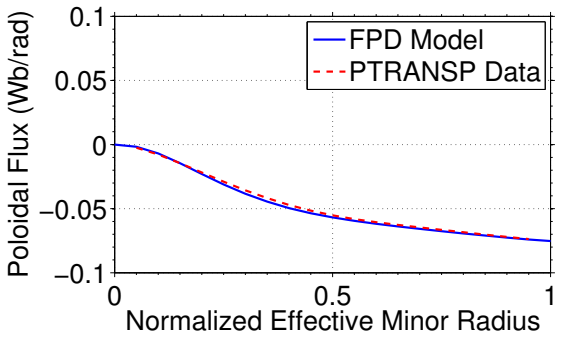

(6) $t = 15$ sec.

Fig. 8: Poloidal magnetic flux profile evolution comparison.

Safety Factor Comparison - Time Traces

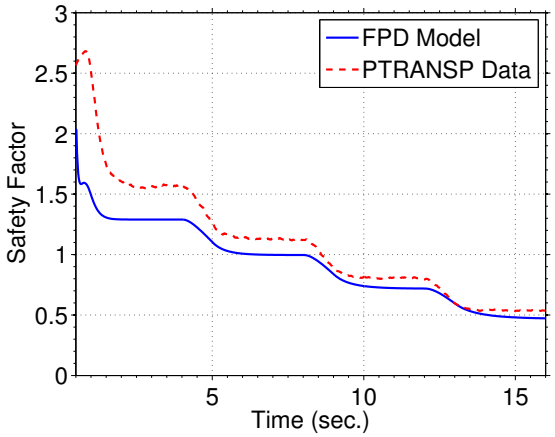

(1) $\hat{\rho} = 0.1$ sec.

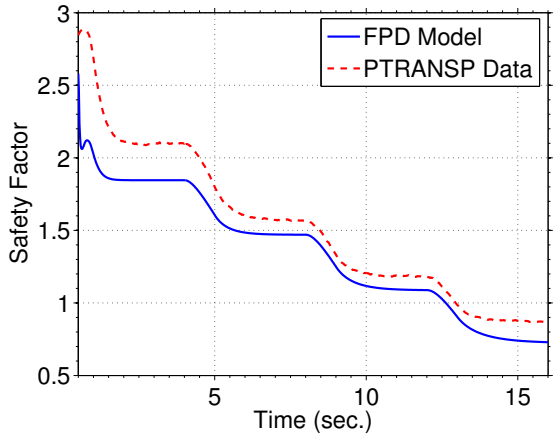

(2) $\hat{\rho} = 0.2$ sec.

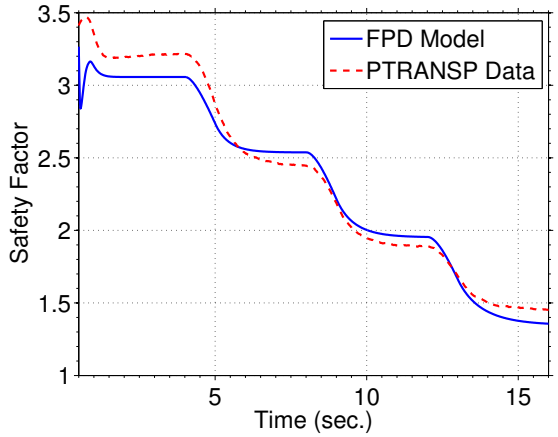

(3) $\hat{\rho} = 0.3$ sec.

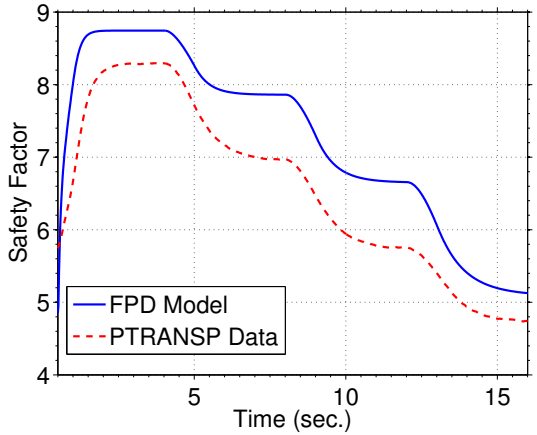

(4) $\hat{\rho} = 0.5$ sec.

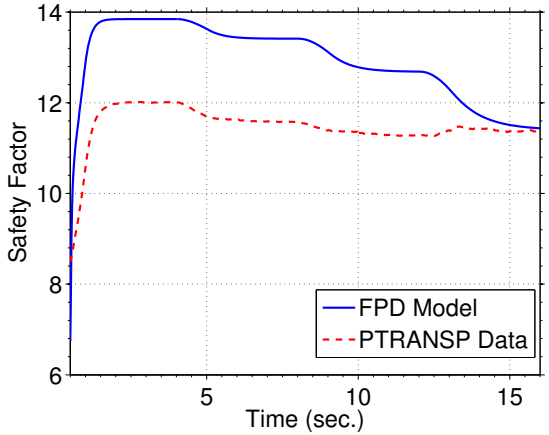

(5) $\hat{\rho} = 0.7$ sec.

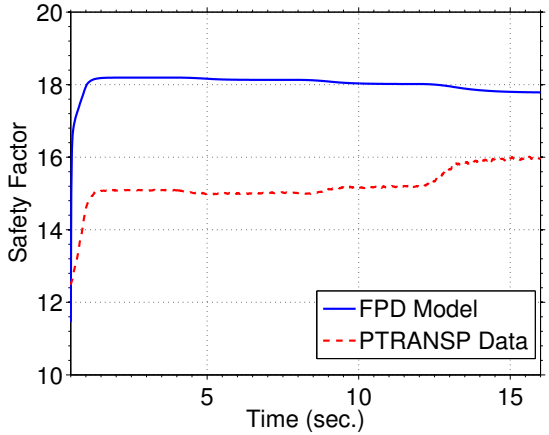

(6) $\hat{\rho} = 0.9$ sec.

Fig. 9: Safety factor evolution comparison.

Safety Factor Profile Comparison

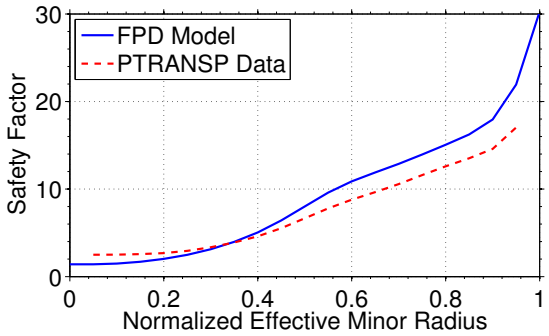

(1) $t = 1$ sec.

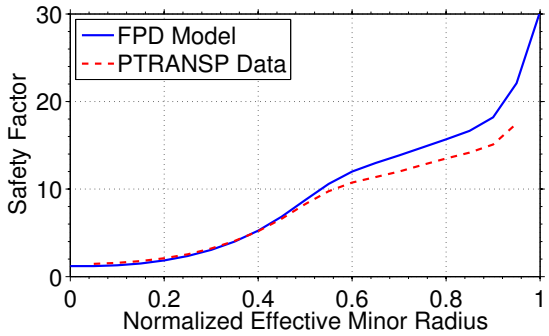

(2) $t = 3$ sec.

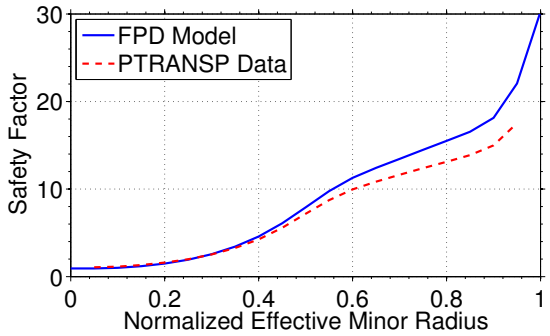

(3) $t = 6$ sec.

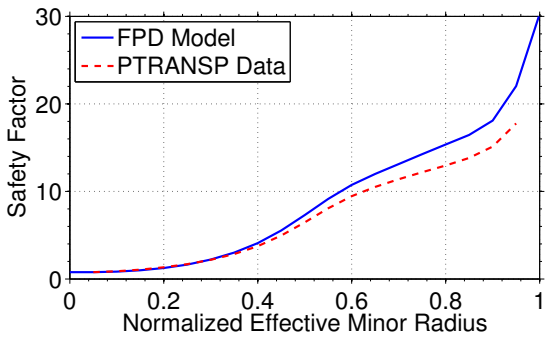

(4) $t = 9$ sec.

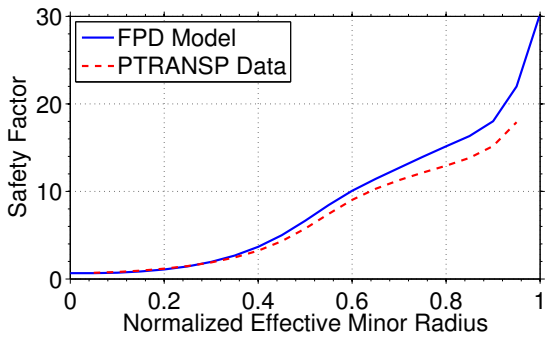

(5) $t = 12$ sec.

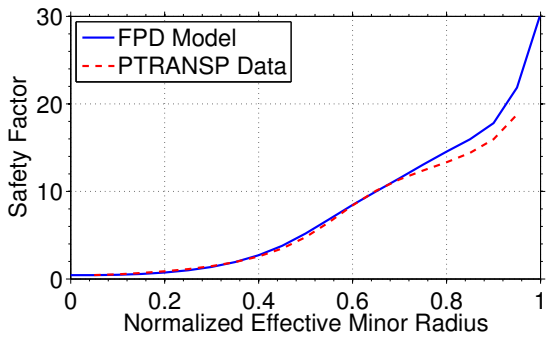

(6) $t = 15$ sec.

Fig. 10: Safety factor profile evolution comparison.

Status of Work

- The nonlinear magnetic-diffusion PDE coupled with empirical models for the electron density, electron temperature and non-inductive current drive (neutral beams) has been already implemented in a Matlab/Simulink using a numerical integration scheme.
- The numerical integration scheme was also coded in C language in order to run Simserver simulations during the implementation stage.
- A code has been developed to extract significant data from NSTX-U PTRANSP simulations and generate control-oriented model parameters.
- Bootstrap current model and q-profile prediction in the outer region still need work. More data is necessary for model tailoring and validation.
- Improved control-oriented model expected by the end of the summer.
  - Several issues need to be discussed.
- We are ready to start working on applications that make use of the FPD control-oriented model.
  - Several issues need to be discussed.

FPD Modeling: Topics to Discuss

- Reference shot numbers to tailor and validate the FPD model?
- Typical durations of discharges in NSTX-U?
  - Shot 142301M21: 16 sec.
  - Shot 121014P01: 1 sec.
  - Shot 130356A01: 0.7 sec.
- Should we use a different scaling for the current drives? Is data available?
- How good is the $T_e \approx T_i$ assumption in the interested scenarios?
- Should we use a different confinement scaling? $H_{98y,2}$ or ST?
- How many neutral beam injectors available for actuation? All of them? Can we group them as a function of their characteristics? Which beam will have off-axis capability? Are simulations available? Energy limit?
- Should we consider high-harmonic fast wave (HHFW) as actuator? Are simulations/data available? Any other heating source or current drive?
- How is density control achieved? Gas feeders or pellet launchers? Effectiveness?

Utilization of First-principles-driven, Physics-based Models in Plasma Profile Control Applications

1. **Feedforward control design:**
   - **Actuator trajectory optimization:** Achieve target plasma state evolution throughout discharge by specifying actuator trajectory waveforms, with goal of numerically supporting experimental effort of scenario development.
   - Study effects different auxiliary heating/current-drive schemes (e.g. deposition location) have on ability to achieve a certain plasma state.
2. **Feedback control design:**
   - Track target plasma state evolution and reject effects external disturbances have on plasma dynamics, with goal of running repeatable discharges.
3. **Plasma state observers:**
   - Simulate model in real-time/faster-than-real-time as discharge evolving to obtain current/future plasma state for feedback-control/disruption-mitigation.
     - Can be combined with real-time measurements of plasma state.
4. **Control algorithm implementation and testing:**
   - Execute simulations to determine correctness of algorithm implementation in Plasma Control System (PCS) as well as performance and robustness of control algorithms before experimental testing.

Plasma Profile and Parameter Control Components

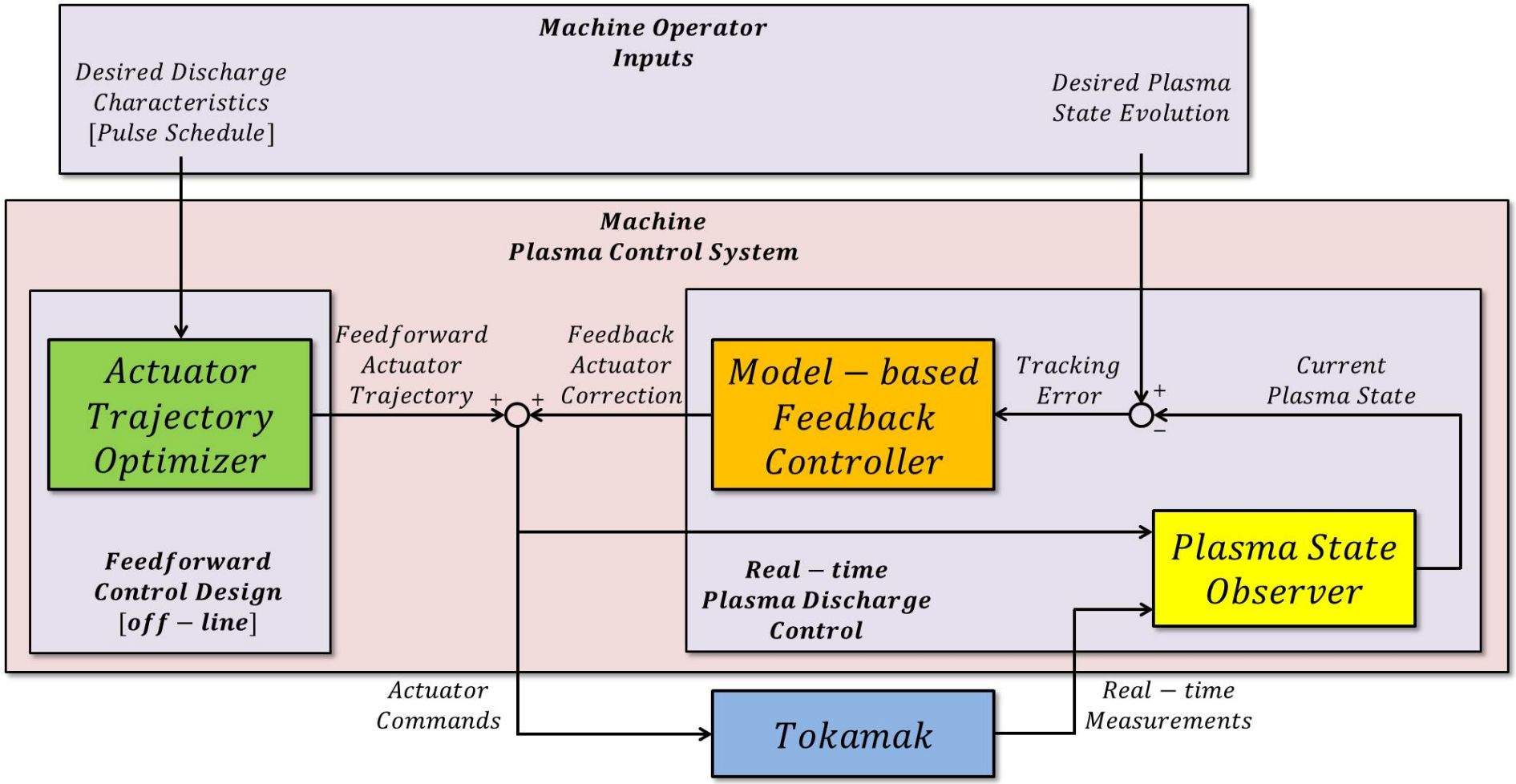

Fig.: Plasma profile and parameter control components.

Physics-based Model of Plasma Parameter Evolutions

- Evolution of plasma poloidal magnetic flux profile is given by:

$$\frac{\partial \psi}{\partial t} = \frac{\eta(T_e)}{\mu_0 \rho_b^2 \hat{F}^2} \frac{1}{\hat{\rho}} \frac{\partial}{\partial \hat{\rho}} \left(\hat{\rho} \hat{F} \hat{G} \hat{H} \frac{\partial \psi}{\partial \hat{\rho}} \right) + R_0 \hat{H} \eta(T_e) \frac{< \bar{j}_{ni} \cdot \bar{B} >}{B_{\phi,0}}$$

$$\left. \frac{\partial \psi}{\partial \hat{\rho}} \right|_{\hat{\rho}=0} = 0 \qquad \left. \frac{\partial \psi}{\partial \hat{\rho}} \right|_{\hat{\rho}=1} = -\frac{\mu_0}{2\pi} \frac{R_0}{\hat{G}\Big|_{\hat{\rho}=1} \hat{H}\Big|_{\hat{\rho}=1}} I_p(t)$$

- Volume-averaged energy balance in plasma is given by:

$$\frac{dE}{dt} = -\frac{E}{\tau_E} + P_{ohm}(t) + P_{aux}(t) - P_{rad}(t)$$

- **Physics-based, control-oriented models** for electron density and temperature profiles, plasma resistivity and noninductive current-drive sources (auxiliary and bootstrap) tailored to H-mode scenarios in DIII-D.
- Using $\Phi = \pi B_{\phi,0} \rho^2$ and $\hat{\rho} = \rho / \rho_b$, safety factor ($q$) profile expressed as:

$$q(\hat{\rho}, t) = -\frac{d\Phi}{d\Psi} = -\frac{d\Phi}{2\pi d\psi} = -\frac{B_{\phi,0} \rho_b^2 \hat{\rho}}{\partial \psi / \partial \hat{\rho}}$$

- Normalized plasma beta (β_N) expressed as:

$$\beta_N = \beta_t [\%] \frac{a B_{\phi,0}}{I_p} \qquad \beta_t = \frac{2 \langle n_e T_e \rangle_V}{B_{\phi,0}^2 / (2\mu_0)} \qquad E = 3 \langle n_e T_e \rangle_V V \qquad n_i = n_e \text{ and } T_i = T_e$$

Model Parameters Tailored to DIII-D H-mode Scenario

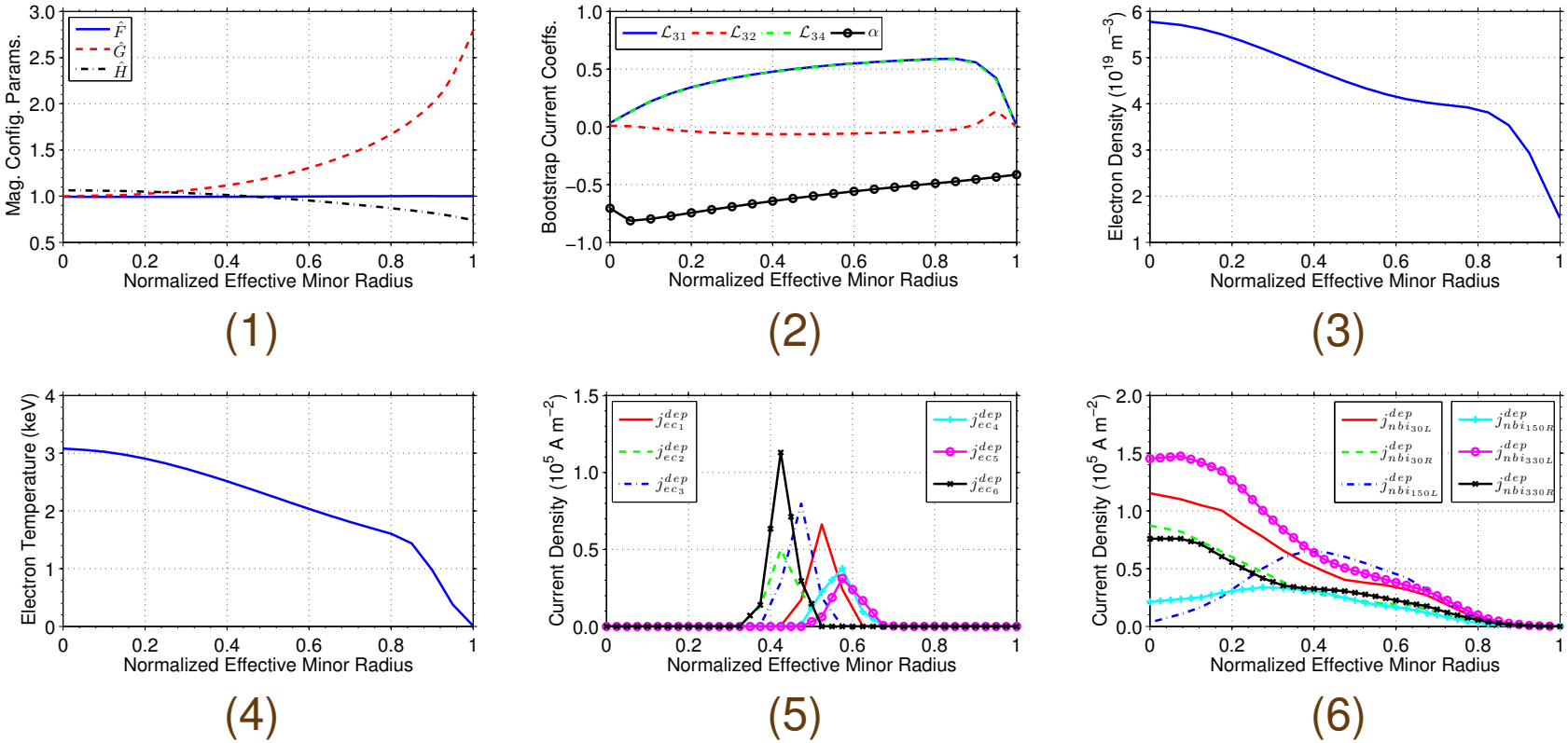

Fig.: Model parameters tailored to DIII-D H-mode scenario.

Model Prediction Comparison to Experimental Data I

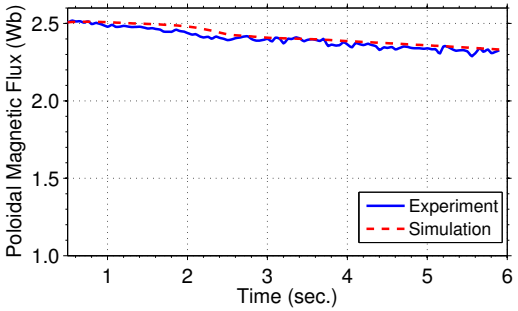

(1) $\hat{\rho} = 0.1$

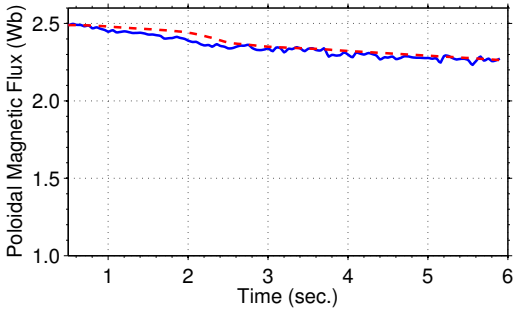

(2) $\hat{\rho} = 0.2$

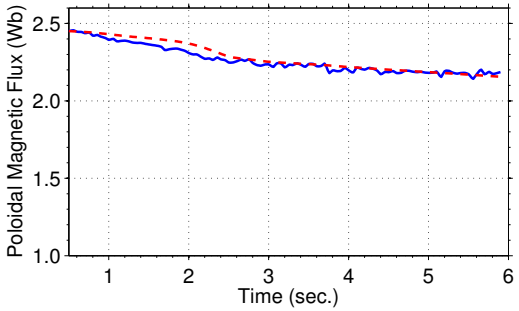

(3) $\hat{\rho} = 0.3$

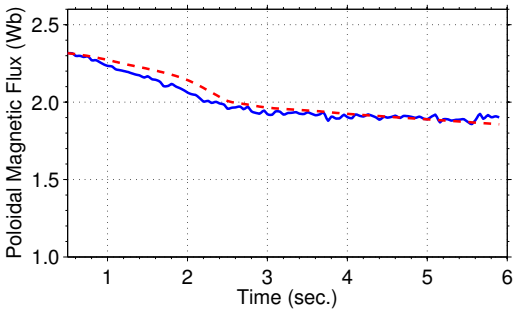

(4) $\hat{\rho} = 0.5$

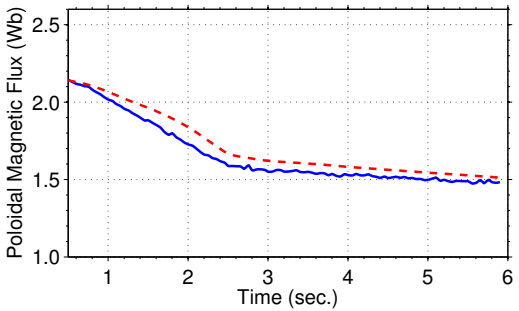

(5) $\hat{\rho} = 0.7$

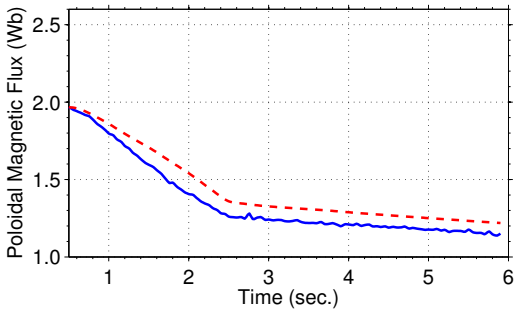

(6) $\hat{\rho} = 0.9$

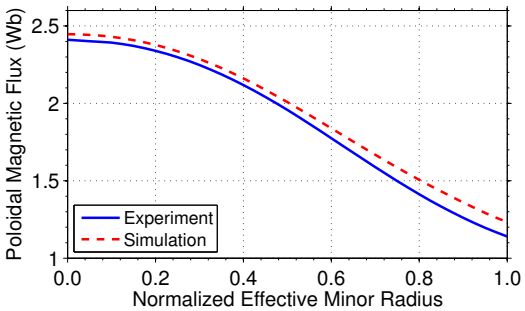

(7) $t = 2.5$ sec.

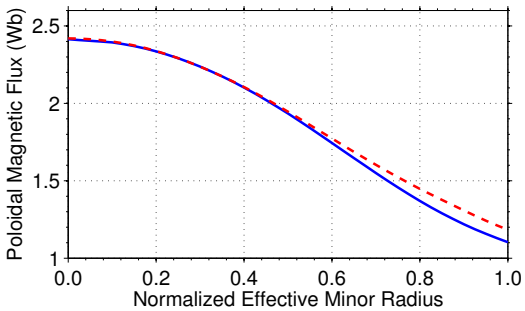

(8) $t = 3.5$ sec.

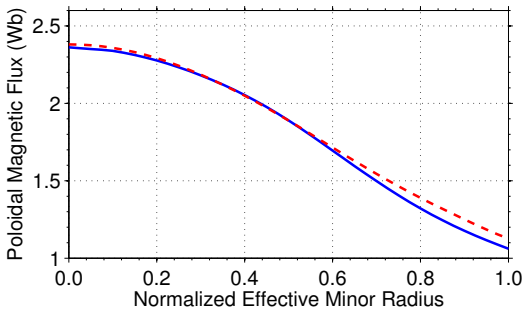

(9) $t = 5.0$ sec.

Fig.: Poloidal flux time traces and profiles. Note: experiment (solid) and simulated (dash).

Model Prediction Comparison to Experimental Data II

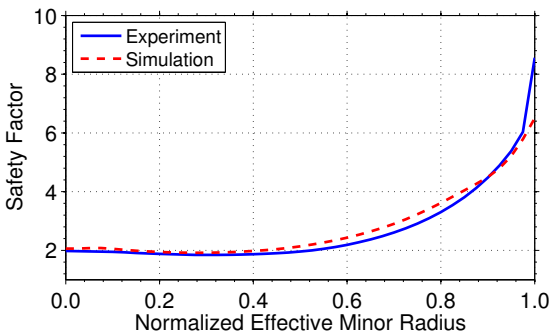

(1) $t = 2.5$ sec.

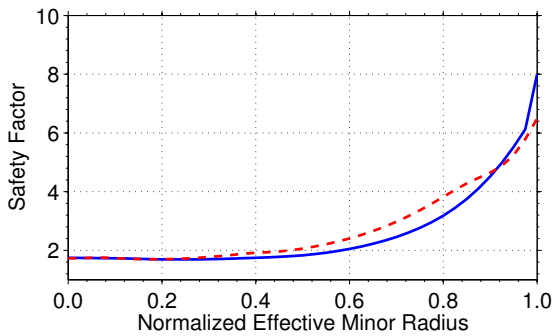

(2) $t = 3.5$ sec.

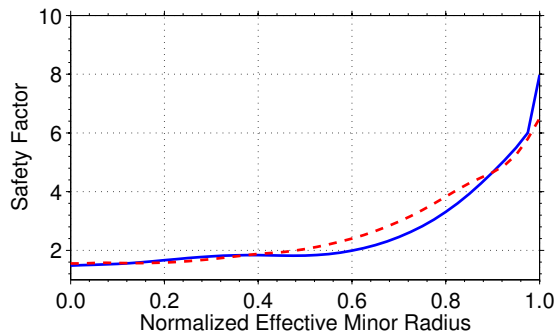

(3) $t = 5.0$ sec.

Fig.: Safety factor profile $q(\hat{\rho})$ at various time instances. Note: experiment (solid) and simulated (dash).

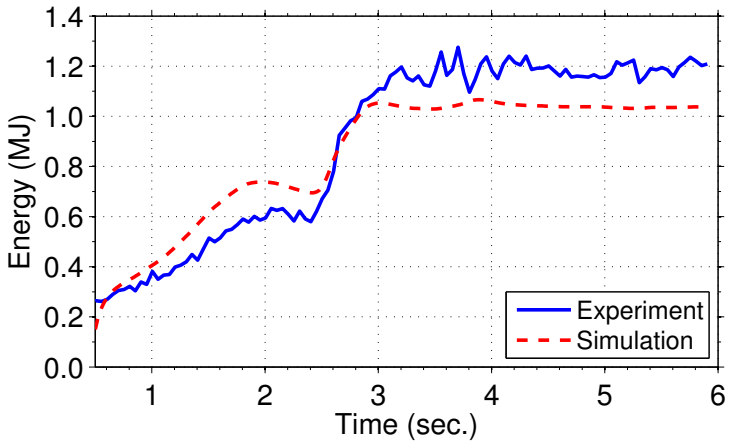

(1) $E(t)$

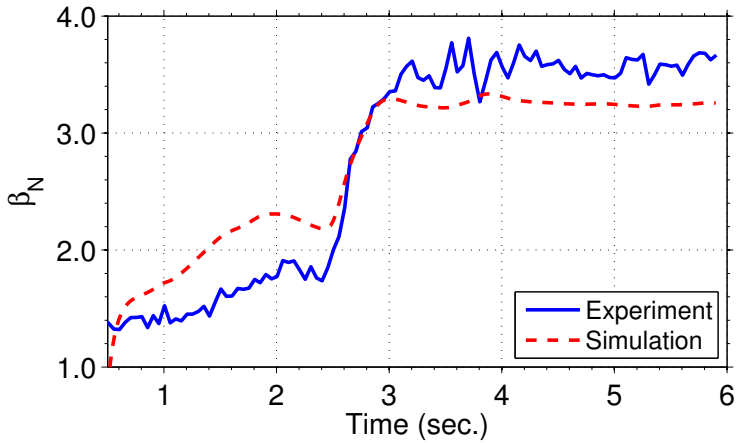

(2) $\beta_N(t)$

Fig.: Plasma stored energy and normalized plasma beta versus time. Note: experiment (solid) and simulated (dash).

1. Feedforward Control Design

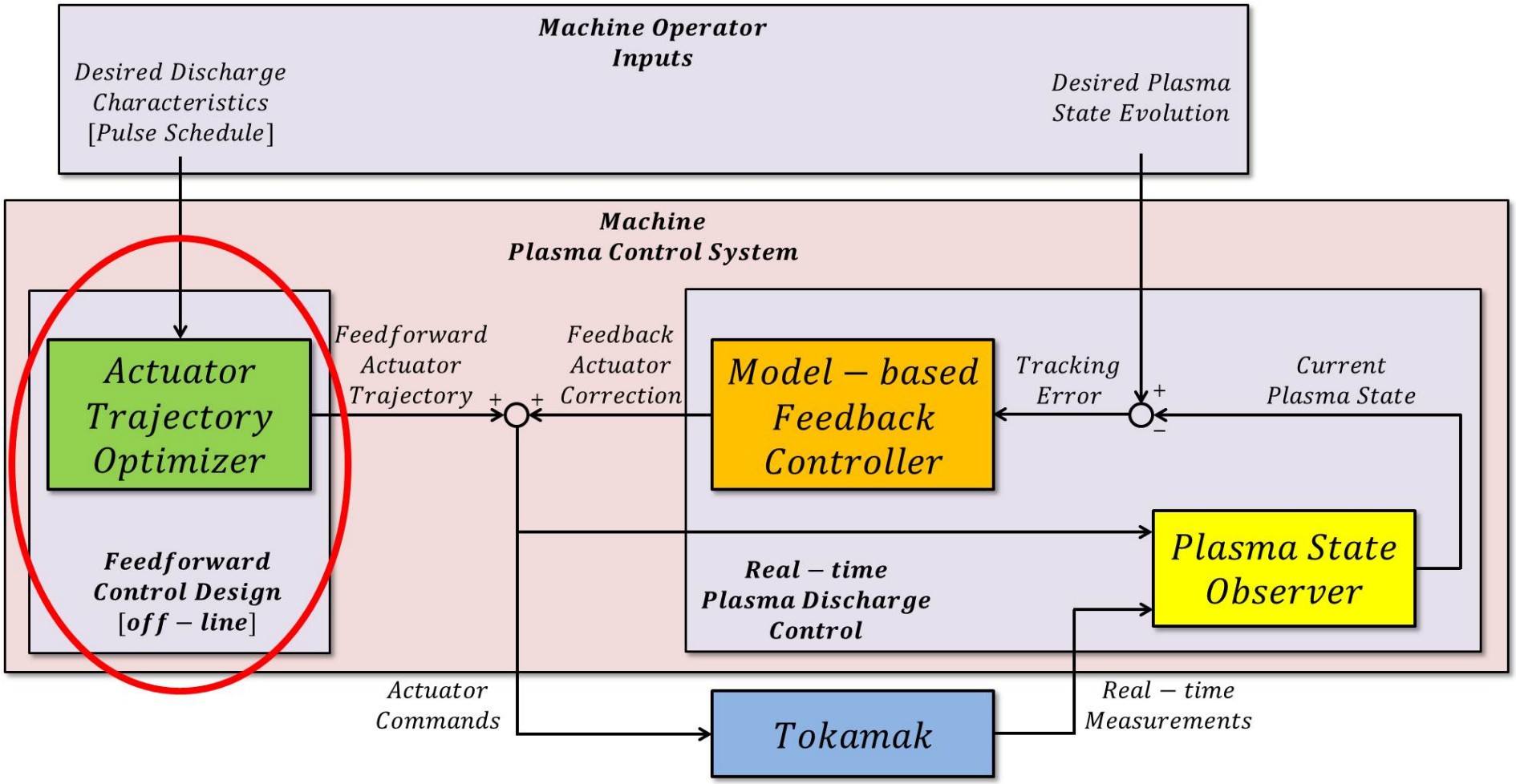

Fig.: Plasma profile and parameter control components.

1. Actuator Trajectory Optimization

- **Objective:** Reach desired target safety factor profile $q^{tar}(\hat{\rho}, t_f)$ and normalized beta $\beta_N^{tar}(t_f)$ at time t_f during flattop phase of discharge in such a way that desired plasma state is as stationary in time as possible by specifying **actuator trajectory waveforms**.
  - Cost functional defined as:

$$J(t_f) = J_{ss} + J_q + J_{\beta_N}$$

- **Constraints:** Limits on solution of optimization problem.
  - Actuator magnitude constraints: min/max plasma current, min/max gyrotron power, min/max neutral beam power.
  - Actuator rate constraints: min/max rate of change of plasma current.
  - Plasma state constraints: min safety factor value, max normalized beta.
  - Actuator-magnitude/state constraints: power across plasma surface $>$ L-H threshold power.

1. Optimized Actuator Trajectories

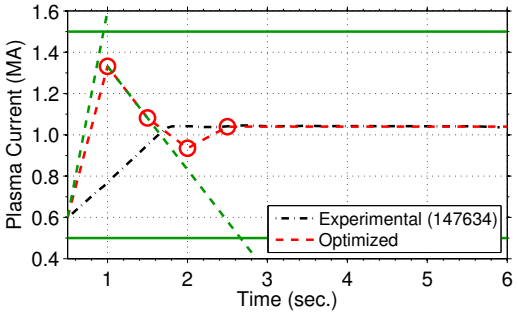

(1) $I_p(t)$

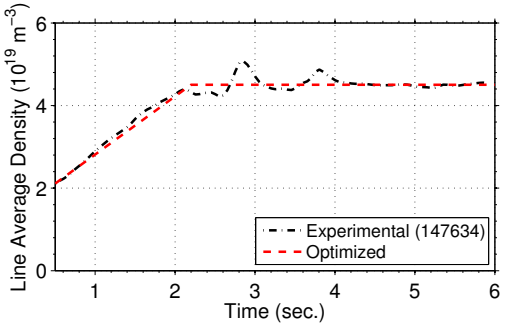

(2) $\bar{n}_e(t)$

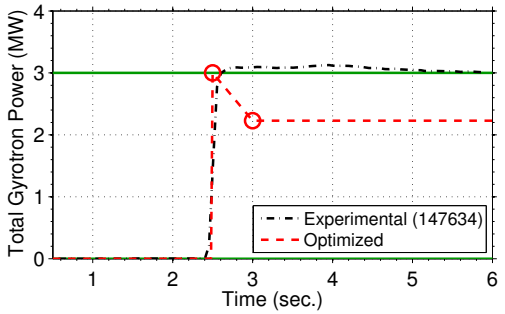

(3) $P_{ec_{tot}}(t)$

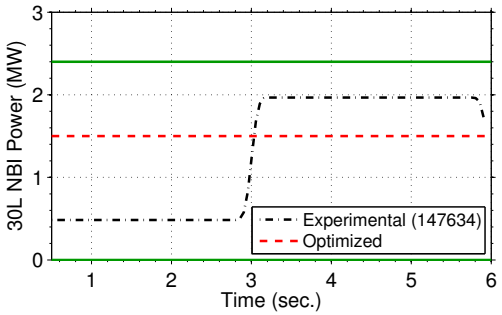

(4) $P_{nbi_{30L}}(t)$

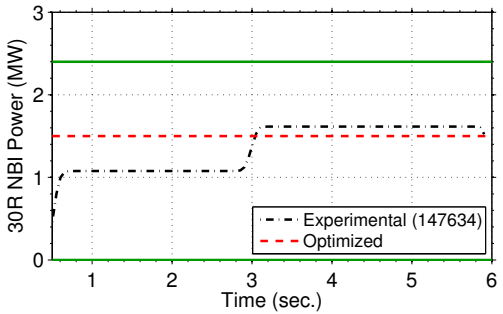

(5) $P_{nbi_{30R}}(t)$

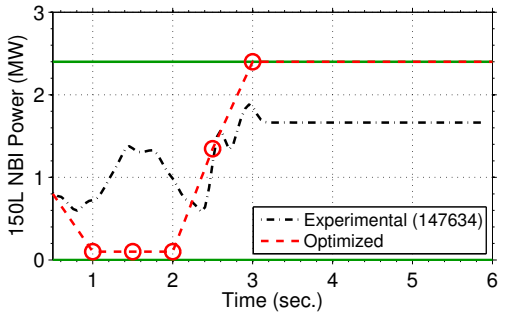

(6) $P_{nbi_{150L}}(t)$

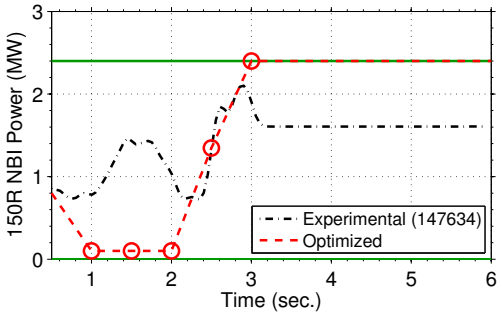

(7) $P_{nbi_{150R}}(t)$

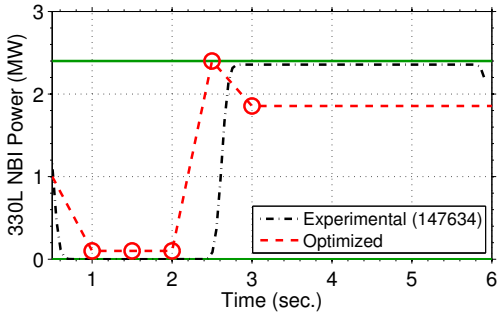

(8) $P_{nbi_{330L}}(t)$

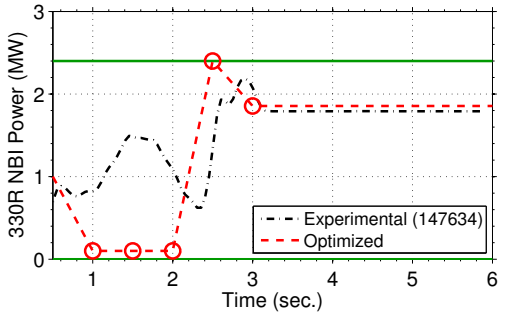

(9) $P_{nbi_{330R}}(t)$

Fig.: Comparison of actuator trajectories: optimized and utilized in DIII-D shot 147634.

1. Target State Achieved with Optimized Trajectories

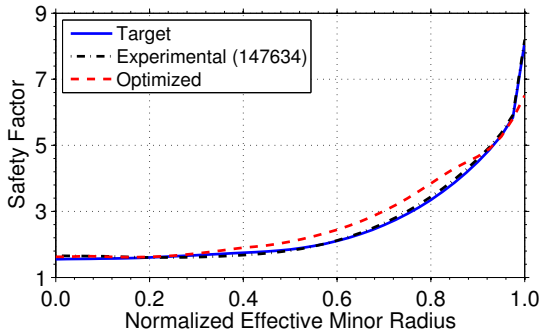

(1) $t = 3.0$ sec.

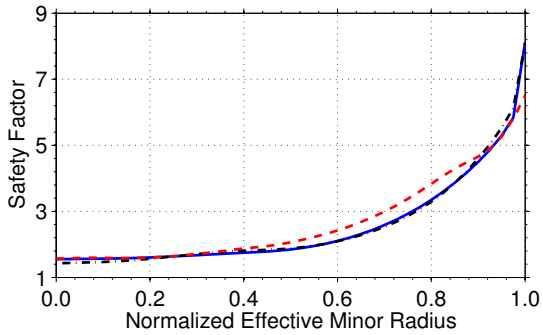

(2) $t = 4.0$ sec.

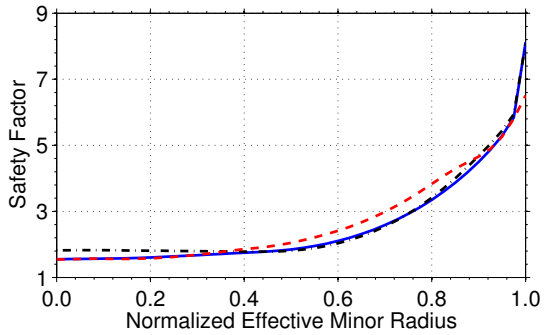

(3) $t = 5.5$ sec.

Fig.: Safety factor profile $q(\hat{\rho})$ at various time instances. Note: target (solid), experiment (dash-dotted), and simulated with optimized actuator trajectories (dash).

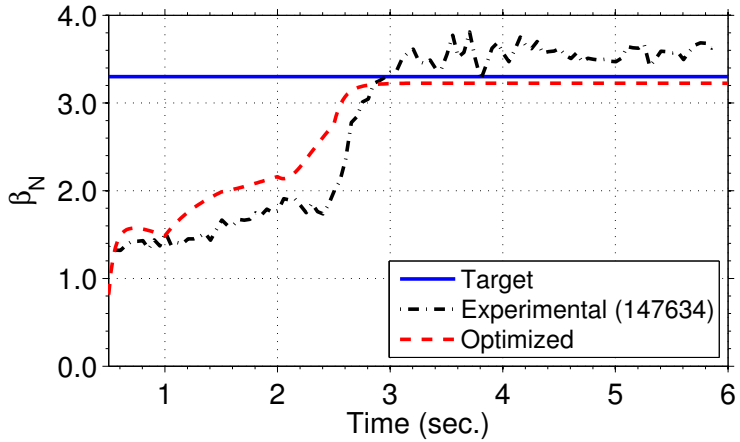

(1)

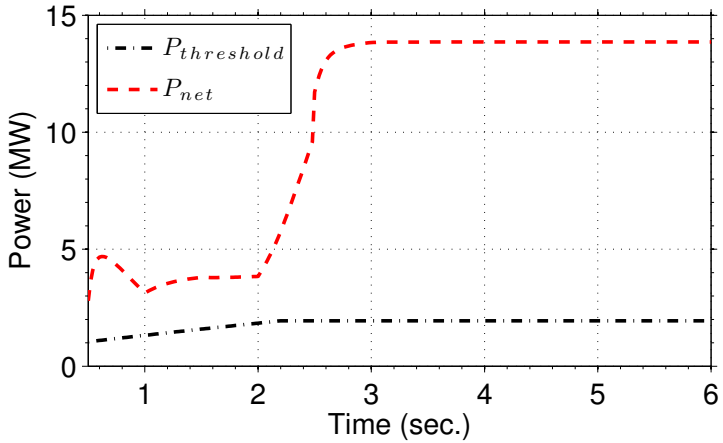

(2)

Fig.: (1) Normalized beta versus time. Note: optimization target (solid), experiment (dash-dotted), and simulated with optimized actuator trajectories (dash). (2) simulated L-to-H threshold and net power through the plasma surface.

1. Achieved Target State is Stationary in Time

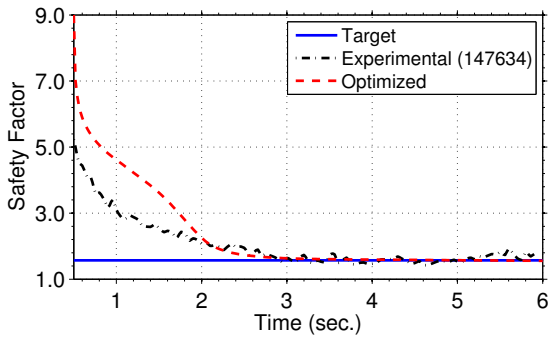

(1) $\hat{\rho} = 0.1$

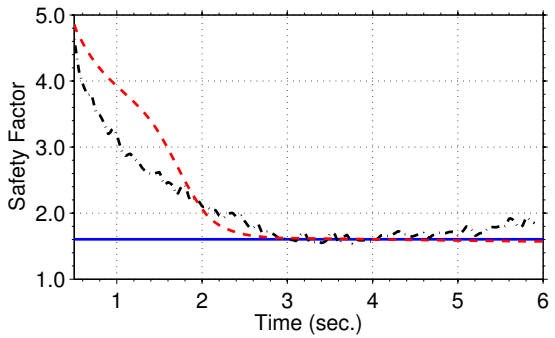

(2) $\hat{\rho} = 0.2$

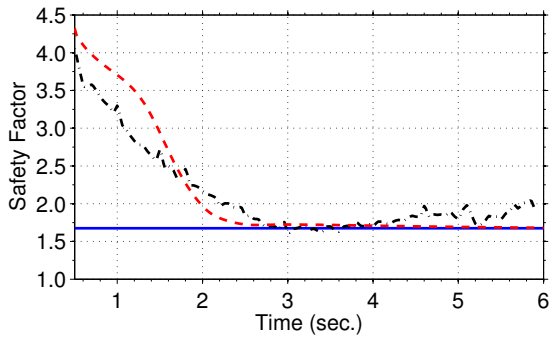

(3) $\hat{\rho} = 0.3$

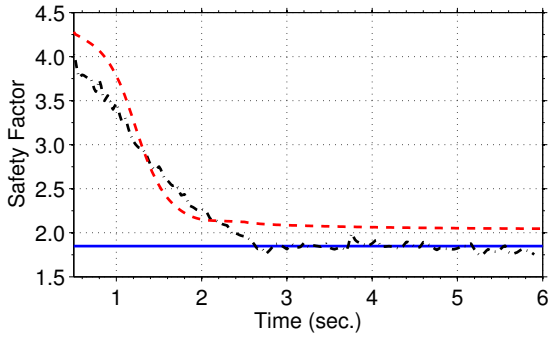

(4) $\hat{\rho} = 0.5$

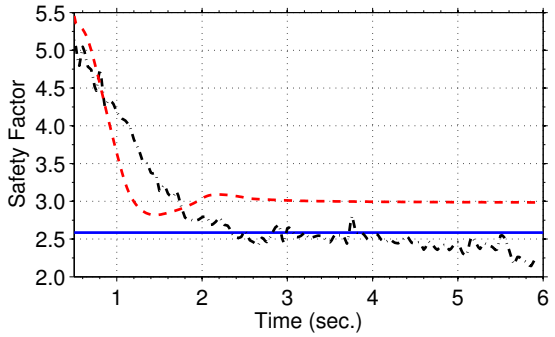

(5) $\hat{\rho} = 0.7$

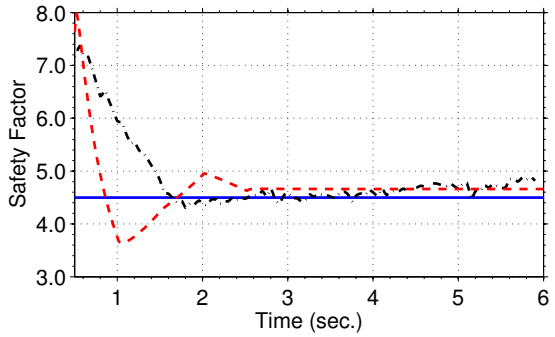

(6) $\hat{\rho} = 0.9$

Fig.: Time trace of safety factor q at various spatial locations. Note: target (solid), experiment (dash-dotted), and simulated with optimized actuator trajectories (dash).

1. Actuator Trajectory Optimization: Topics to Discuss

- Definition of desired plasma state.
  - Other important plasma parameters to include?
- Definition of actuator and plasma state constraints.
  - Other constraints necessary to include from a physics standpoint, i.e., onset of MHD instabilities, etc?
- Optimized actuator trajectories.
  - Have you ever experimentally tried actuator trajectories similar to these, particularly plasma current trajectory?
  - For see potential of inducing MHD instabilities with actuator trajectories?
- Plasma state evolution achieved with optimized actuator trajectories.
  - Does L-to-H threshold power seem reasonable?

2. Feedback Control Design

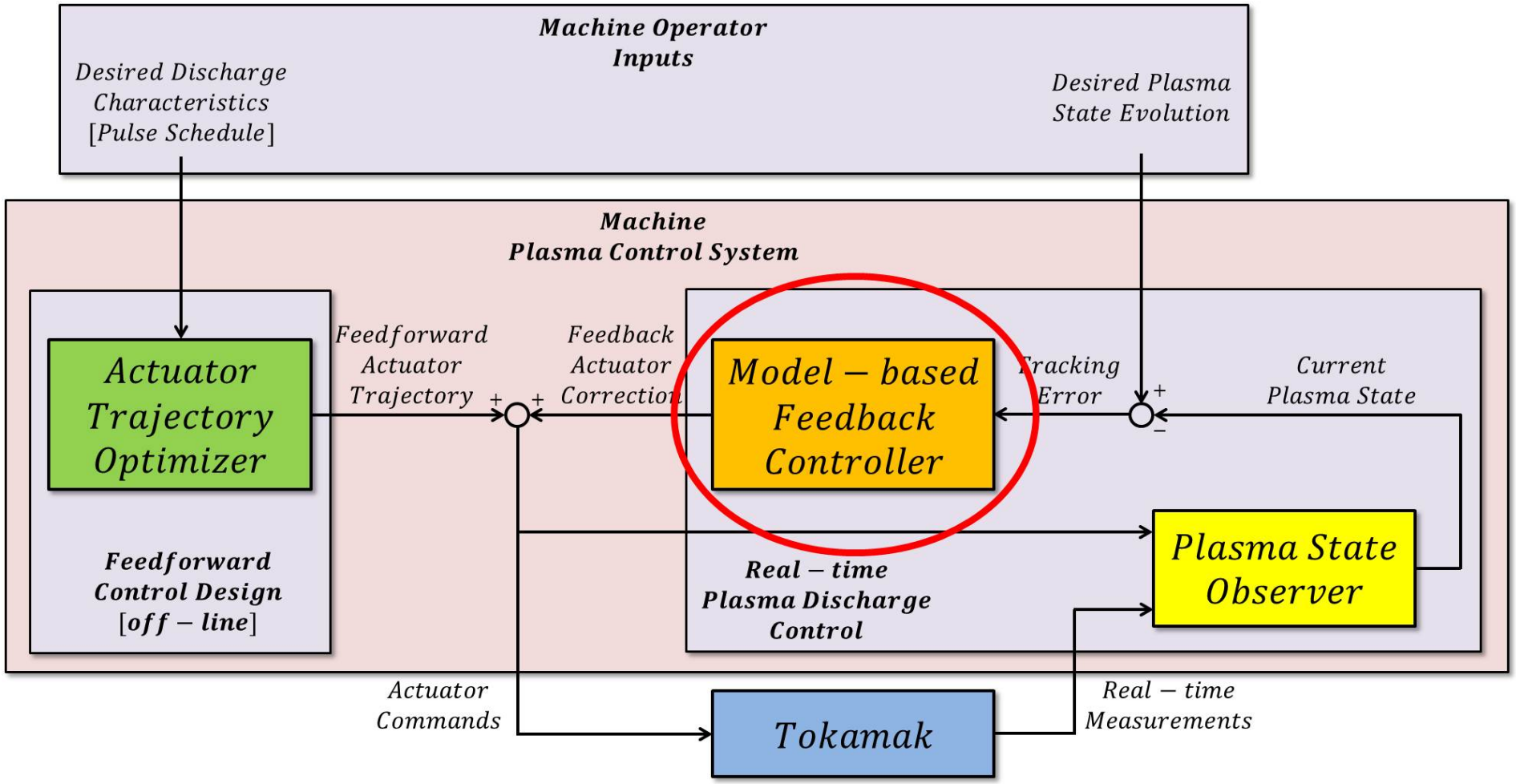

Fig.: Plasma profile and parameter control components.

2. Feedback Control Design – H-mode

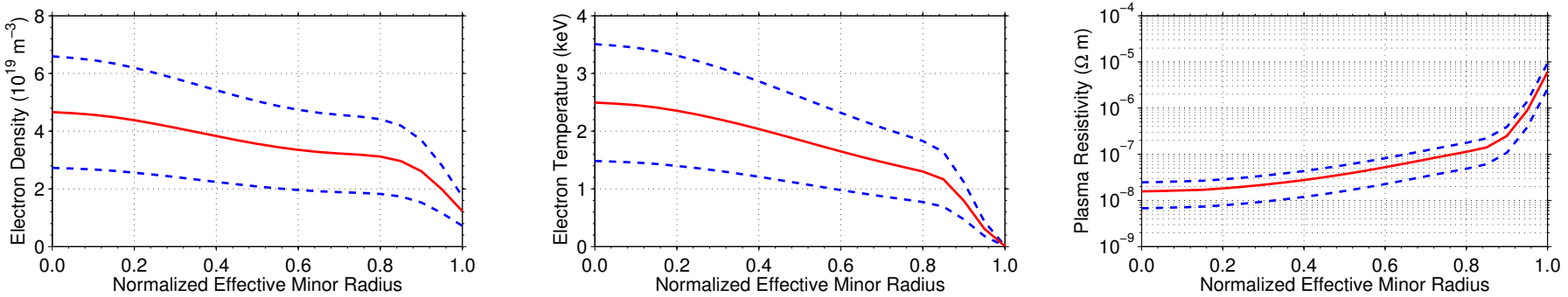

(1) (2) (3)

Fig.: Plasma parameter uncertainty ranges: (1) electron density, (2) electron temperature, and (3) plasma resistivity. Note: nominal values (solid) and minimum/maximum values (dash).

- Electron density and temperature profiles and plasma resistivity modeled as a nominal profile plus bounded uncertain component.
- Feedback controller designed to:
  - Track target poloidal flux gradient $\theta(\hat{\rho}, t)$ profile and stored energy $E(t)$ evolution.
  - Maintain closed-loop system stability in presence of uncertainty in kinetic plasma parameters.

2. Implemented Control Architecture in DIII-D PCS

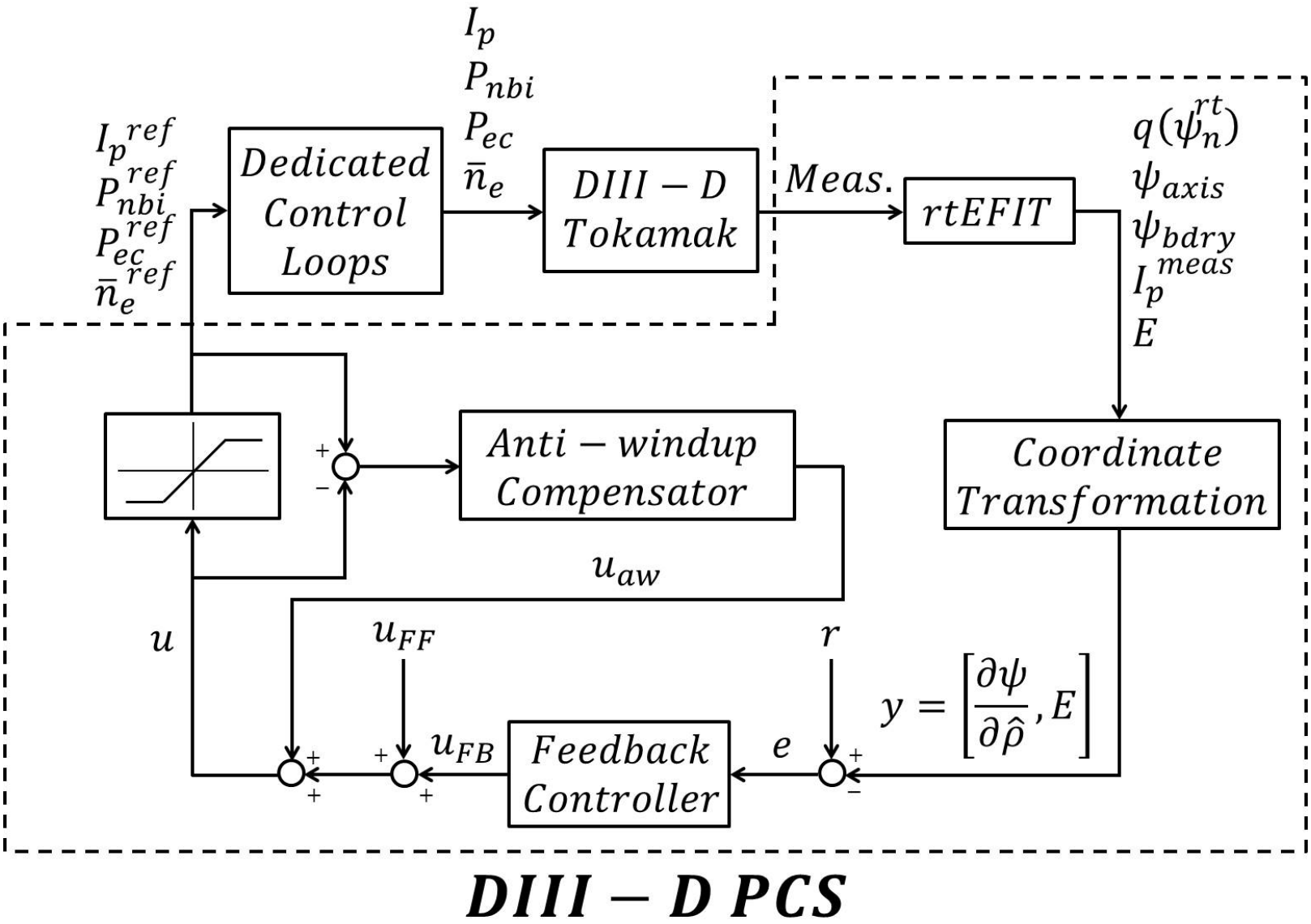

Fig.: Schematic of plasma profile and parameter control structure in DIII-D PCS.

2. Disturbance Rejection: Target State Achieved I

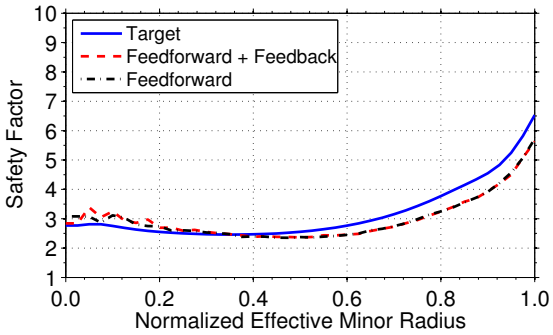

(1) $t = 2.0$ sec. {FB−OFF}

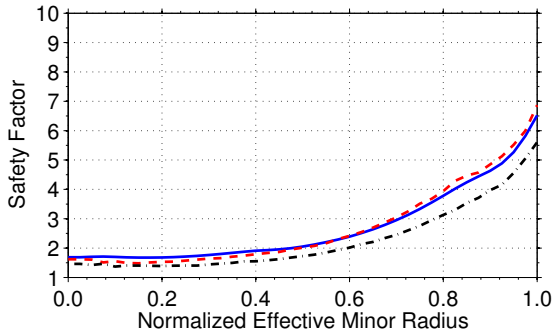

(2) $t = 4.0$ sec. {FB−ON}

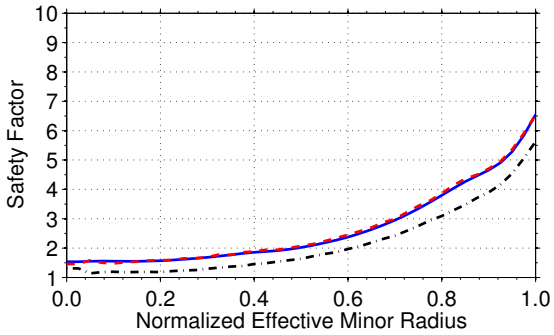

(3) $t = 5.5$ sec. {FB−ON}

Fig.: Safety factor profile $q(\hat{\rho})$ at various time instances. Note: target (solid blue), feedforward + feedback (dash red), and feedforward (dash-dotted black).

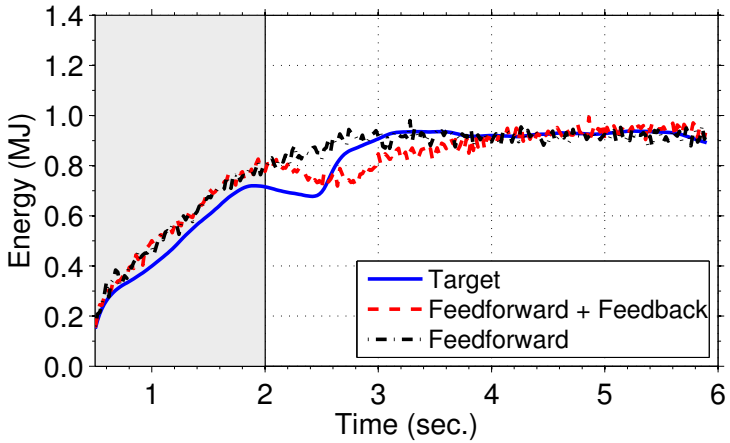

(1) E

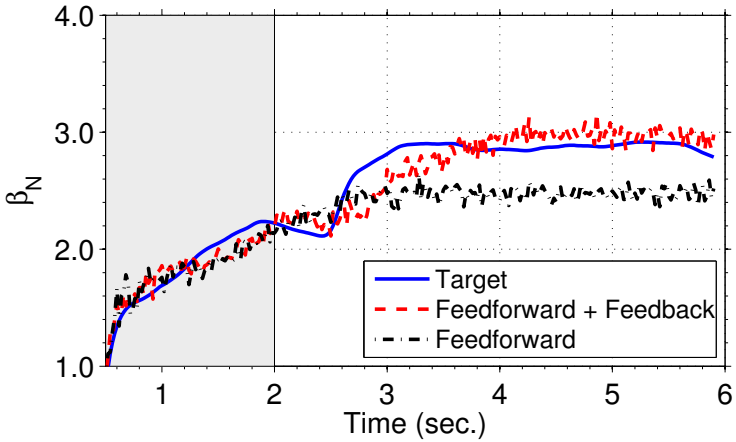

(2) β_N

Fig.: Plasma stored energy and normalized beta versus time. The shaded gray region denotes when the feedback controller is not active. Note: target (solid blue), feedforward + feedback (dash red), and feedforward (dash-dotted black).

2. Disturbance Rejection: Target State Achieved II

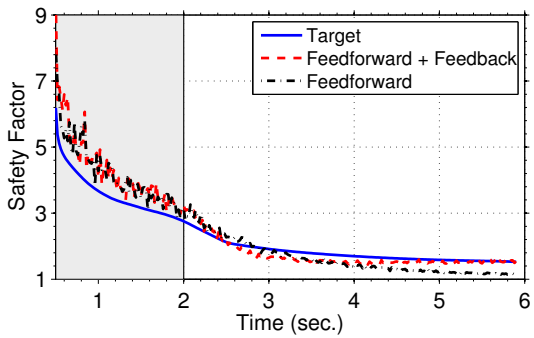

(1) $\hat{\rho} = 0.1$

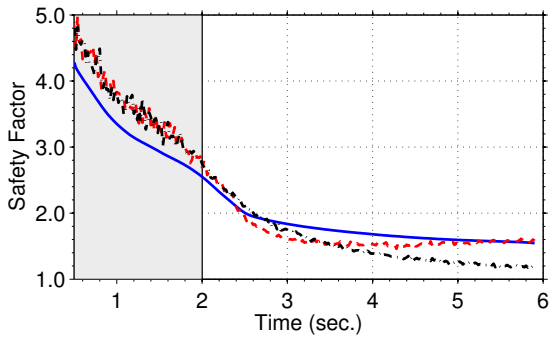

(2) $\hat{\rho} = 0.2$

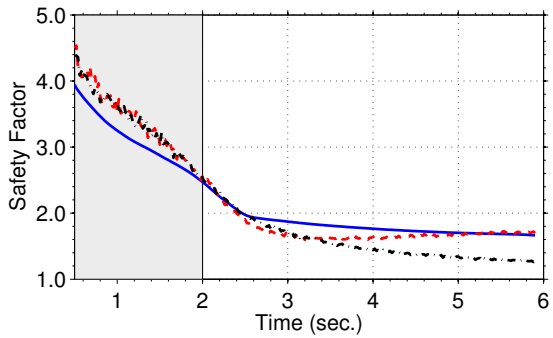

(3) $\hat{\rho} = 0.3$

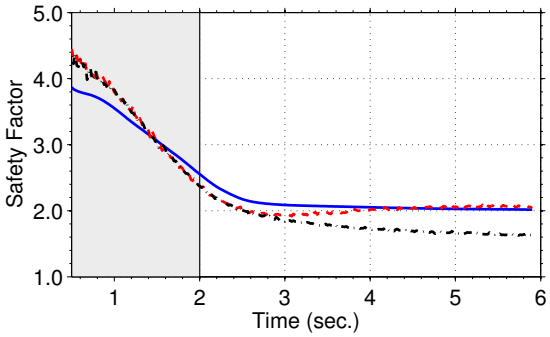

(4) $\hat{\rho} = 0.5$

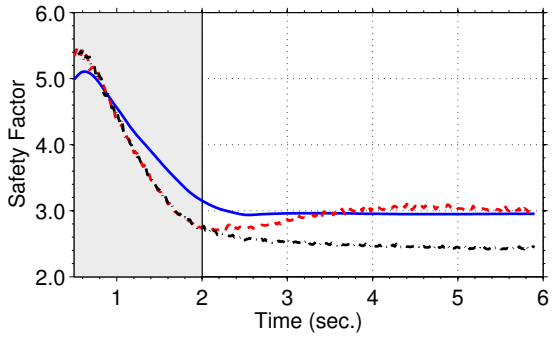

(5) $\hat{\rho} = 0.7$

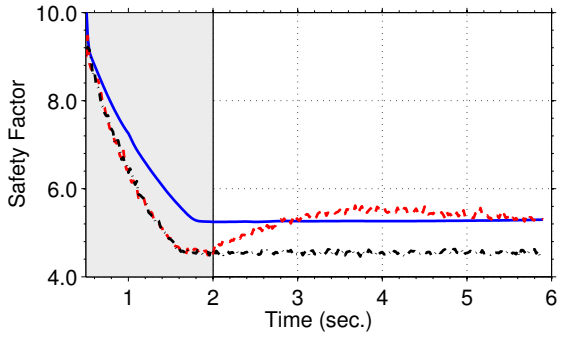

(6) $\hat{\rho} = 0.95$

Fig.: Time trace of safety factor q at various spatial locations. The shaded gray region denotes when the feedback controller is not active. Note: target (solid blue), feedforward + feedback (dash red), and feedforward (dash-dotted black).

2. Disturbance Rejection: Actuator Comparison

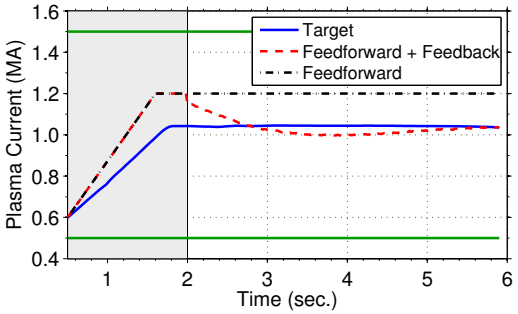

(1) $I_p(t)$

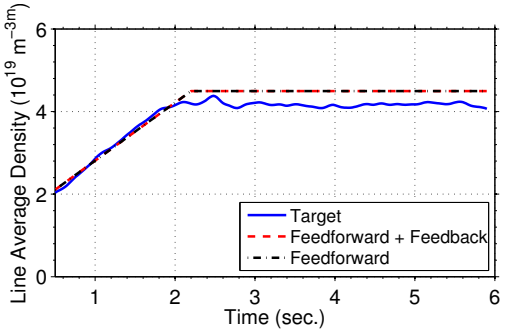

(2) $\bar{n}_e(t)$

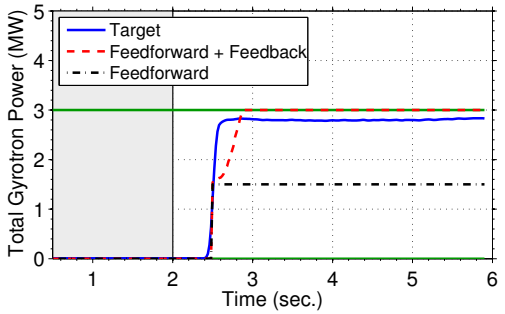

(3) $P_{ec_{tot}}(t)$

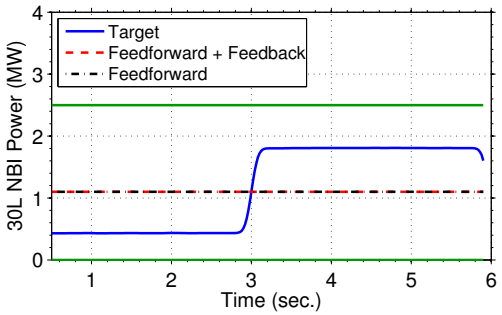

(4) $P_{nbi_{30L}}(t)$

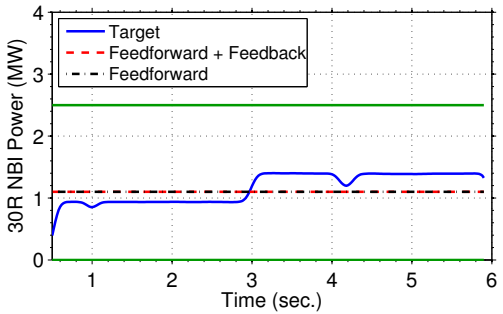

(5) $P_{nbi_{30R}}(t)$

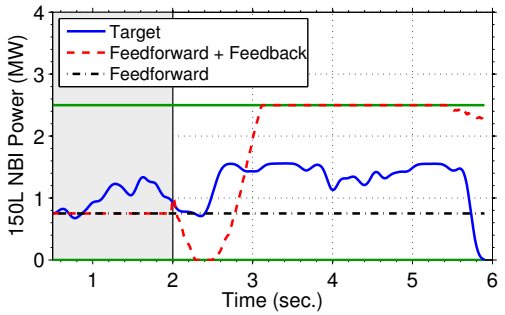

(6) $P_{nbi_{150L}}(t)$

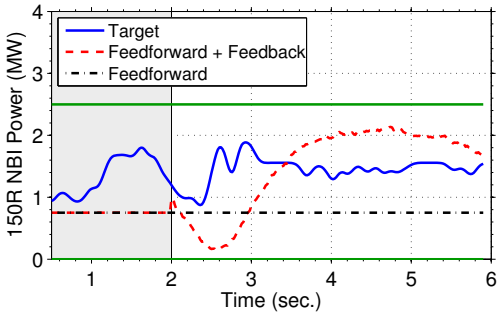

(7) $P_{nbi_{150R}}(t)$

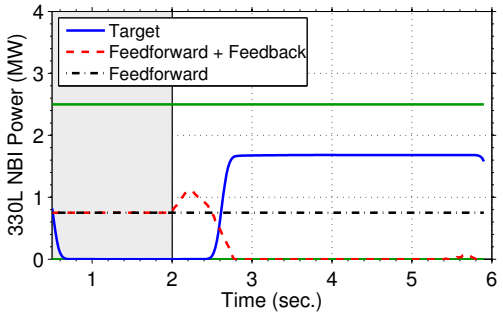

(8) $P_{nbi_{330L}}(t)$

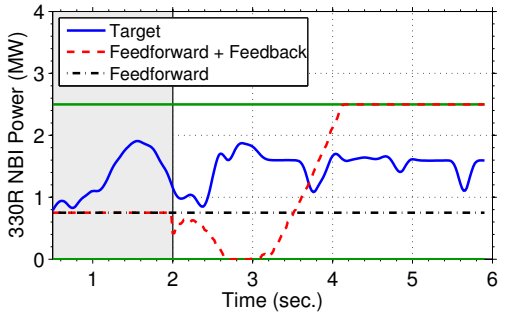

(9) $P_{nbi_{330R}}(t)$

Fig.: Control actuator trajectory comparison.

2. Reference Tracking: Target State Achieved I

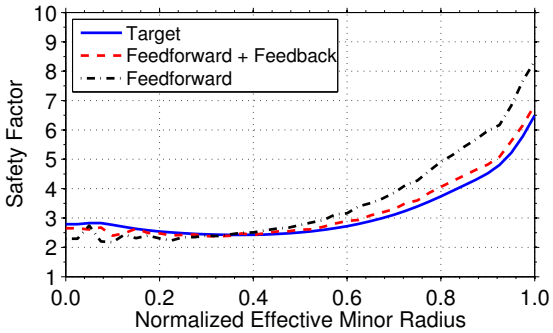

(1) $t = 2.0$ sec. {FB−OFF}

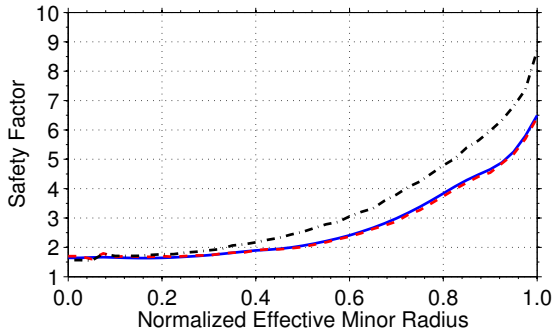

(2) $t = 4.0$ sec. {FB−ON}

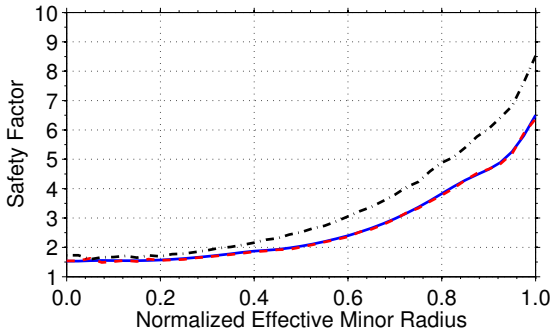

(3) $t = 5.5$ sec. {FB−ON}

Fig.: Safety factor profile $q(\hat{\rho})$ at various time instances. Note: target (solid blue), feedforward + feedback (dash red), and feedforward (dash-dotted black).

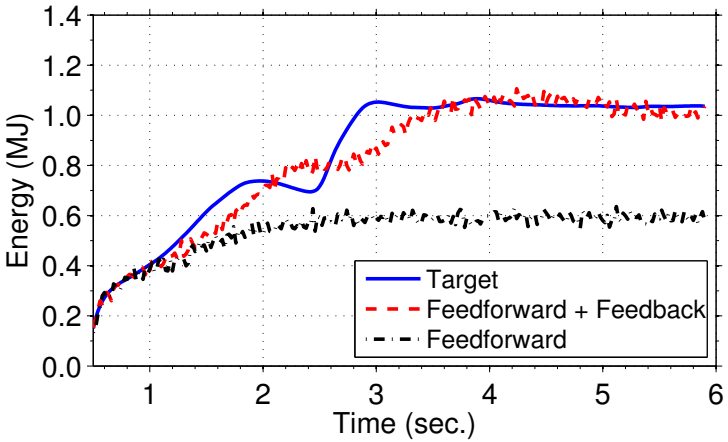

(1) E

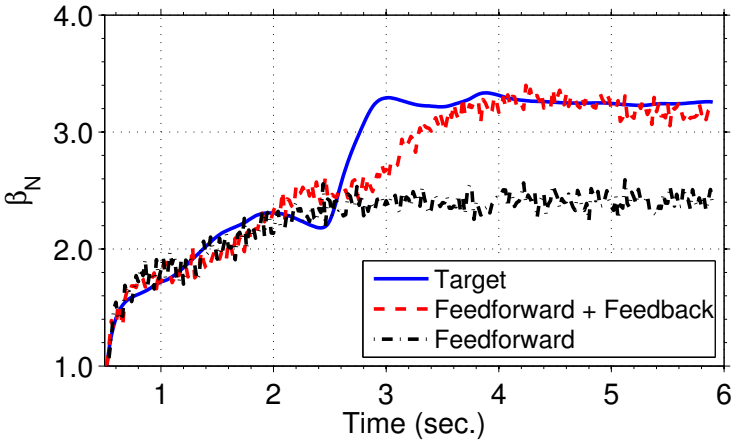

(2) β_N

Fig.: Plasma stored energy and normalized beta versus time. Note: target (solid blue), feedforward + feedback (dash red), and feedforward (dash-dotted black).

2. Reference Tracking: Target State Achieved II

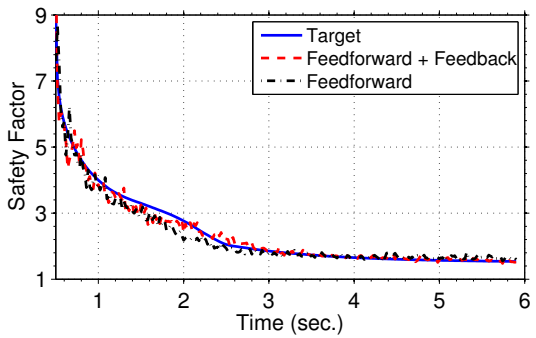

(1) $\hat{\rho} = 0.1$

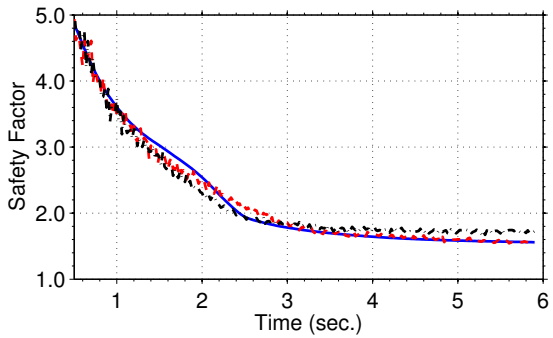

(2) $\hat{\rho} = 0.2$

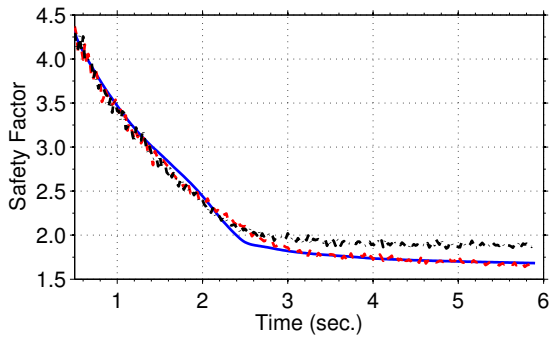

(3) $\hat{\rho} = 0.3$

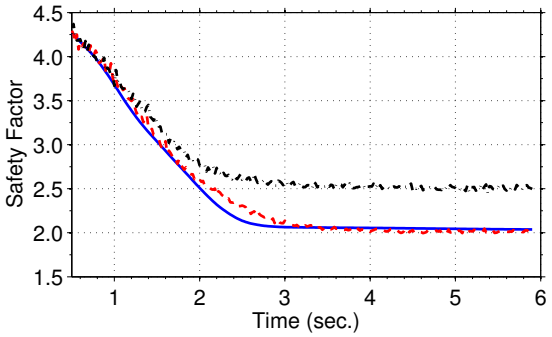

(4) $\hat{\rho} = 0.5$

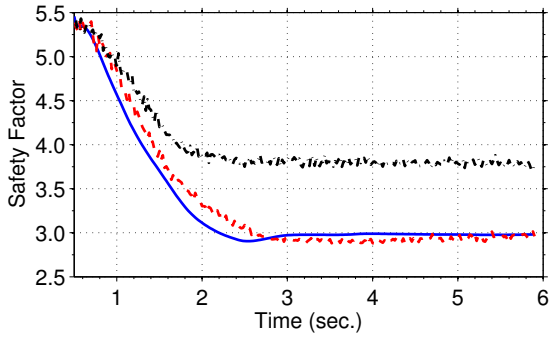

(5) $\hat{\rho} = 0.7$

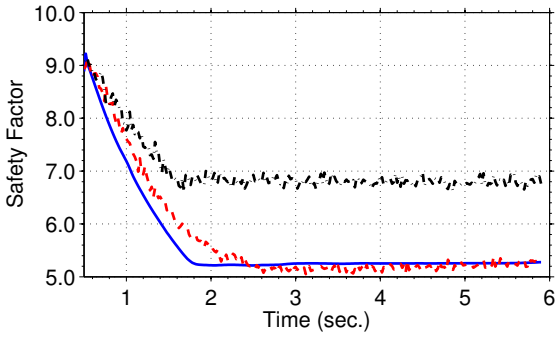

(6) $\hat{\rho} = 0.95$

Fig.: Time trace of safety factor q at various spatial locations. Note: target (solid blue), feedforward + feedback (dash red), and feedforward (dash-dotted black).

2. Reference Tracking: Actuator Comparison

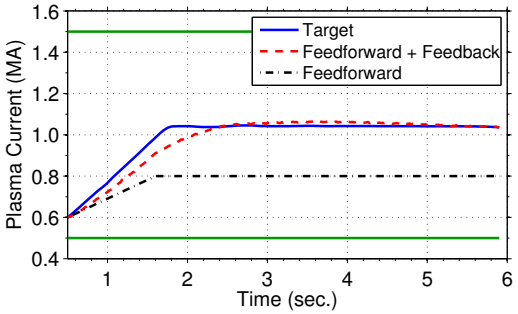

(1) $I_p(t)$

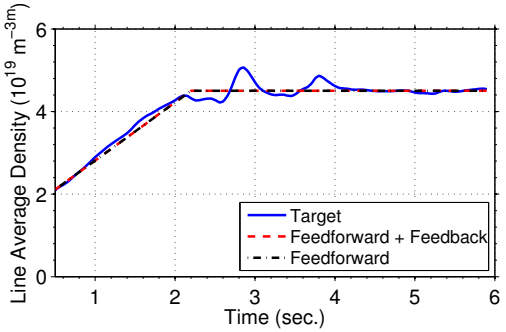

(2) $\bar{n}_e(t)$

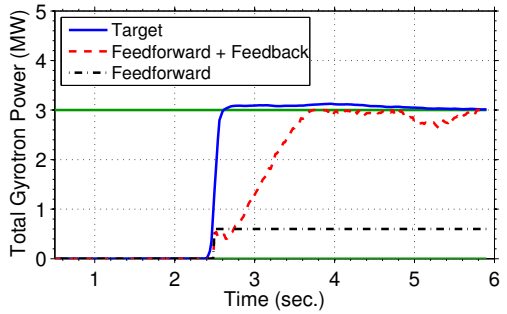

(3) $P_{ec_{tot}}(t)$

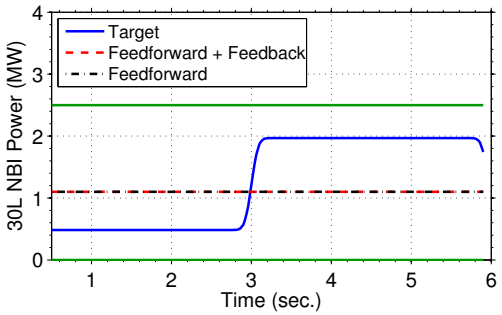

(4) $P_{nbi_{30L}}(t)$

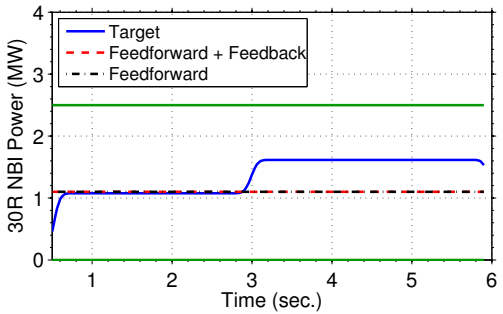

(5) $P_{nbi_{30R}}(t)$

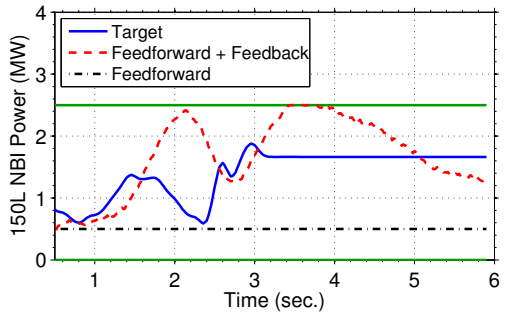

(6) $P_{nbi_{150L}}(t)$

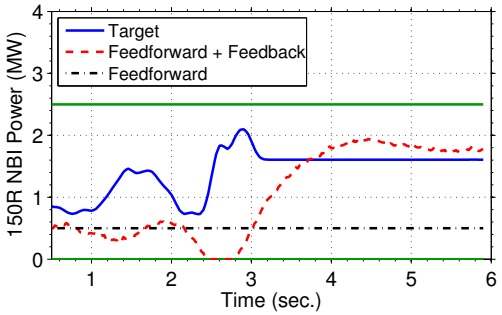

(7) $P_{nbi_{150R}}(t)$

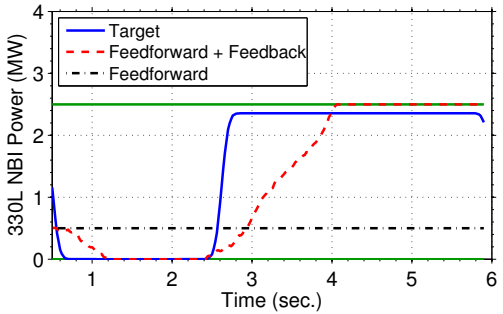

(8) $P_{nbi_{330L}}(t)$

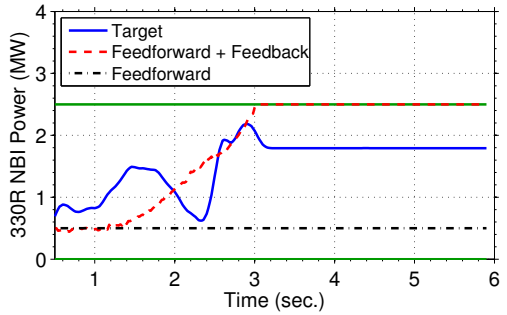

(9) $P_{nbi_{330R}}(t)$

Fig.: Control actuator trajectory comparison.

2. Current Profile Evolution Model – L-mode

- Empirical scaling laws are used for density, temperature, and non-inductive current drive
  - **Density:**

$$n(\hat{\rho},t) = n^{profile}(\hat{\rho})\bar{n}(t) \tag{28}$$

  - **Temperature:**

$$T_e(\hat{\rho},t) = k_{T_e} T_e^{profile} \frac{I(t)\sqrt{P_{tot}(t)}}{\bar{n}(t)} \tag{29}$$

  - **Non-inductive current drive:**

$$\frac{\langle j_{NI}\cdot B\rangle}{B_{\phi,0}}(\hat{\rho},t) = C(\hat{\rho})\frac{P_{tot}(t)\sqrt{T_e(\hat{\rho},t)}}{\bar{n}(t)} \tag{30}$$

$$= k_{NI} j_{NI}^{profile}(\hat{\rho})\frac{I(t)^{1/2}P_{tot}^{5/4}}{\bar{n}(t)^{3/2}} \tag{31}$$

- **Bootstrap current is neglected.**

2. Current Profile Evolution Model – L-mode

- Resulting model:

$$\frac{\partial \theta}{\partial t} = \left[h_0(\hat{\rho}) \frac{\partial^2 \theta}{\partial \hat{\rho}^2} + h_1(\hat{\rho}) \frac{\partial \theta}{\partial \hat{\rho}} + h_2(\hat{\rho}) \theta \right] u_1(t) + h_3(\hat{\rho}) u_2(t) \tag{32}$$

with boundary conditions:

$$\theta\Big|_{\hat{\rho}=0} = 0 \qquad \theta\Big|_{\hat{\rho}=1} = -k_3 u_3(t) \tag{33}$$

where

$$u_1(t) = \left(\bar{n}(t) / (I(t)\sqrt{P_{tot}}) \right)^{3/2} \tag{34}$$

$$u_2(t) = \sqrt{P_{tot}(t)} / I(t) \tag{35}$$

$$u_3(t) = I(t) \tag{36}$$

2. Magnetic Control Architecture in DIII-D PCS

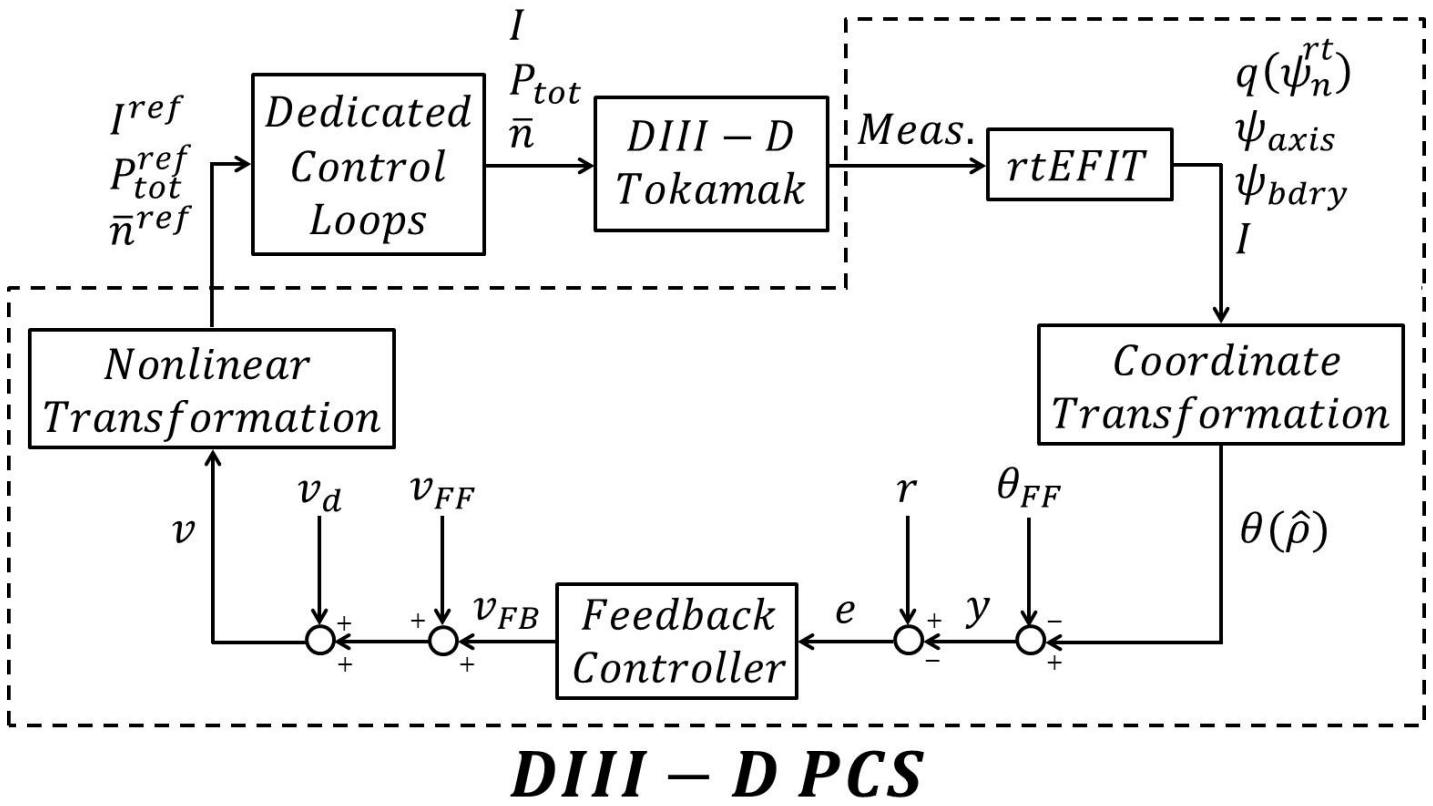

- Feedback portion of controller interfaced with real-time EFIT (rtEFIT) equilibrium reconstruction code for magnetic profile control.

2. Input Disturbance Experiment - Scenario

- **Feedforward Actuator Trajectories:** Shot #145477
- **Target Profile Evolution:** Shot #145477
- **Artificial Disturbances:** -0.15 MA in I_p, -0.5 MW in P_{tot} (Disturbance I)
  0.15 MA in I_p, 0.5 MW in P_{tot} (Disturbance II)

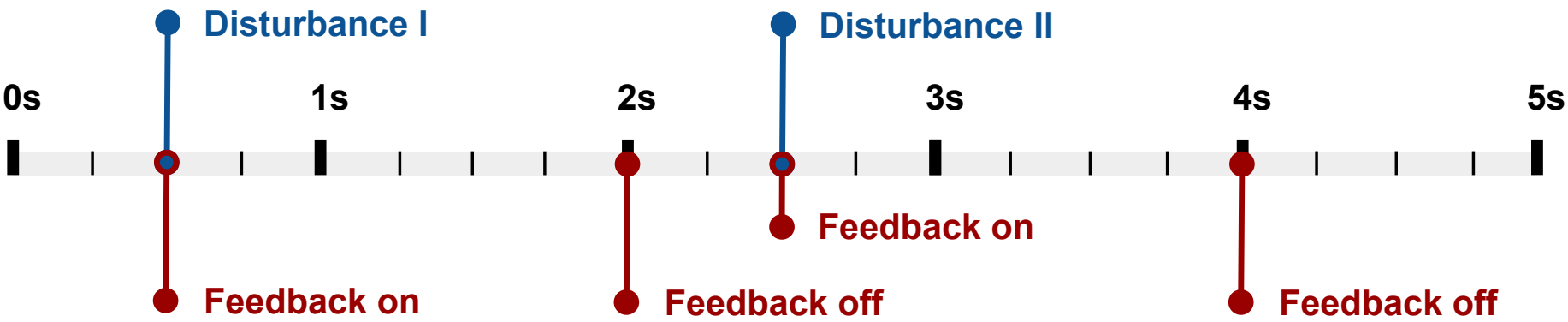

2. Input Disturbance Experiment - Time Traces

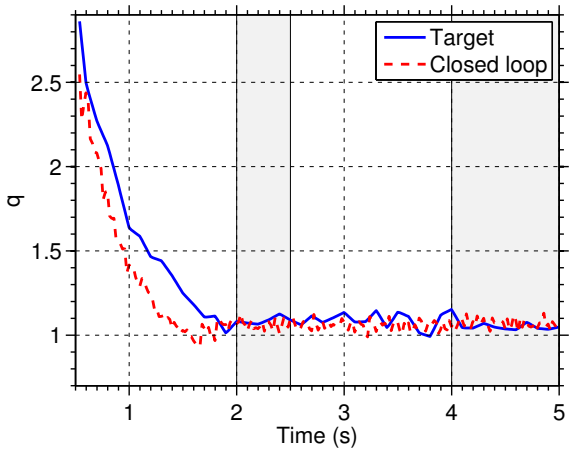

(1) $\hat{\rho} = 0.1$

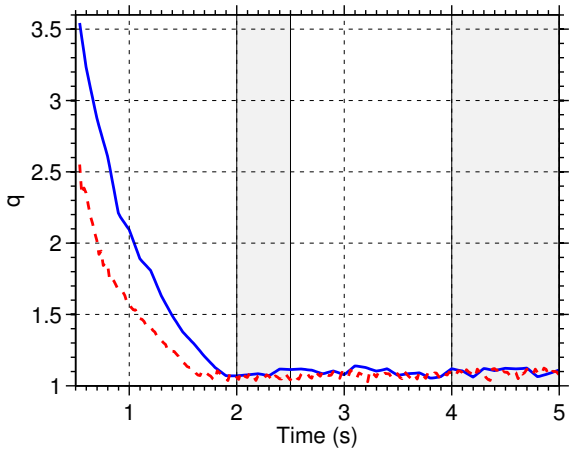

(2) $\hat{\rho} = 0.25$

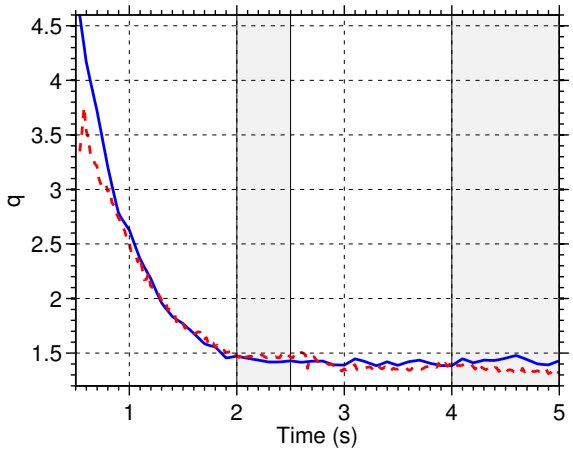

(3) $\hat{\rho} = 0.5$

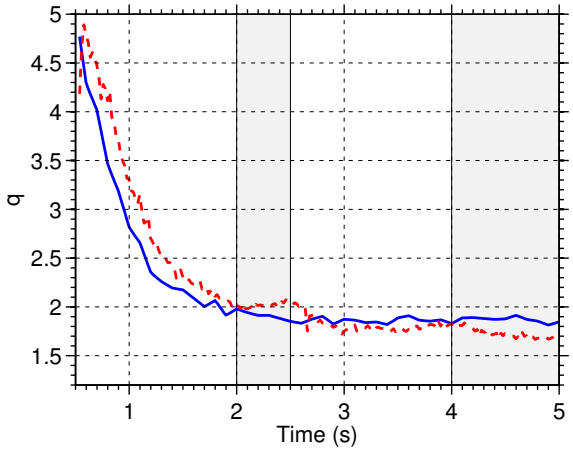

(4) $\hat{\rho} = 0.65$

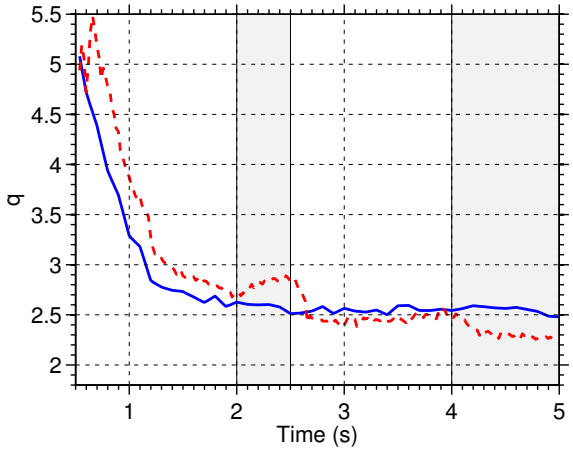

(5) $\hat{\rho} = 0.8$

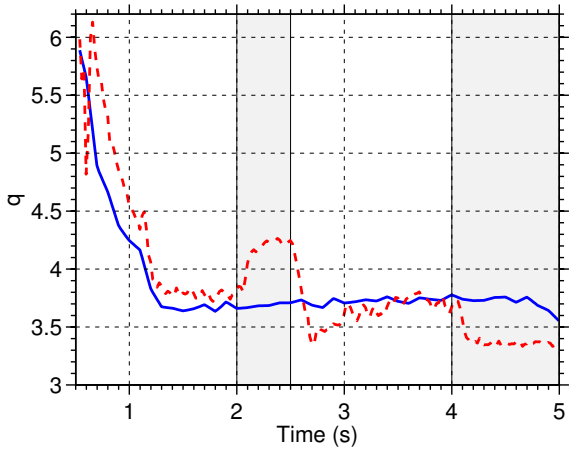

(6) $\hat{\rho} = 0.95$

2. Input Disturbance Experiment - Profiles

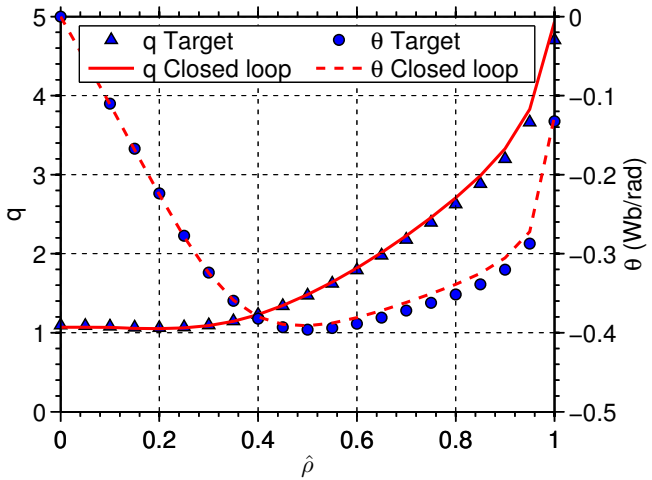

(1) $t = 2.00$s (feedback on)

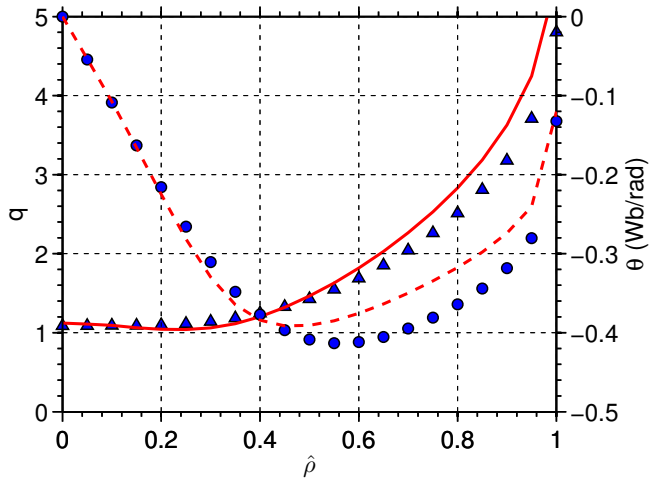

(2) $t = 2.5$s (feedback off)

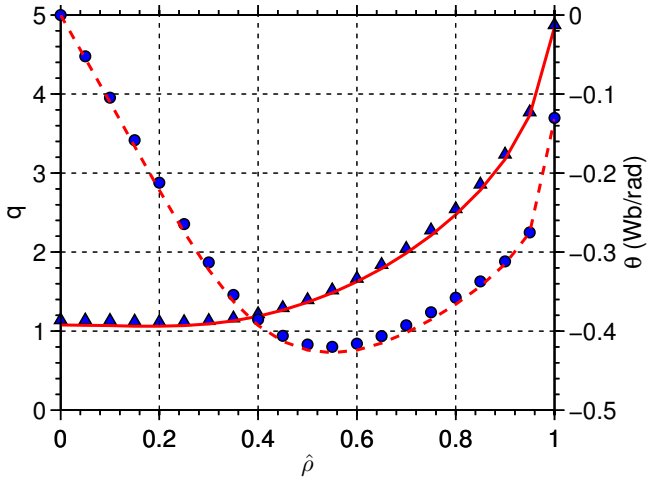

(3) $t = 4.00$s (feedback on)

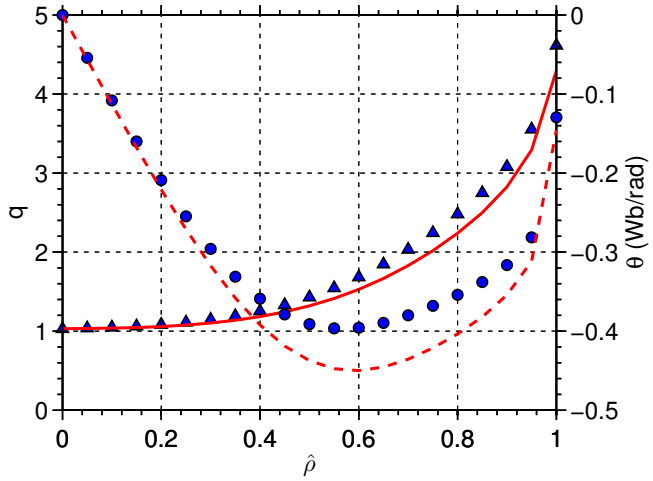

(4) $t = 5.00$s (feedback off)

2. Input Disturbance Experiment - Actuators

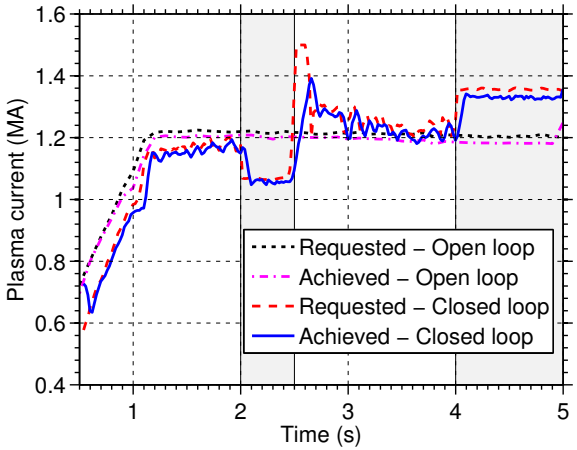

(1) Plasma current I_p

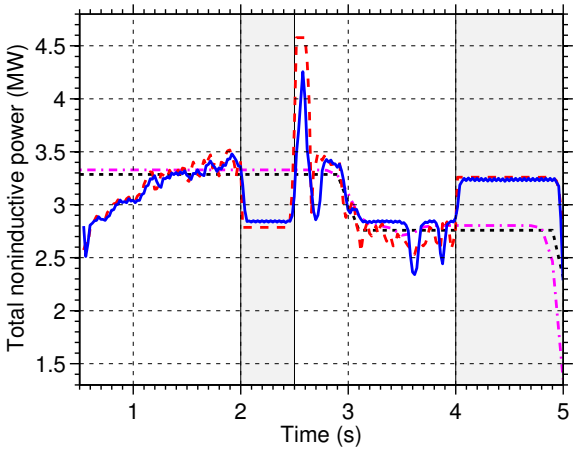

(2) Non-inductive power P_{tot}

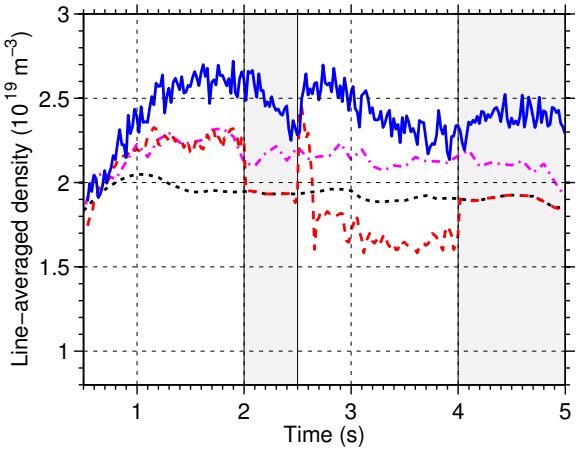

(3) Line averaged density $\bar{n}$

2. Target Tracking Experiment - Scenario

- **Feedforward Actuator Trajectories:** Shot #146411
- **Target Profile Evolution:** Shot #145477
- **Artificial Disturbances:** None

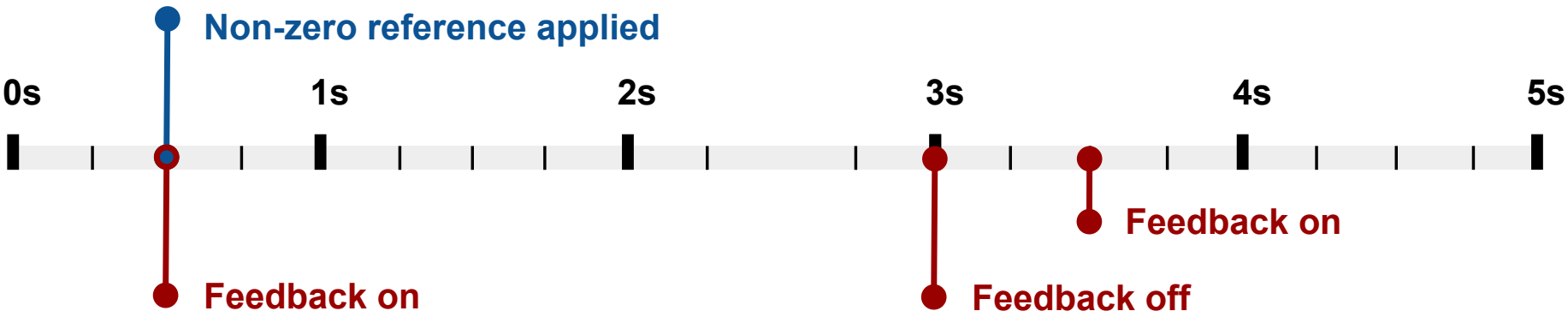

2. Target Tracking Experiment - Time Traces

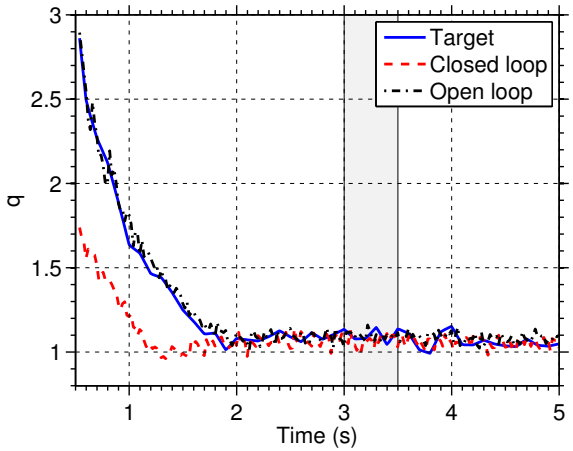

(1) $\hat{\rho} = 0.1$

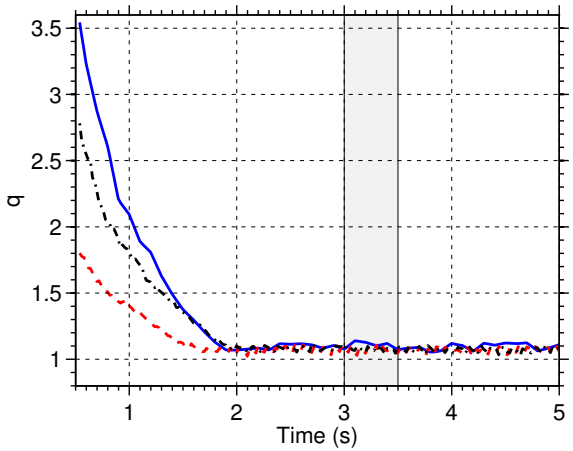

(2) $\hat{\rho} = 0.25$

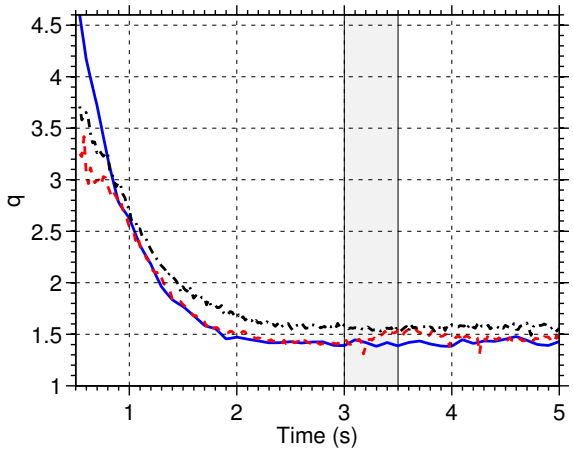

(3) $\hat{\rho} = 0.5$

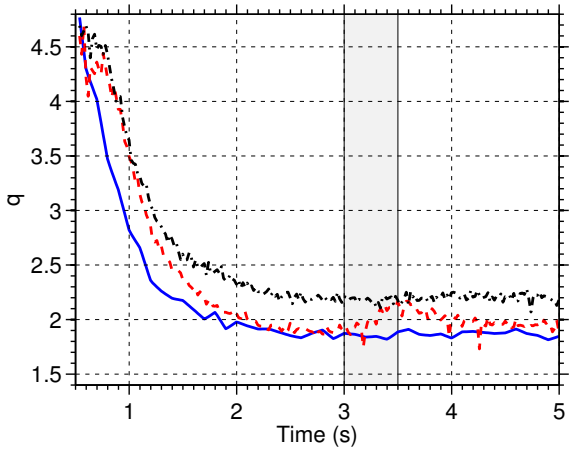

(4) $\hat{\rho} = 0.65$

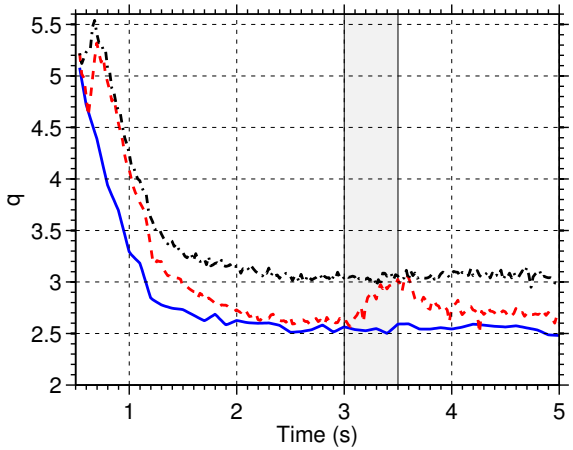

(5) $\hat{\rho} = 0.8$

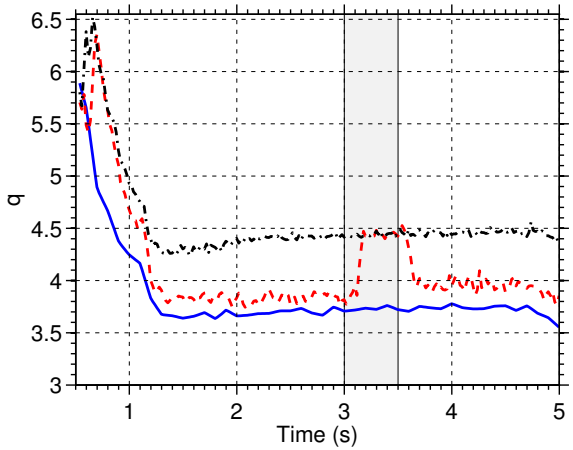

(6) $\hat{\rho} = 0.95$

2. Target Tracking Experiment - Profiles

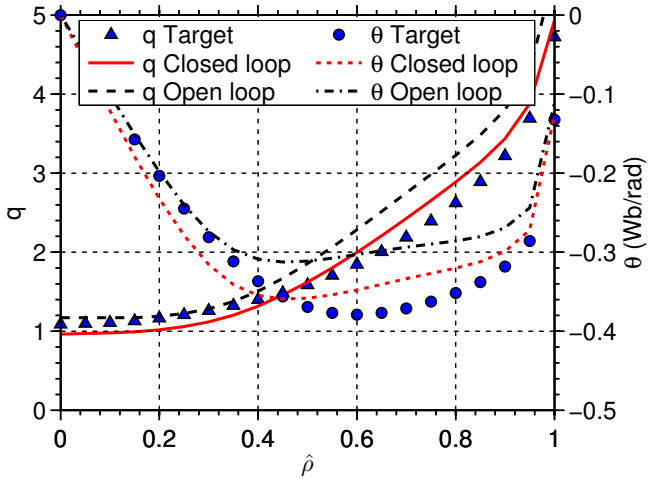

(1) $t = 1.70$s (feedback on)

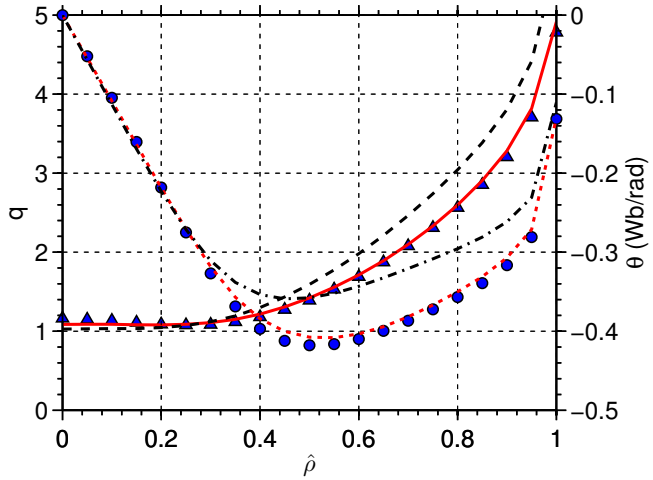

(2) $t = 3.00$s (feedback on)

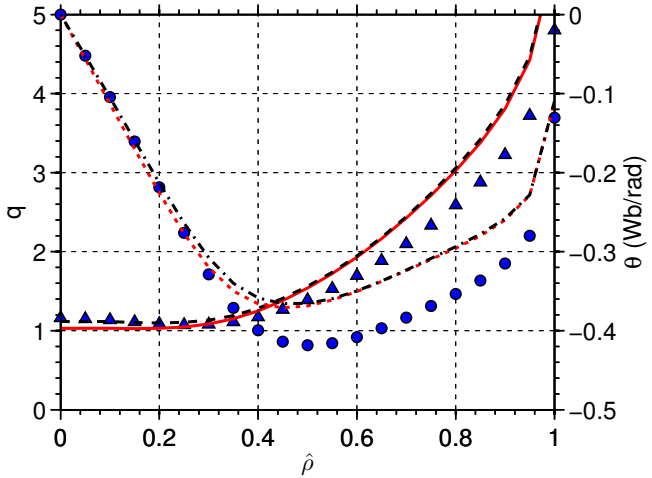

(3) $t = 3.50$s (feedback off)

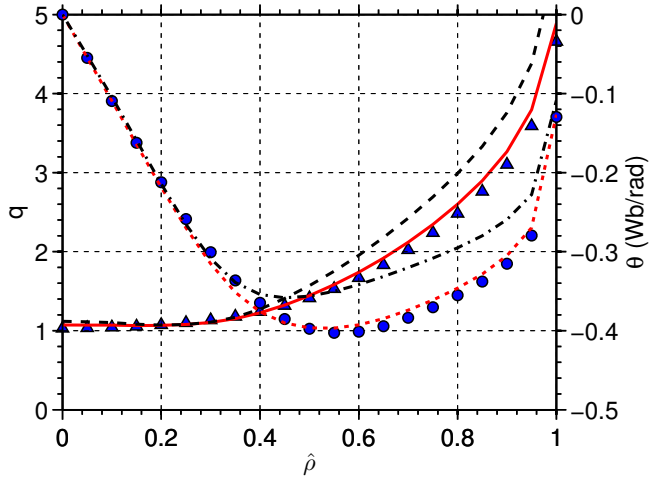

(4) $t = 4.96$s (feedback on)

2. Target Tracking Experiment - Actuators

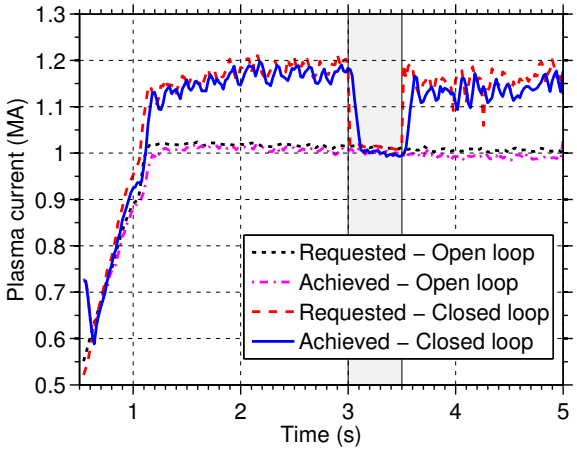

(1) Plasma current I_p

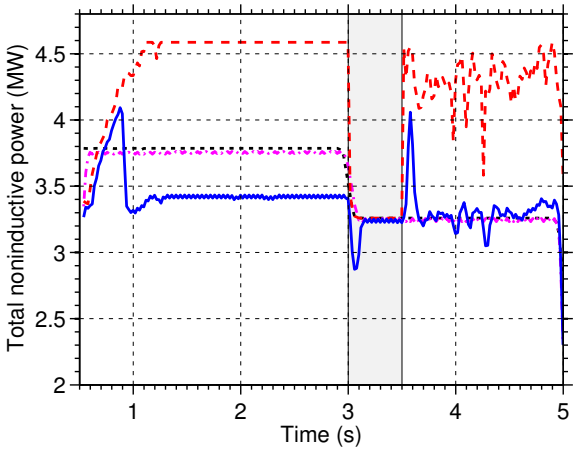

(2) Non-inductive power P_{tot}

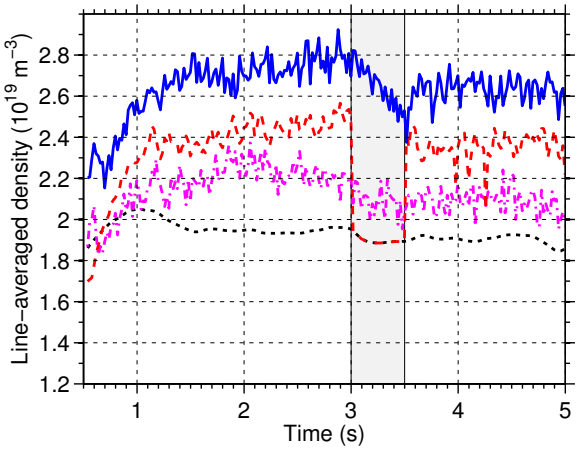

(3) Line averaged density $\bar{n}$

2. Feedback Control Design: Topics to Discuss

- Control performance goals, robustness requirements
- Demonstrations for controller qualification (disturbance rejection, tracking, etc.)
- Available actuators, capabilities of existing dedicated controllers
- State and actuator constraints
- PCS implementation

3. Plasma State Observers

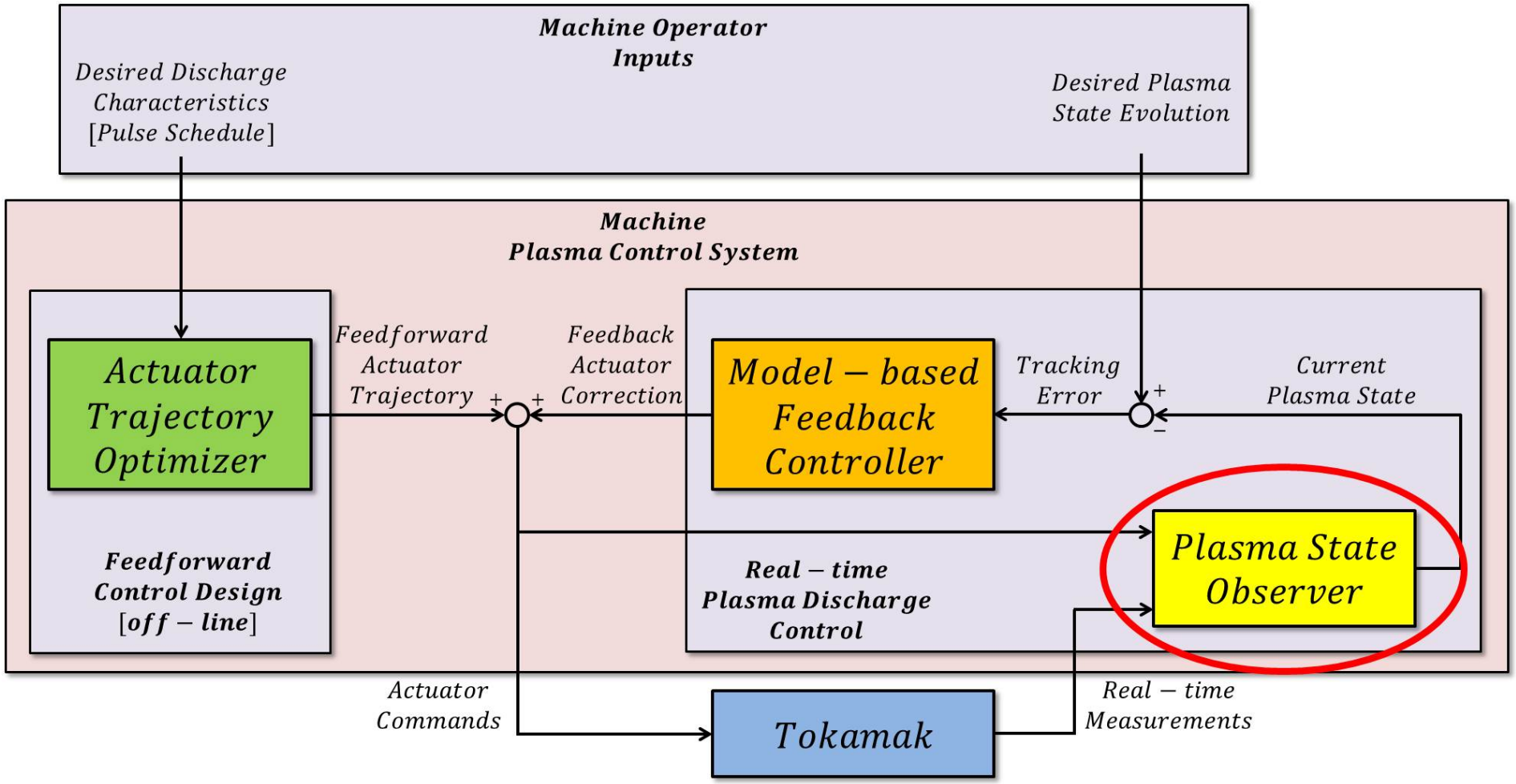

Fig.: Plasma profile and parameter control components.

3. Plasma State Observers

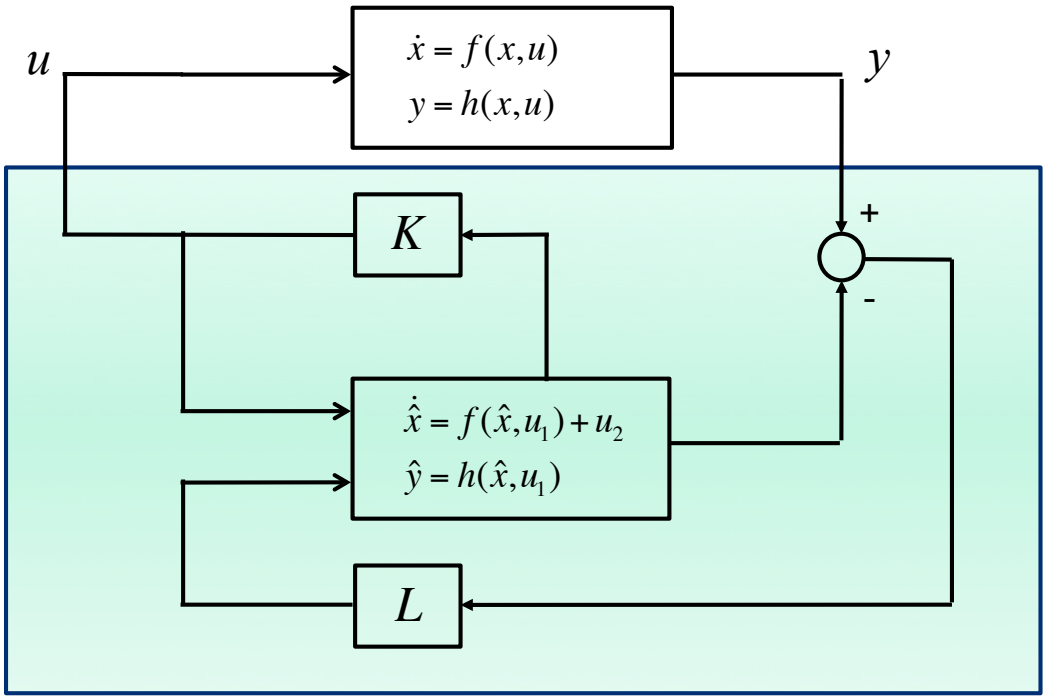

- Core of observer is control-oriented, first-principles-driven model [1, 2, 3].
- Observer filters measurement noise not consistent with physics (model).
- Gain L regulates tradeoff between model prediction and measurement.

[1] OU, Y., WALKER, M.L., SCHUSTER, E., FERRON, J.R., Fusion Eng. Des. (2007).
[2] IN, Y., SCHUSTER, E., OKABAYASHI, M., NAVRATIL, G.A., SABBAGH, S., ... (RWM)
[3] FELICI, F. et al., Nuclear Fusion (2011).

3. Plasma State Observers: Topics to Discuss

- Availability of real-time measurements.
- Measurement sampling times and sensor quality.

4. Simserver Simulations

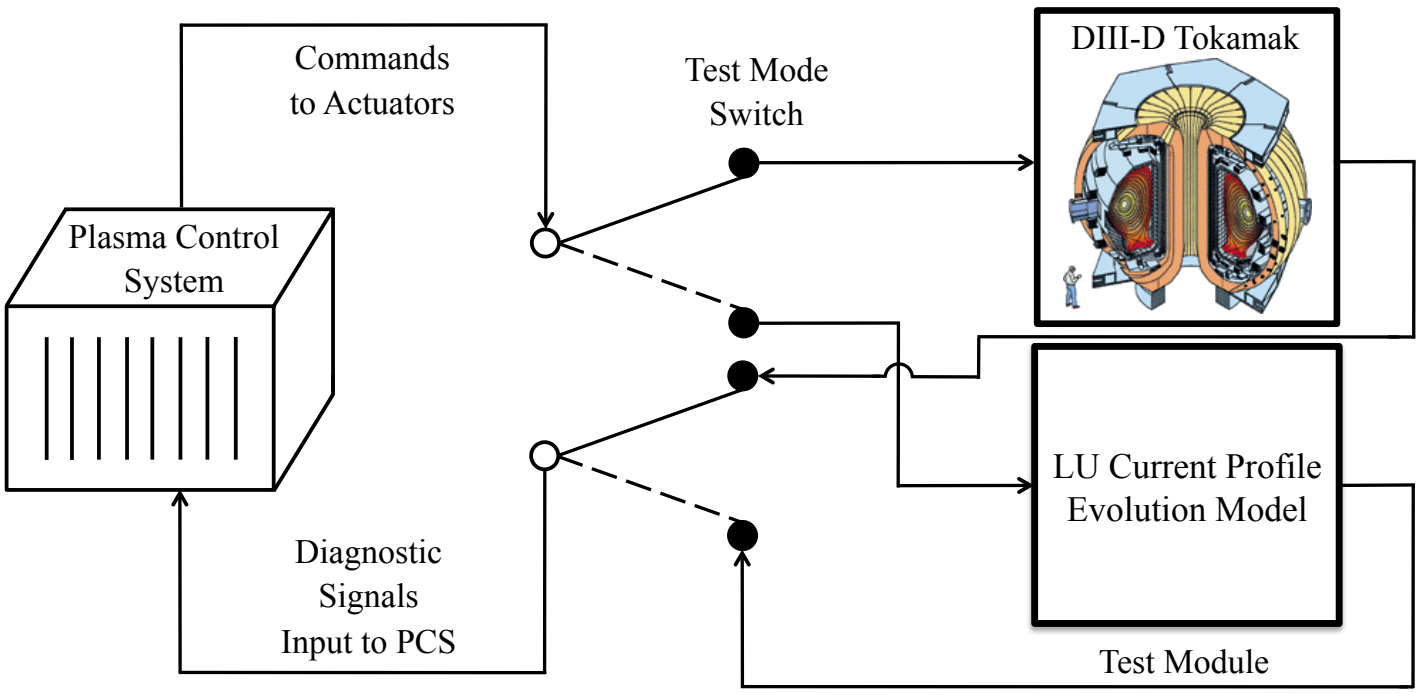

- Simserver architecture [1] used for testing algorithms running in PCS.
- LU current profile evolution model implemented in Simserver [2] and used to determine effectiveness of controllers and debug real-time implementation before experimental tests.

[1] WALKER, M., et al., Fusion Eng. Des., (2007).

[2] BARTON, J.E., OU, Y., XU, C., SCHUSTER, E., WALKER, M., Fusion Eng. Des., (2011).

4. Simserver Simulations: Things to Discuss

- Availability of and experience with Simserver at NSTX
- Simserver implementation

Model Tailoring for NSTX Shot 121014P01

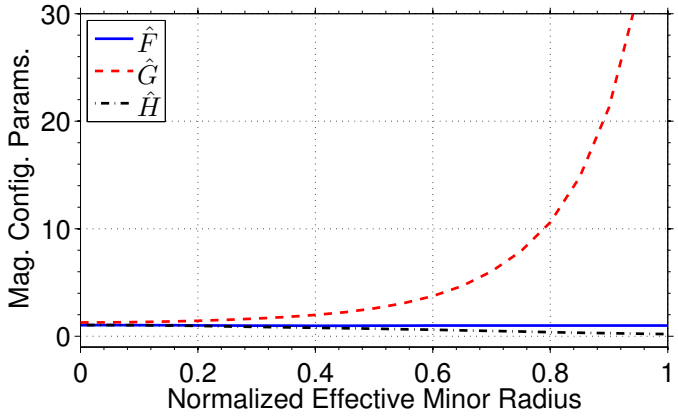

(1) $\hat{F}(\hat{\rho})$, $\hat{G}(\hat{\rho})$, $\hat{H}(\hat{\rho})$

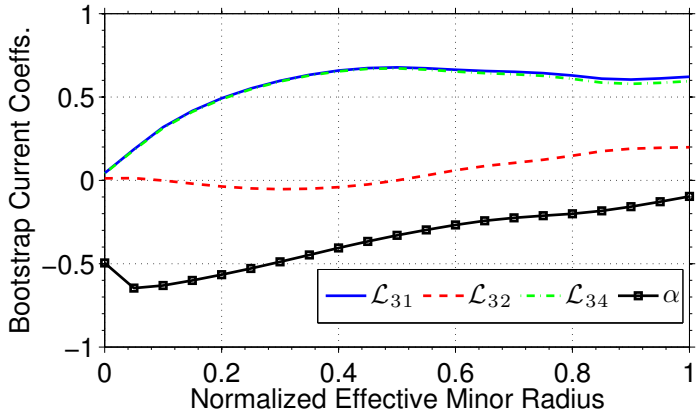

(2) $\mathcal{L}_{31}(\hat{\rho})$, $\mathcal{L}_{32}(\hat{\rho})$, $\mathcal{L}_{34}(\hat{\rho})$, $\alpha(\hat{\rho})$

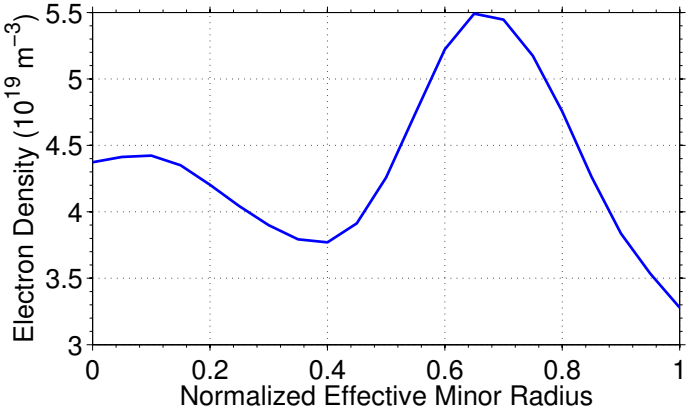

(3) $n_e^{prof}(\hat{\rho})$

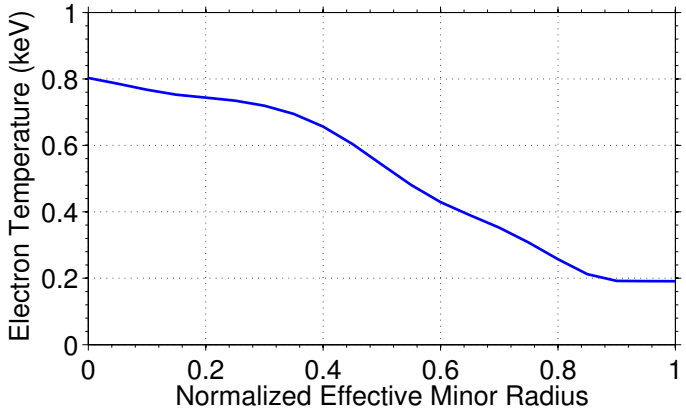

(4) $T_e^{prof}(\hat{\rho})$

Fig. 11: Reference (1) magnetic configuration parameters, (2) bootstrap current coefficients, (3) electron density profile and (4) electron temperature profile.

Model Coefficients and Actuators

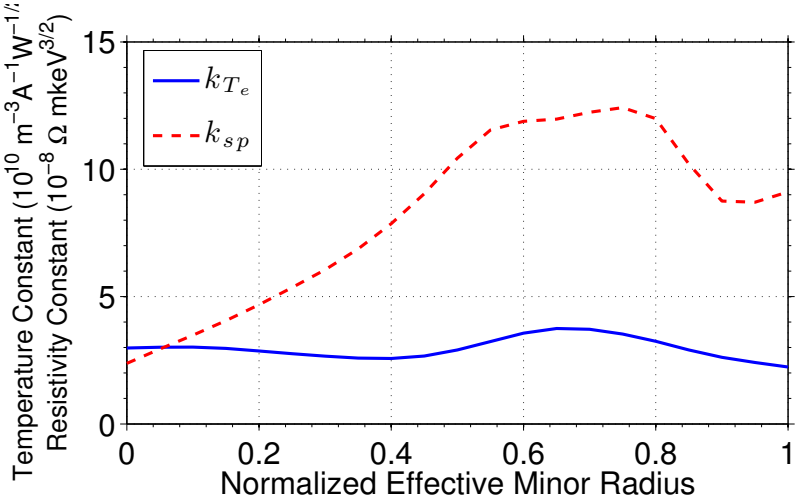

(1) k_{T_e}, k_{sp}

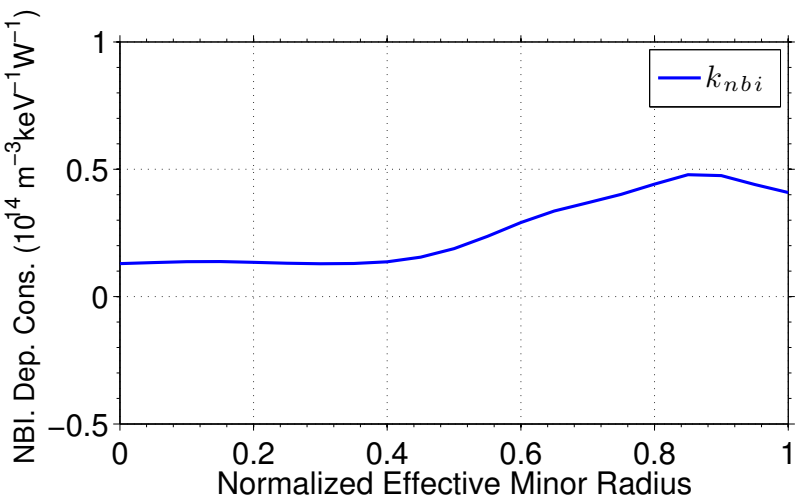

(2) k_{nbi}

Fig. 2: (1) Electron temperature, plasma resistivity, (2) neutral beam model coefficients.

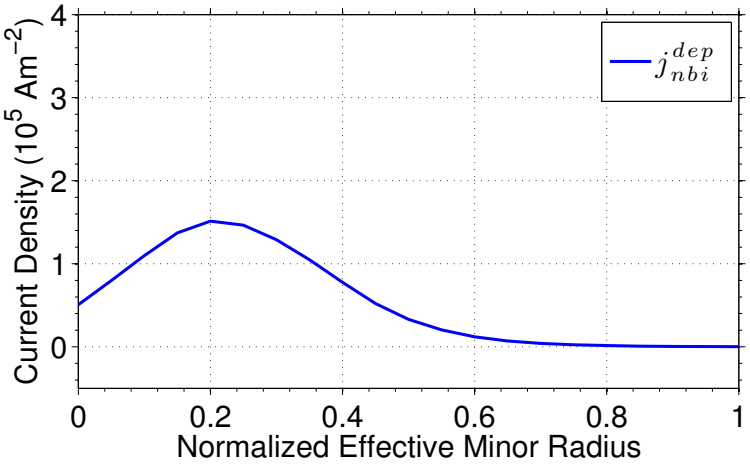

(1) $L_{nbi}^{dep}(\hat{\rho})$

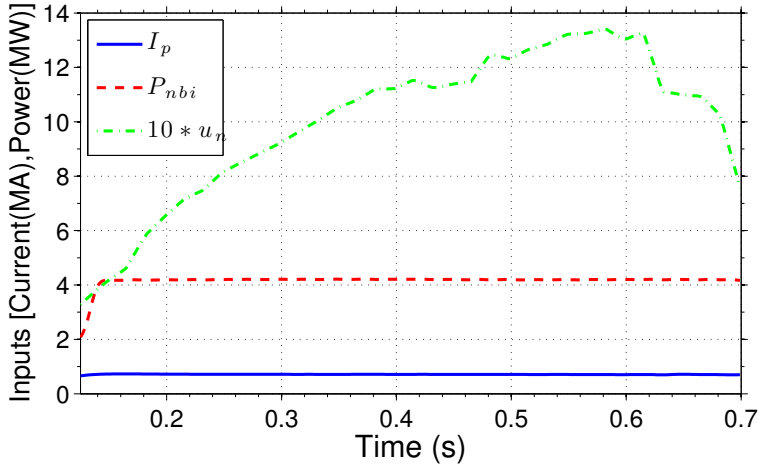

(2) Control Inputs

Fig. 12: (2) Reference NB current deposition profile. (1) Control inputs applied during simulation.

Electron Density and Electron Temperature Profile Comparisons

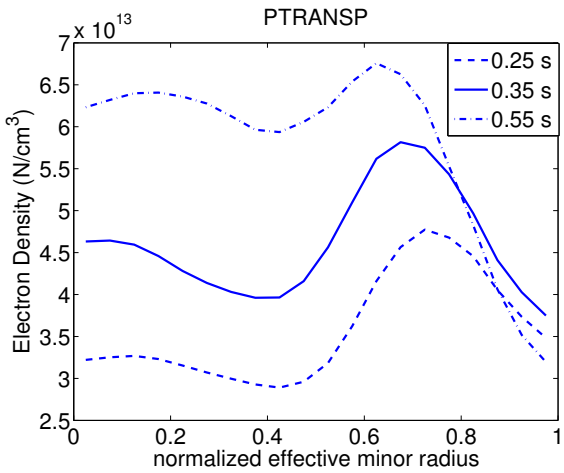

(1) $n_e(\hat{\rho})$

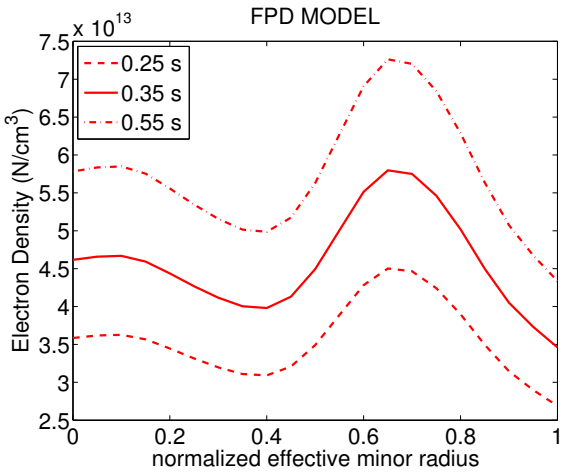

(2) $n_e(\hat{\rho})$

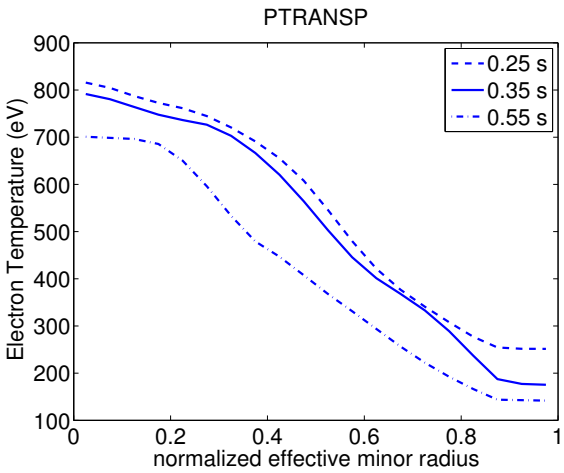

(3) $T_e(\hat{\rho})$

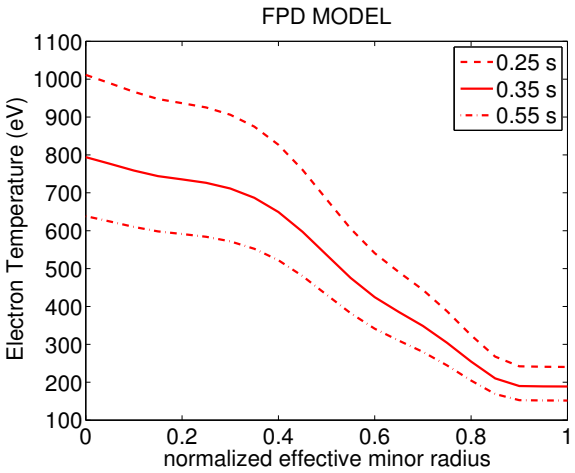

(4) $T_e(\hat{\rho})$

Fig. 13: Plasma profile evolutions comparison: PTRANSP [(1),(3)], control-oriented model [(2),(4)]

Noninductive Current Deposition Profile Comparison

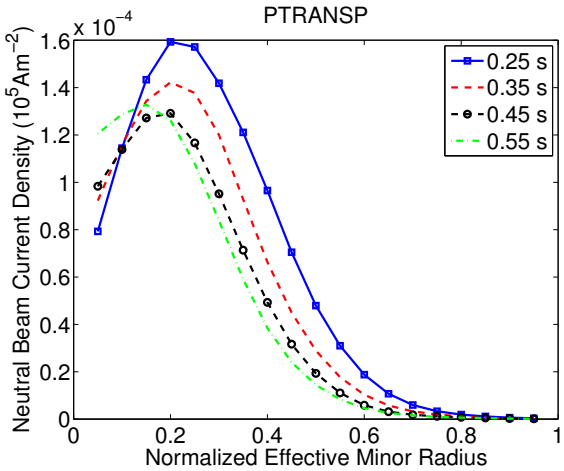

(1) Total Neutral Beam

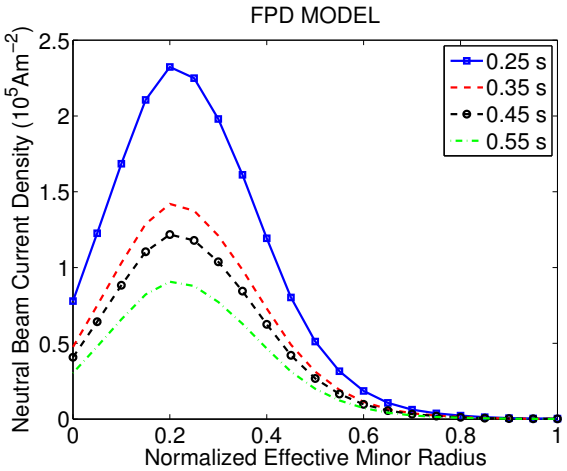

(2) Total Neutral Beam

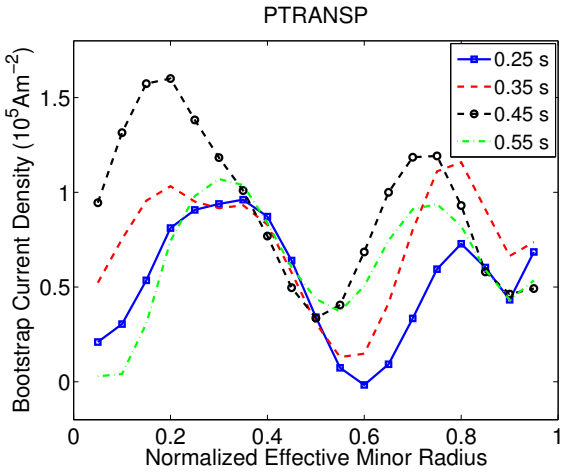

(3) Bootstrap

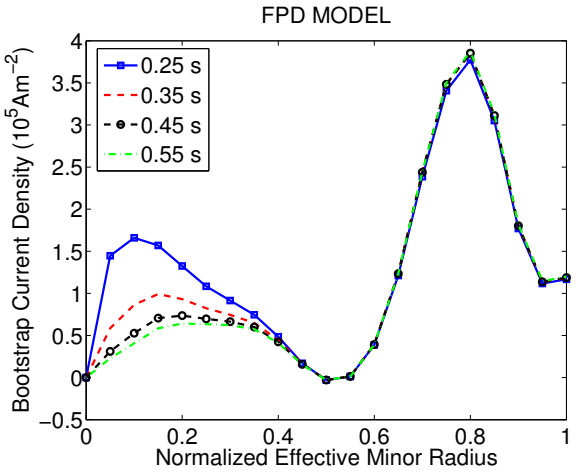

(4) Bootstrap

Fig. 14: Noninductive current deposition profile evolution comparison: PTRANSP [(1),(3)], control-oriented model [(2),(3)].

Noninductive Current Deposition Profile Comparison

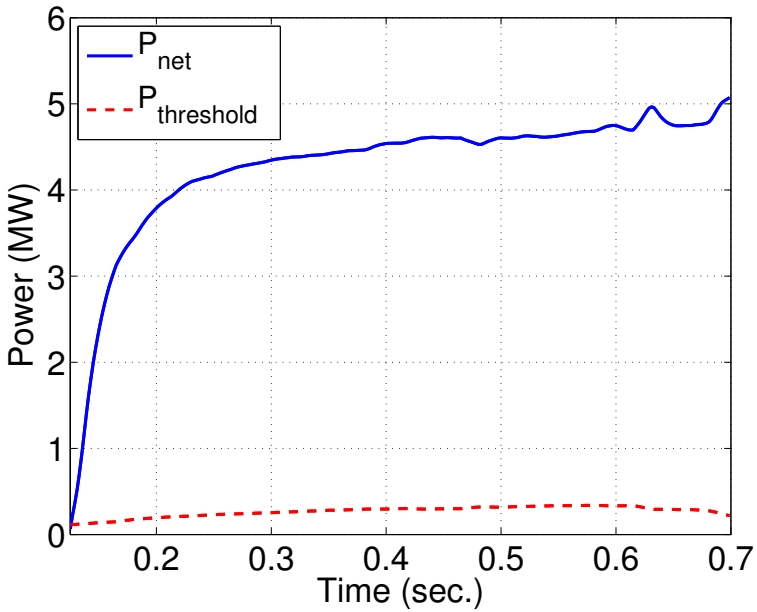

(1) Total Neutral Beam

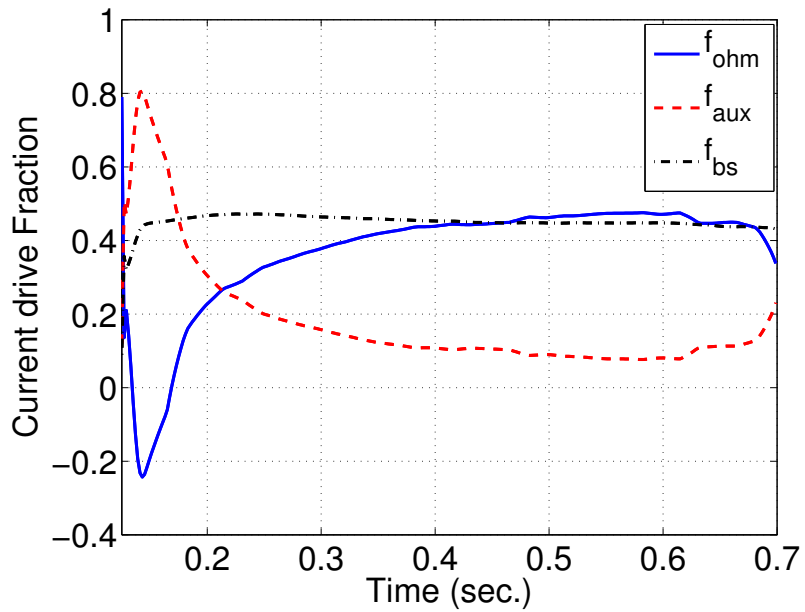

(2) Total Neutral Beam

Fig. 15: (2) Net power across separatrix and L-H threshold power and (3) Current drive fraction.

Poloidal Magnetic Flux Comparison - Time Traces

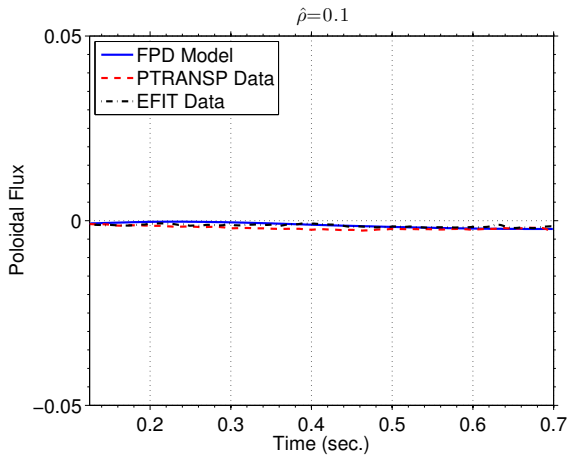

(1) $\hat{\rho} = 0.1$ sec.

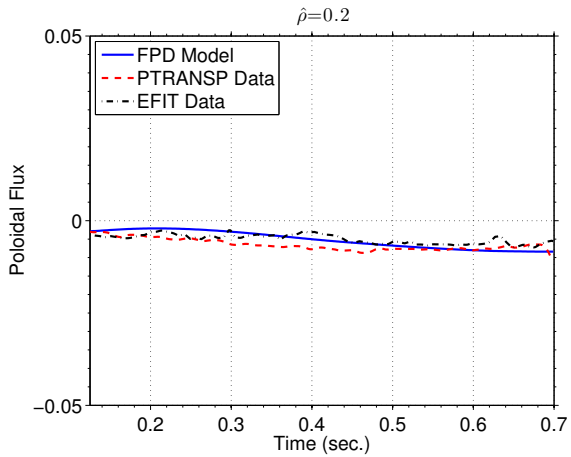

(2) $\hat{\rho} = 0.2$ sec.

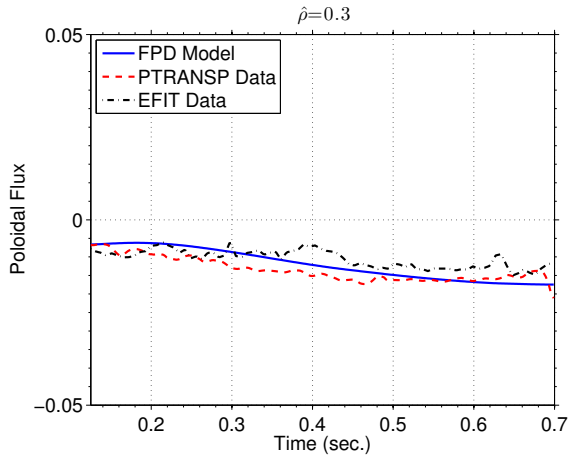

(3) $\hat{\rho} = 0.3$ sec.

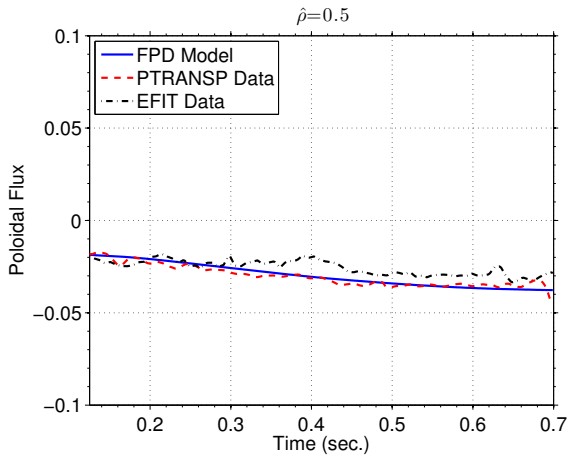

(4) $\hat{\rho} = 0.5$ sec.

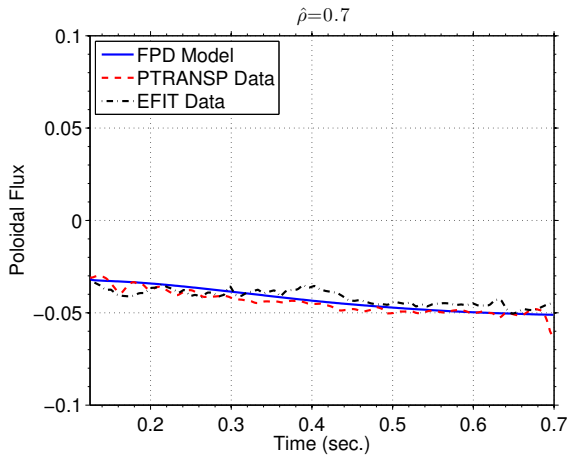

(5) $\hat{\rho} = 0.7$ sec.

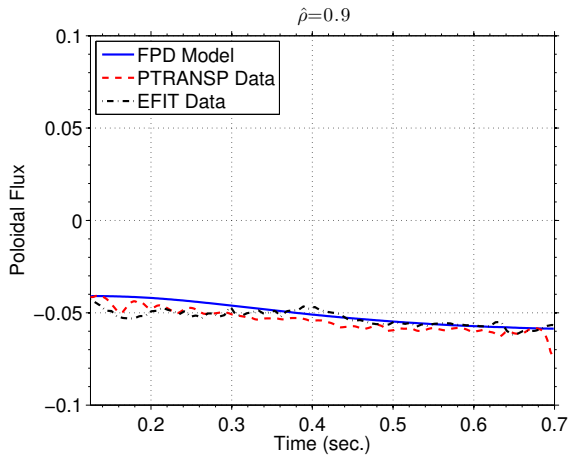

(6) $\hat{\rho} = 0.9$ sec.

Fig. 16: Poloidal magnetic flux evolution comparison.

Poloidal Magnetic Flux Profile Comparison

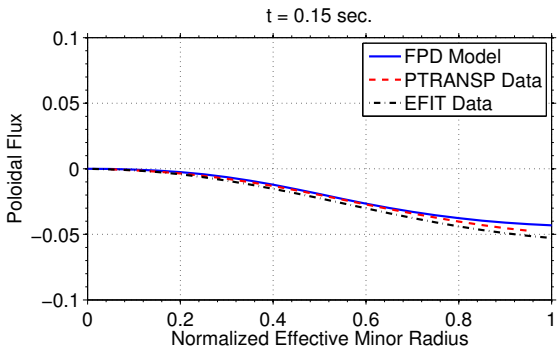

(1) $t = 1$ sec.

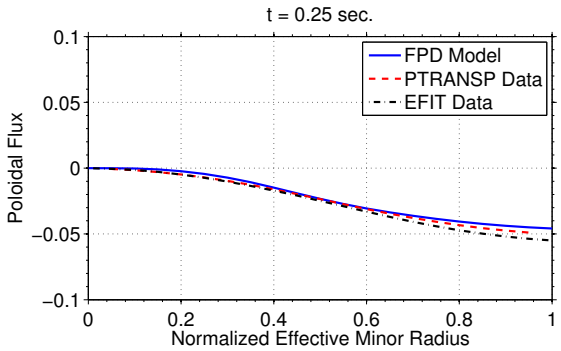

(2) $t = 3$ sec.

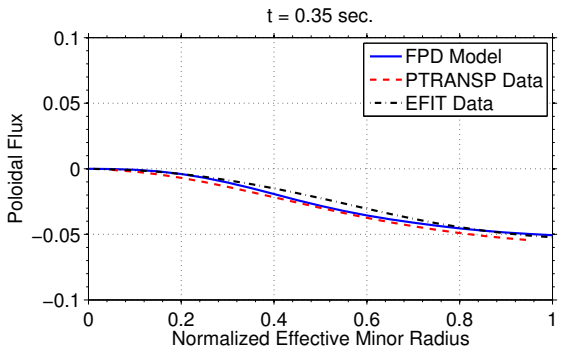

(3) $t = 6$ sec.

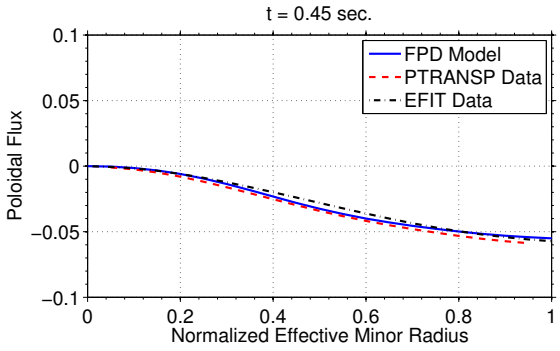

(4) $t = 9$ sec.

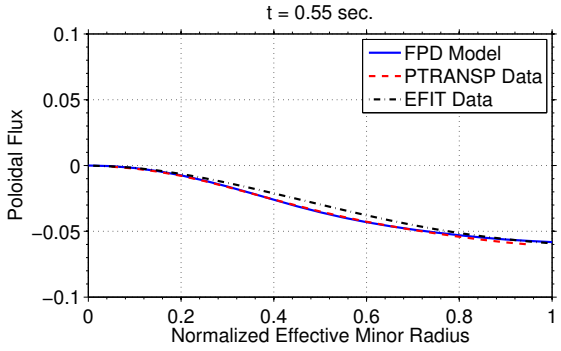

(5) $t = 12$ sec.

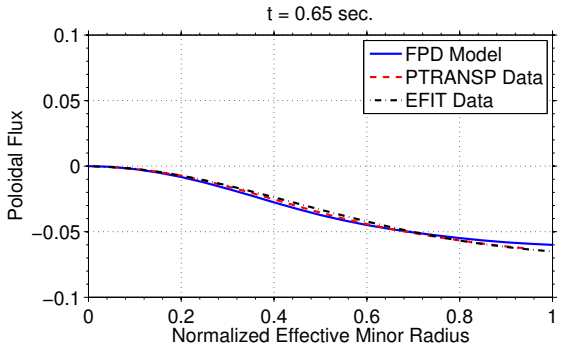

(6) $t = 15$ sec.

Fig. 17: Poloidal magnetic flux profile evolution comparison.

Safety Factor Profile Comparison

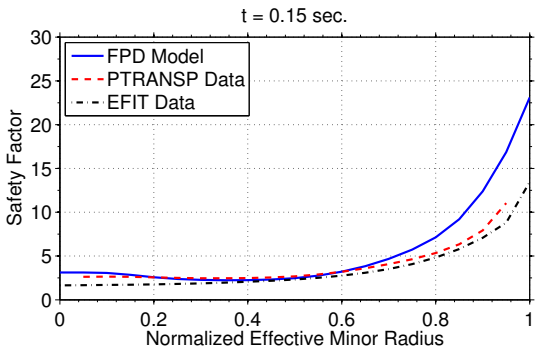

(1) $t = 1$ sec.

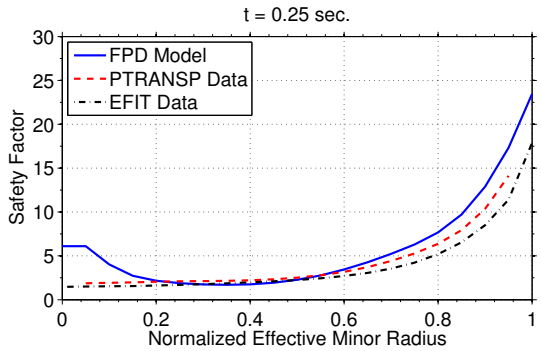

(2) $t = 3$ sec.

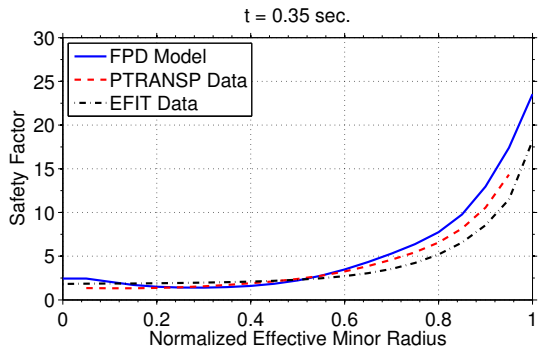

(3) $t = 6$ sec.

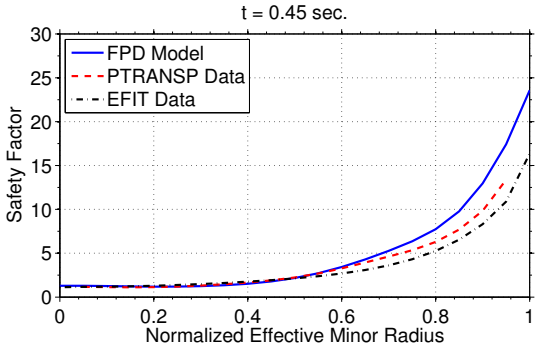

(4) $t = 9$ sec.

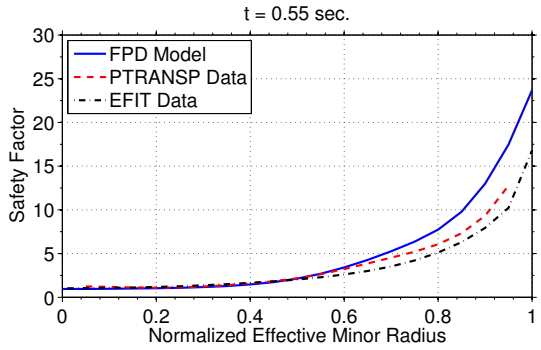

(5) $t = 12$ sec.

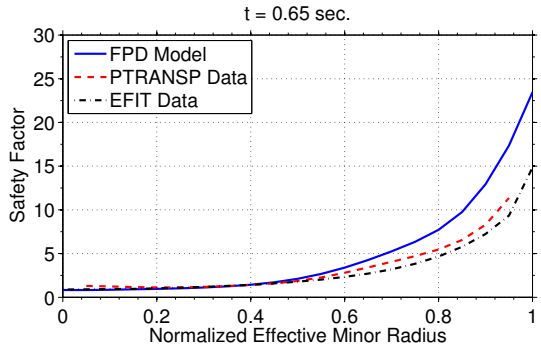

(6) $t = 15$ sec.

Fig. 18: Safety factor profile evolution comparison.

Model Tailored for ITER

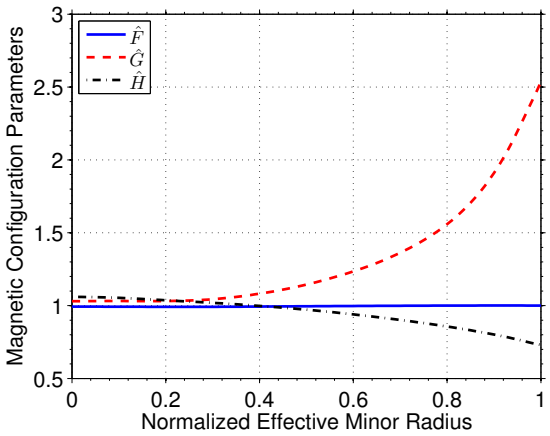

(1) $\hat{F}(\hat{\rho})$, $\hat{G}(\hat{\rho})$, $\hat{H}(\hat{\rho})$

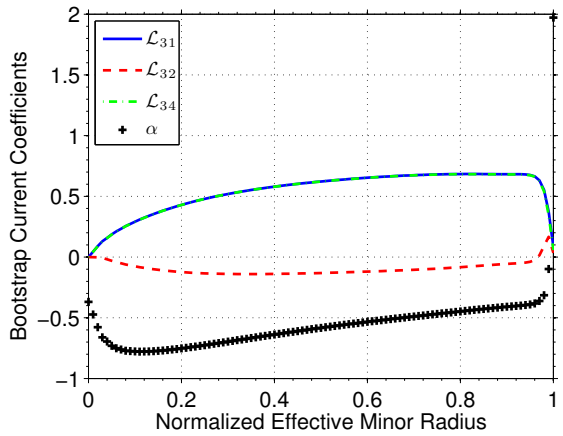

(2) $\mathcal{L}_{31}(\hat{\rho})$, $\mathcal{L}_{32}(\hat{\rho})$, $\mathcal{L}_{34}(\hat{\rho})$, $\alpha(\hat{\rho})$

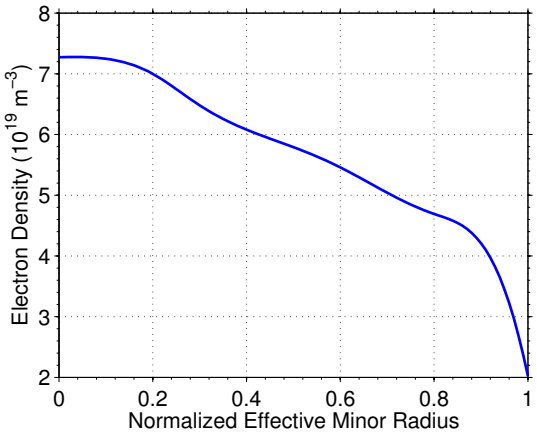

(3) $n_e^{prof}(\hat{\rho})$

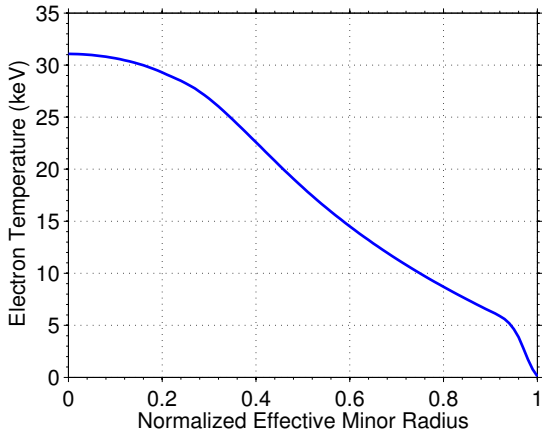

(4) $T_e^{prof}(\hat{\rho})$

Fig. 1: Reference (1) magnetic configuration parameters, (2) bootstrap current coefficients, (3) electron density profile and (4) electron temperature profile.

Model Coefficients and Current Deposition Profiles

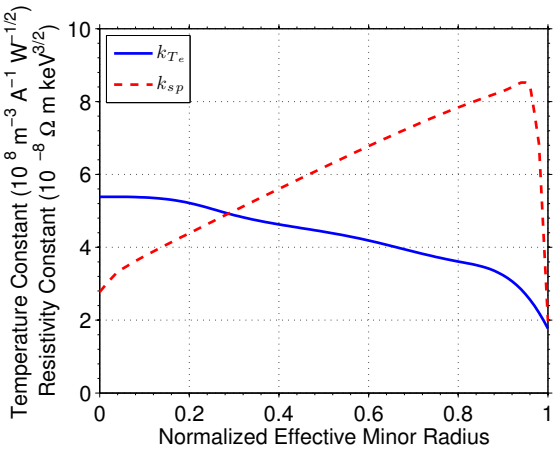

(1) k_{T_e}, k_{sp}

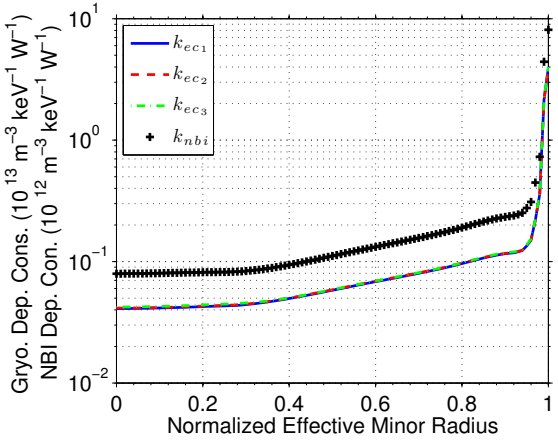

(2) k_{ec_1}, k_{ec_2}, k_{ec_3}, k_{nbi}

Fig. 2: (1) Electron temperature, plasma resistivity, (2) gyrotron, neutral beam model coefficients.

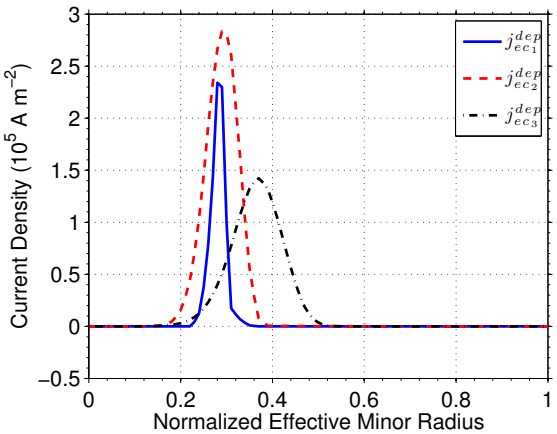

(1) $j_{ec_1}^{dep}(\hat{\rho})$, $j_{ec_2}^{dep}(\hat{\rho})$, $j_{ec_3}^{dep}(\hat{\rho})$

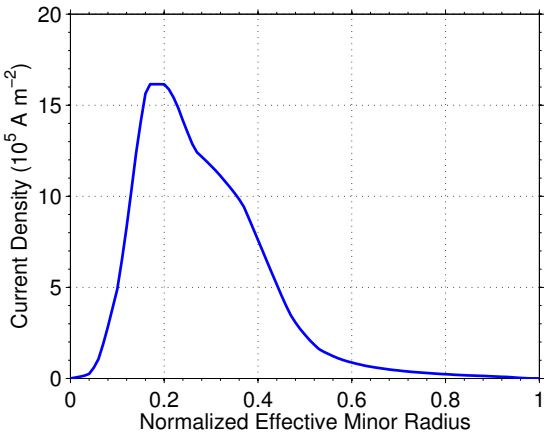

(2) $j_{nbi}^{dep}(\hat{\rho})$ (Note: Off-axis)

Fig. 3: Reference current deposition profiles:
(1) gyrotron and (2) neutral beam.

LEHIGH UNIVERSITY

Model Constants and Simulation Setup

Quantity	Value	Units
μ_0	$4\pi \times 10^{-7}$	$\mathrm{V \cdot s(A \cdot m)^{-1}}$
$B_{\phi,0}$	5.3	T
R_0	6.2	m
a	2.0	m
ρ_b	2.615	m
$\hat{\rho}_{tb}$	0.95	None
κ	1.7	None
$V(\rho_b)$	760	m^3

Quantity	Value	Units
η_{ec_1}	1	None
η_{ec_2}	1	None
η_{ec_3}	1	None
η_{ic}	0.85	None
η_{nbi}	1	None
η_{fus}	0.15	None
Z_{eff}	1.7	None
H_H	1.35	None

- Simulation setup:
  - Plasma ohmically heated during time interval $[1.5, 16]$ sec.
  - During time interval $[16, 38]$ sec., 6.0 MW of electron cyclotron power injected into plasma using first gyrotron launcher.
  - At $t = 38$ sec., 4.0 MW of electron cyclotron power in all three gyrotron launchers, 11.0 MW of ion cyclotron power and 18.5 MW of neutral beam power injected into plasma.
  - Plasma transitions to high confinement mode at $t = 42$ sec.
  - Initial conditions for $\psi(\hat{\rho}, t_0)$ and $\bar{W}(t_0)$ employed in simulation of developed control-oriented model were extracted from the DINA-CH+CRONOS simulation at $t_0 = 45$ sec.

LEHIGH UNIVERSITY

Actuators and Electron Density Profile Comparison

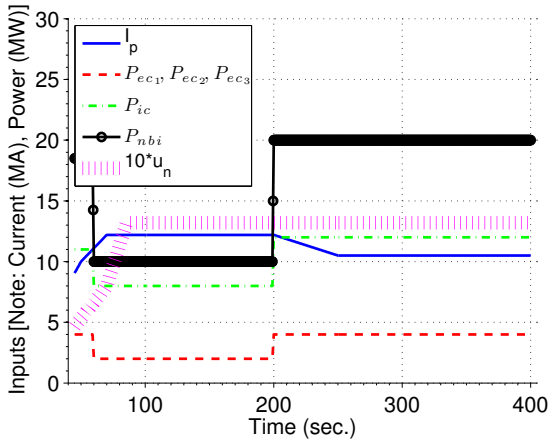

(1) Control Inputs

Fig. 4: Control inputs applied during simulation.

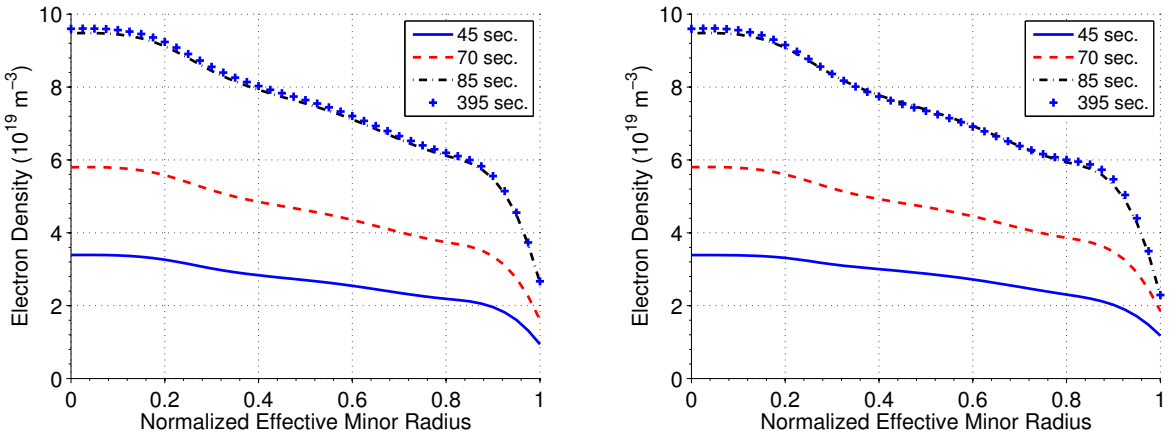

(1) n_e: Control-oriented Model (2) n_e: DINA-CH+CRONOS

Fig. 5: Electron density profile evolution comparison.

Electron Temperature Profile Comparison

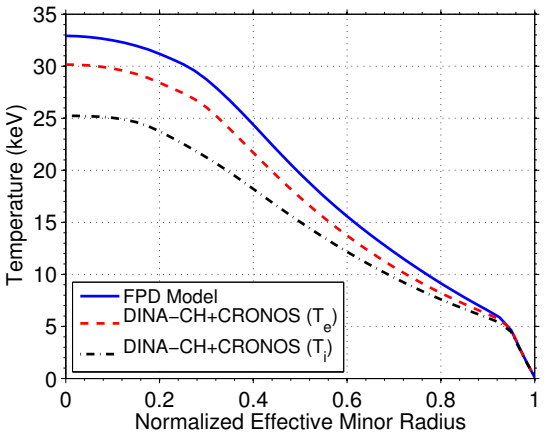

(1) $t = 50$ sec.

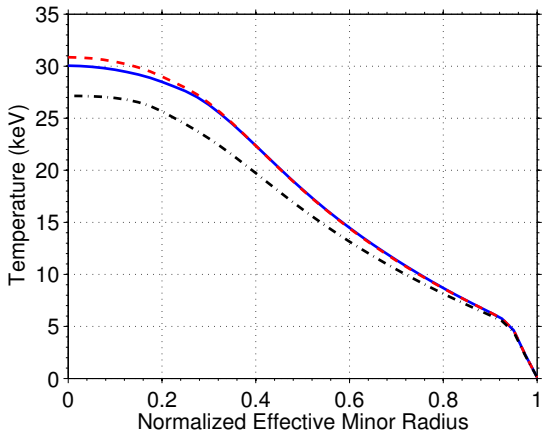

(2) $t = 60$ sec.

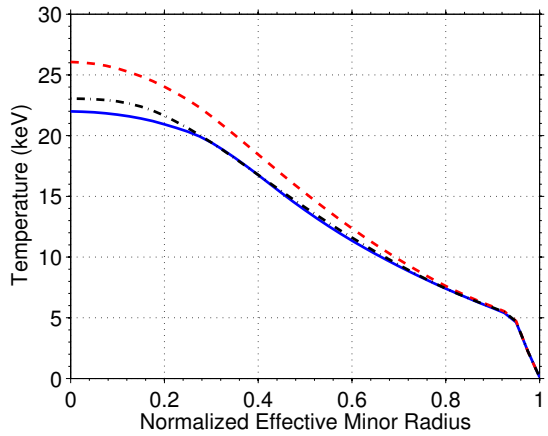

(3) $t = 150$ sec.

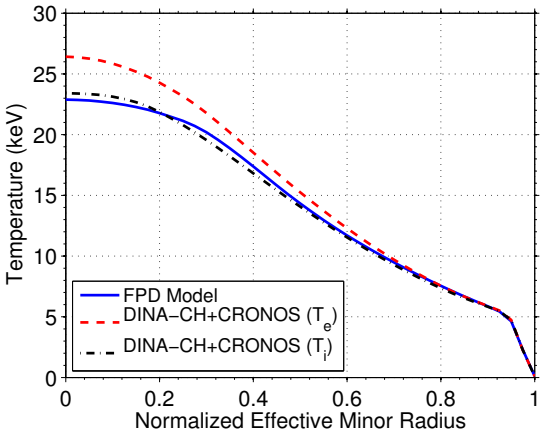

(4) $t = 200$ sec.

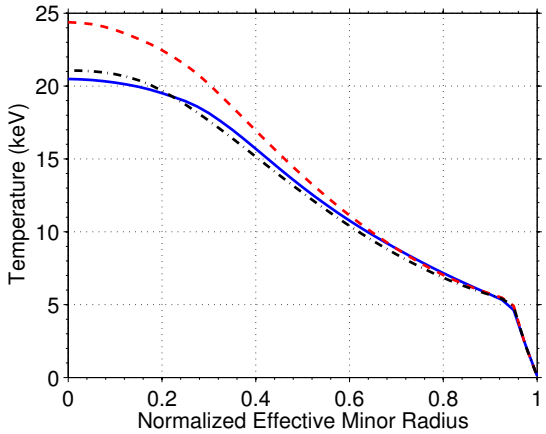

(5) $t = 250$ sec.

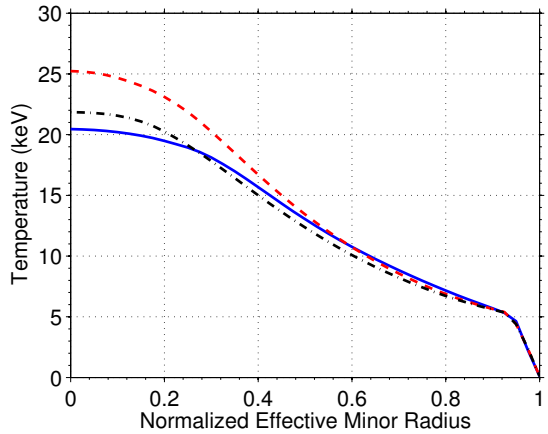

(6) $t = 395$ sec.

Fig. 6: Electron temperature profile evolution comparison.

Noninductive Current Deposition Profile Comparison

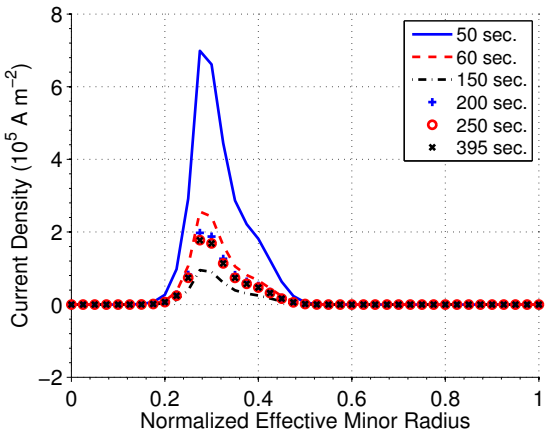

(1) Total Gyrotron

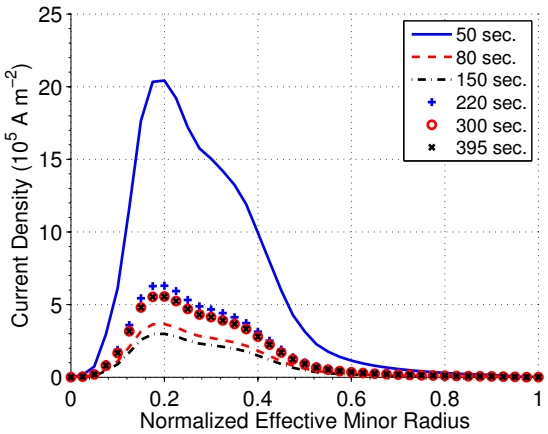

(2) Neutral Beam

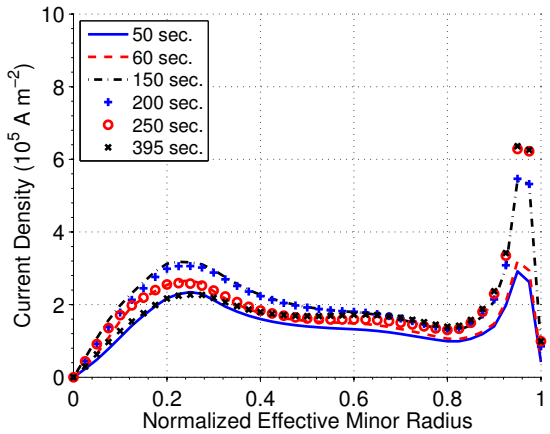

(3) Bootstrap

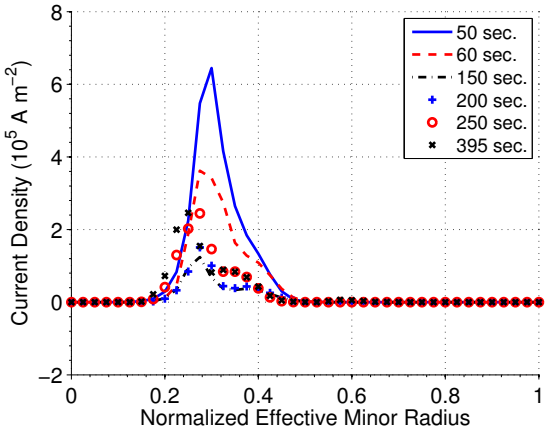

(4) Total Gyrotron

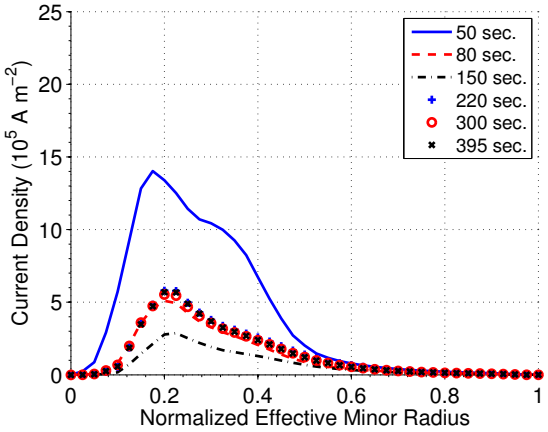

(5) Neutral Beam

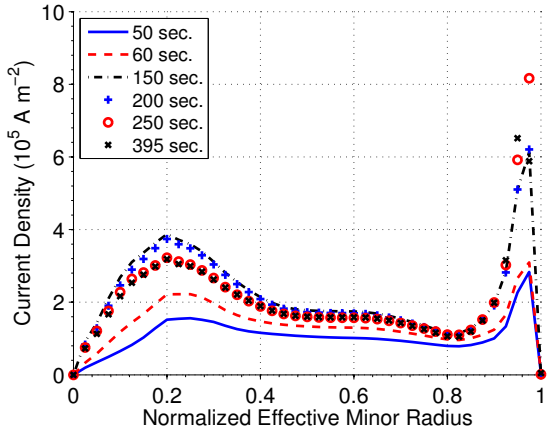

(6) Bootstrap

Fig. 7: Noninductive current deposition profile evolution comparison: control-oriented model [(1),(2),(3)], DINA-CH+CRONOS [(4),(5),(6)].

LEHIGH UNIVERSITY

Stored Energy and Current Drive Fraction

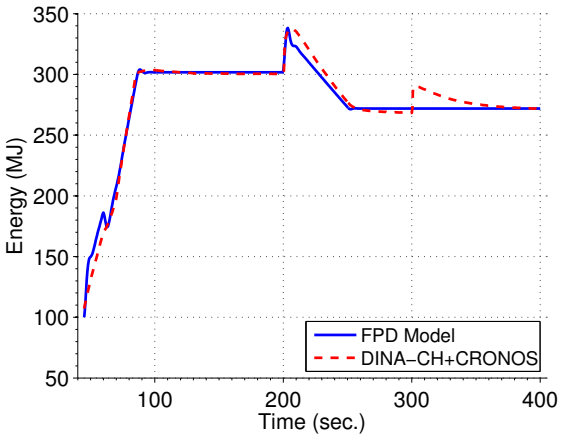

(1) Stored Energy

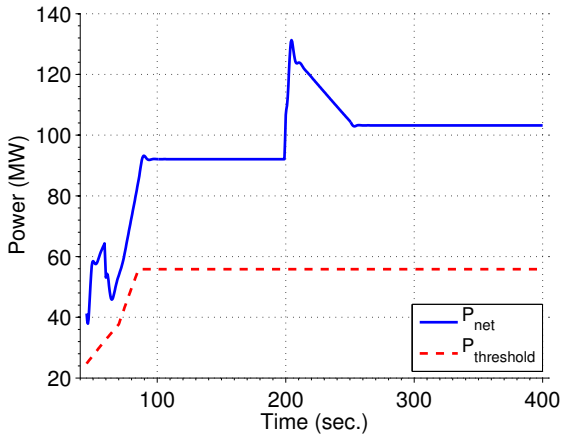

(2) Confinement Regime

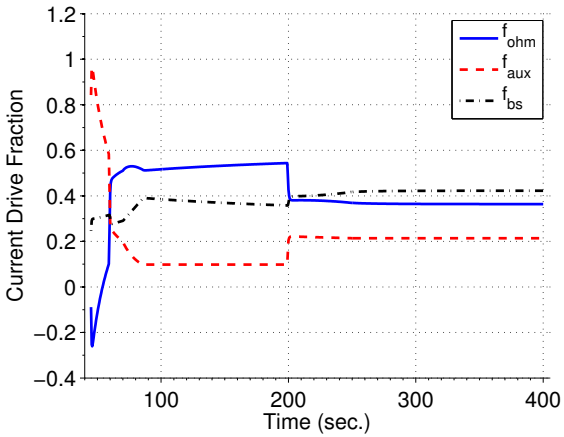

(3) Current Drive Fraction

Fig. 8: (1) Stored energy, (2) net power across separatrix and L-H threshold power and (3) current drive fraction.

- Threshold power to enter H-mode is given by [11,12]:

$$P_{thresh} = \frac{2}{A_{eff}} \left[2.15 e^{\pm 0.107} n_{e20}^{0.782 \pm 0.037} B_{\phi,0}^{0.772 \pm 0.031} a^{0.975 \pm 0.08} R_0^{0.999 \pm 0.101} \right] \quad (37)$$

- If net power through plasma surface $>$ threshold power, plasma will enter H-mode, where

$$P_{net}(t) = P_{tot}(t) - \frac{dW}{dt} \approx \frac{\bar{W}}{\tau_{\bar{W}}} \quad (38)$$

[11] MARTIN, Y. et al., Journal of Physics (2008).
[12] RIGHI, E. et al., Nuclear Fusion (1999).

Poloidal Magnetic Flux Comparison - Time Traces

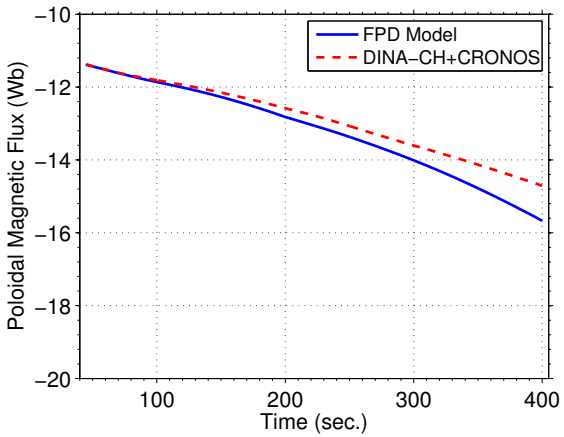

(1) $\hat{\rho} = 0.0$

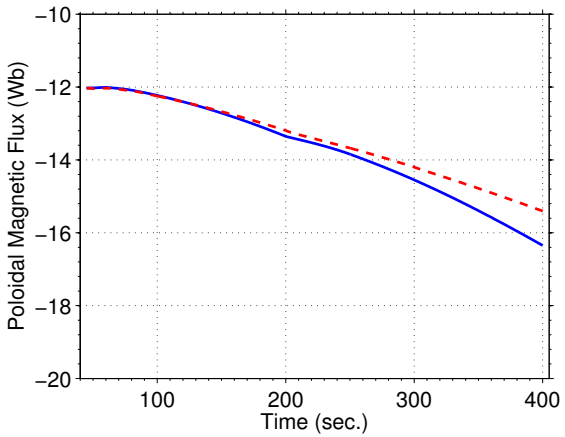

(2) $\hat{\rho} = 0.1$

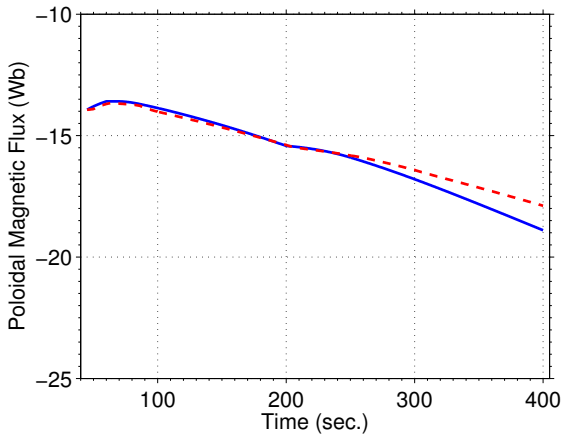

(3) $\hat{\rho} = 0.2$

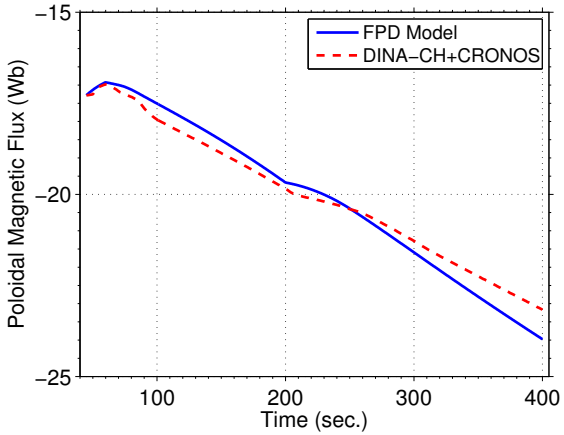

(4) $\hat{\rho} = 0.3$

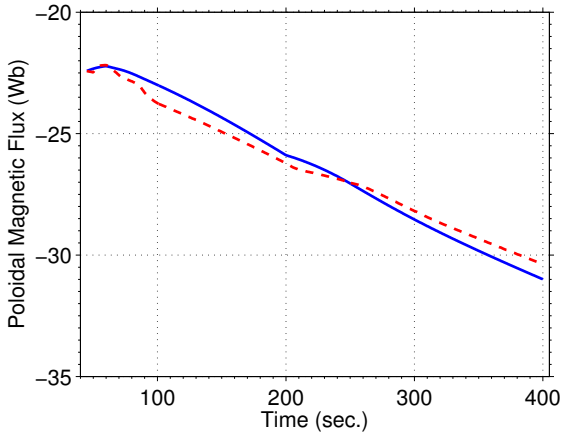

(5) $\hat{\rho} = 0.4$

Fig. 9: Poloidal magnetic flux evolution comparison.

Poloidal Magnetic Flux Comparison - Time Traces

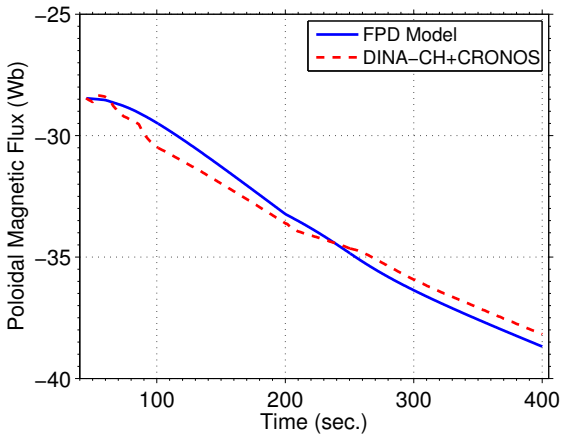

(1) $\hat{\rho} = 0.5$

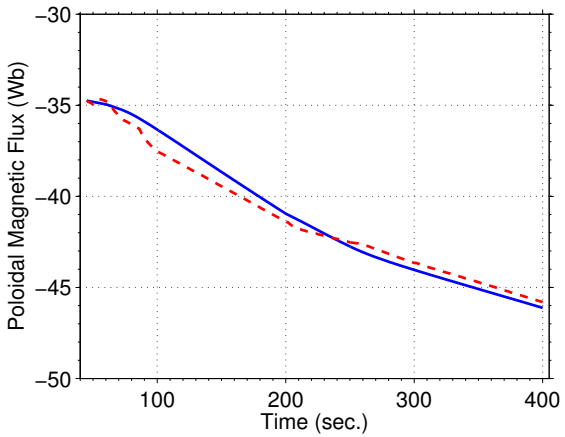

(2) $\hat{\rho} = 0.6$

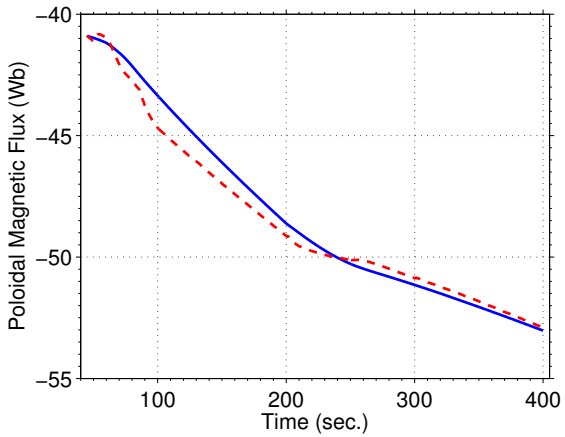

(3) $\hat{\rho} = 0.7$

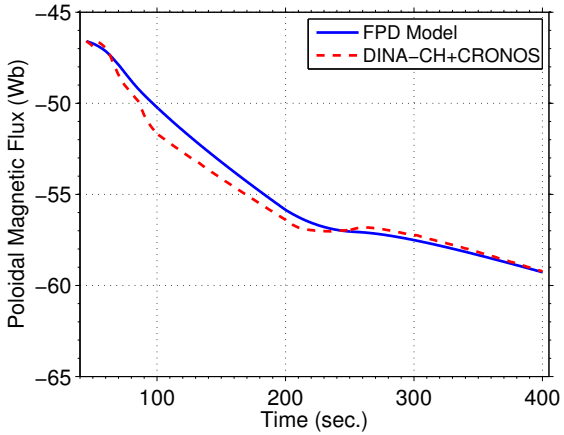

(4) $\hat{\rho} = 0.8$

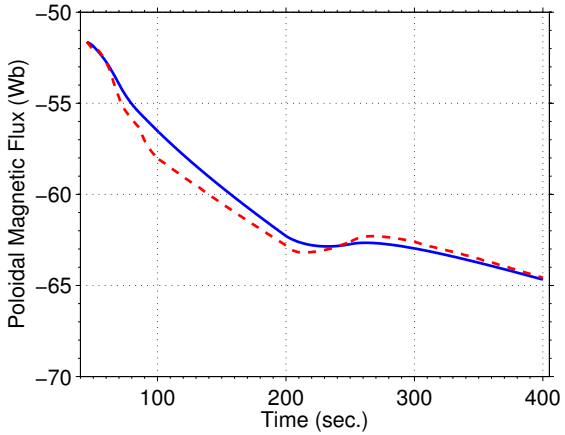

(5) $\hat{\rho} = 0.9$

Fig. 10: Poloidal magnetic flux evolution comparison.

Poloidal Magnetic Flux Profile Comparison

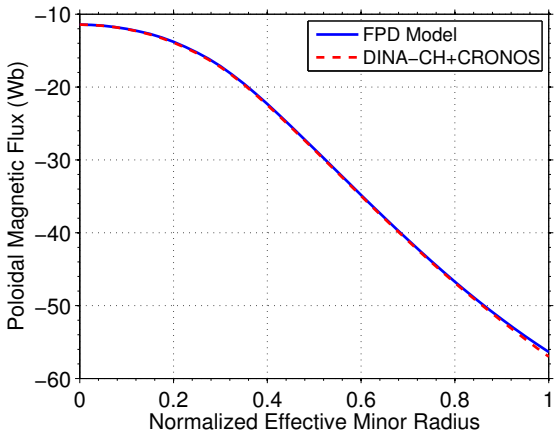

(1) $t = 50$ sec.

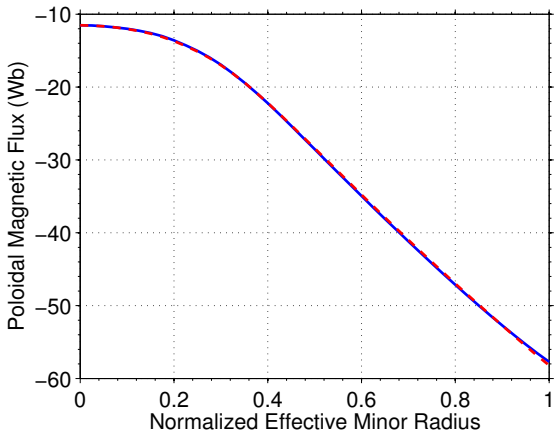

(2) $t = 60$ sec.

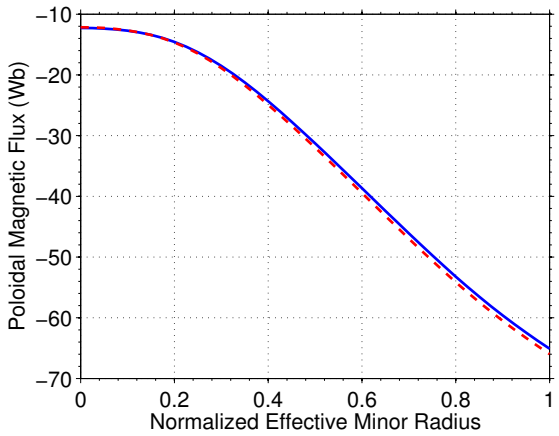

(3) $t = 150$ sec.

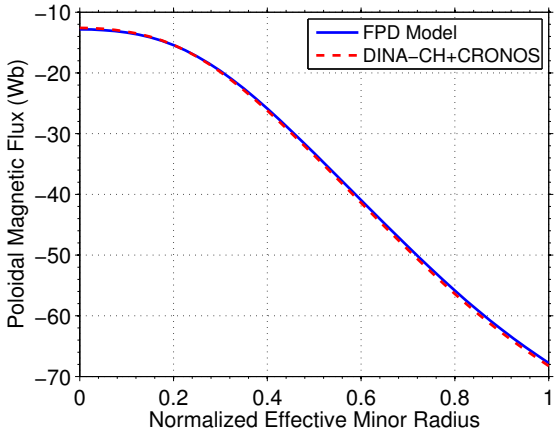

(4) $t = 200$ sec.

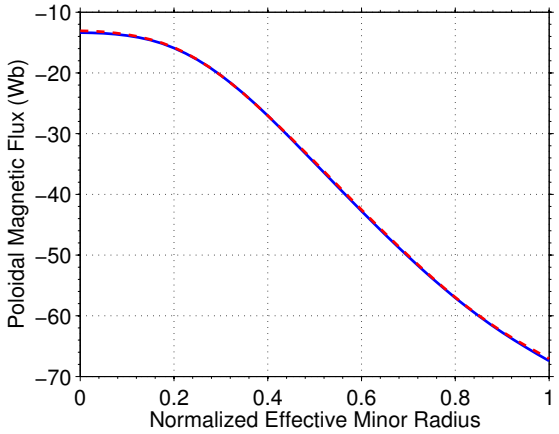

(5) $t = 250$ sec.

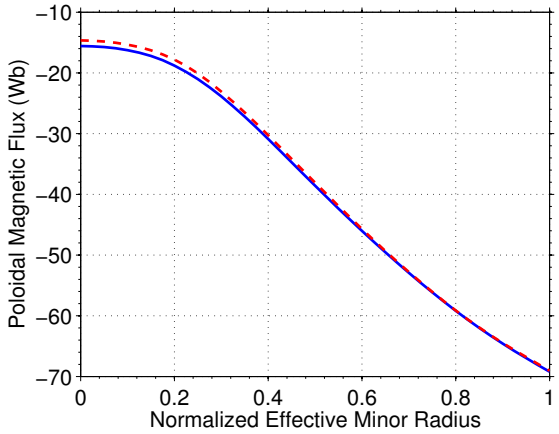

(6) $t = 395$ sec.

Fig. 11: Poloidal magnetic flux profile evolution comparison.

Safety Factor Profile Comparison

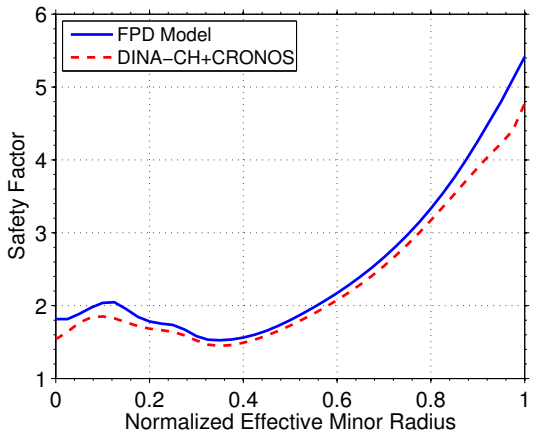

(1) $t = 50$ sec.

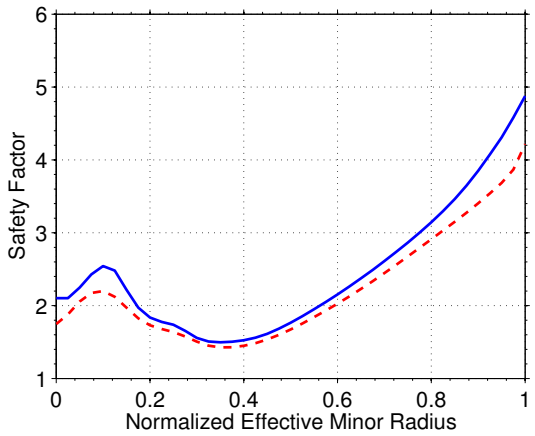

(2) $t = 60$ sec.

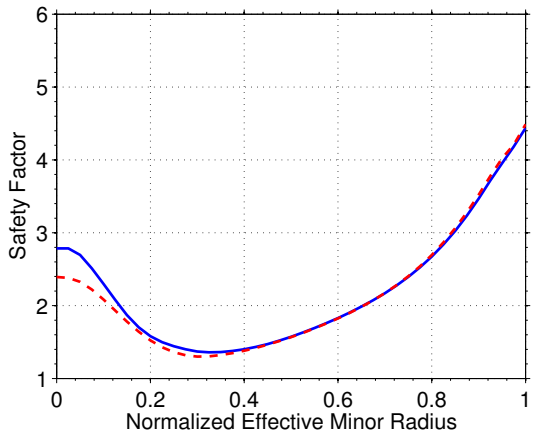

(3) $t = 150$ sec.

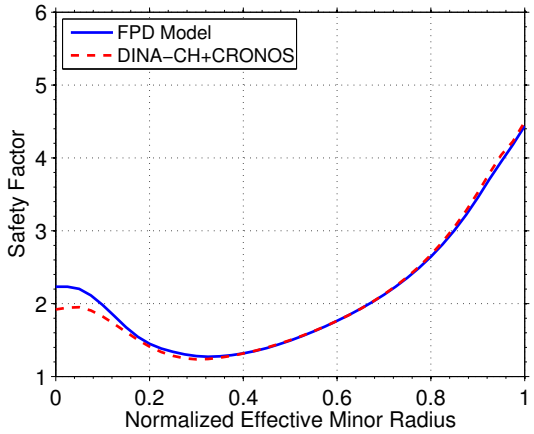

(4) $t = 200$ sec.

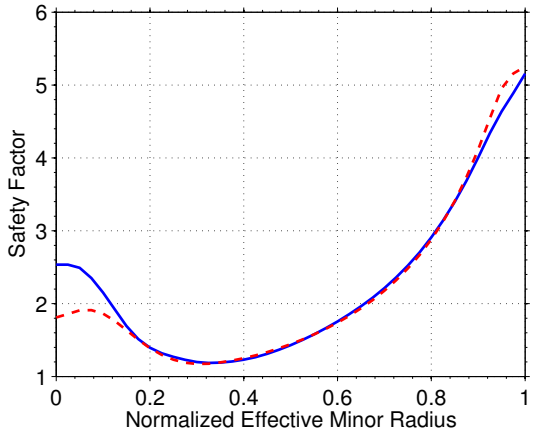

(5) $t = 250$ sec.

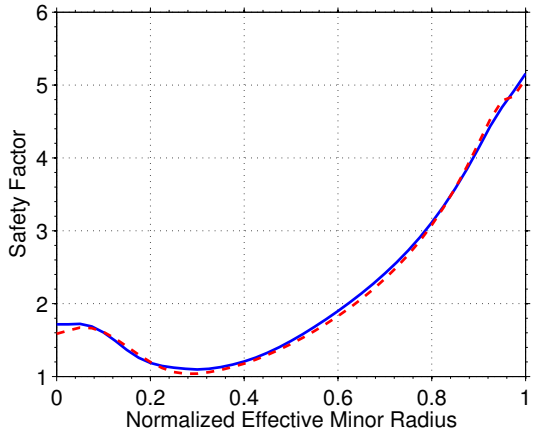

(6) $t = 395$ sec.

Fig. 12: Safety factor q profile evolution comparison.